

Hierarchical Federated Learning in Wireless Networks: Pruning Tackles Bandwidth Scarcity and System Heterogeneity

Md Ferdous Pervej, *Member, IEEE*, Richeng Jin, *Member, IEEE*, and Huaiyu Dai, *Fellow, IEEE*

Abstract—While a practical wireless network has many tiers where end users do not directly communicate with the central server, the users' devices have limited computation and battery powers, and the serving base station (BS) has a fixed bandwidth. Owing to these practical constraints and system models, this paper leverages model pruning and proposes a pruning-enabled hierarchical federated learning (PHFL) in heterogeneous networks (HetNets). We first derive an upper bound of the convergence rate that clearly demonstrates the impact of the model pruning and wireless communications between the clients and the associated BS. Then we jointly optimize the model pruning ratio, central processing unit (CPU) frequency and transmission power of the clients in order to minimize the controllable terms of the convergence bound under strict delay and energy constraints. However, since the original problem is not convex, we perform successive convex approximation (SCA) and jointly optimize the parameters for the relaxed convex problem. Through extensive simulation, we validate the effectiveness of our proposed PHFL algorithm in terms of test accuracy, wall clock time, energy consumption and bandwidth requirement.

Index Terms—Heterogeneous network, hierarchical federated learning, model pruning, resource management.

I. INTRODUCTION

FEDERATED learning (FL) has garnered significant attention as a privacy-preserving distributed edge learning solution in wireless edge networks [1]–[3]. Since the original FL follows the parameter server paradigm, many state-of-the-art works consider a single server with distributed clients as the

general system model in order to study the analytical and empirical performance [2]–[6]. Given that there are $\mathcal{U} := \{u\}_{u=1}^U$ clients, each with a local dataset of $\mathcal{D}_u := \{\mathbf{x}_a, y_a\}_{a=1}^A$, where \mathbf{x}_a and y_a are the a^{th} feature vector and the corresponding label, the central server wants to train a global machine learning (ML) model \mathbf{w} by minimizing a weighted combination of the clients' local objective functions $f_u(\mathbf{w})$'s, as follows

$$f(\mathbf{w}) := \sum_{u=1}^U \alpha_u f_u(\mathbf{w}), \quad (1)$$

$$f_u(\mathbf{w}) := (1/|\mathcal{D}_u|) \sum_{(\mathbf{x}_a, y_a) \in \mathcal{D}_u} l(\mathbf{w}, \mathbf{x}_a, y_a), \quad (2)$$

where α_u is the corresponding weight, and $l(\mathbf{w}, \mathbf{x}_a, y_a)$ denotes the loss function associated with the a^{th} data sample. However, general networks usually follow a hierarchical structure [7], where the clients are connected to edge servers, the edge servers are connected to fog nodes/servers, and these fog nodes/servers are connected to the cloud server [8]. Naturally, some recent works [9]–[14] have extended FL to accommodate this hierarchical network topology.

A client¹ does not directly communicate with the central server in the hierarchical network topology. Instead, the clients usually perform multiple local rounds of model training before sending the updated models to the edge server. The edge server aggregates the received models and updates its edge model, and then broadcasts the updated model to the associated clients for local training. The edge servers repeat this for multiple edge rounds and finally send the updated edge models to the upper-tier servers, which then undergo the same process before finally sending the updated models to the cloud/central server. This is usually known as hierarchical federated learning (HFL) [11]. On the one hand, HFL acknowledges the practical wireless heterogeneous network (HetNet) architecture. On the other hand, it avoids costly direct communication between the far-away cloud server and the capacity-limited clients [14]. Moreover, since local averaging improves learning accuracy [7], the central server ends up with a better-trained model.

While HFL can alleviate communication bottlenecks for the cloud server, data and system heterogeneity amongst the clients still need to be addressed. Since the clients are usually scattered in different locations and have various onboard sensors, the data collected/sensed by these clients are diverse, causing statistical data heterogeneity that the server cannot govern. As such, we need to embrace it in our theoretical and empirical study. Besides, the well-known system heterogeneity

¹The terms client and UE are interchangeably used when there is no ambiguity.

This research was supported in part by the National Natural Science Foundation of China under Grants 62301487, in part by the Zhejiang Provincial Natural Science Foundation of China under Grant No. LQ23F010021 and LD21F010001, in part by the Ng Teng Fong Charitable Foundation in the form of ZJU-SUTD IDEA Grant under Grant No. 188170-11102, and in part by the US National Science Foundation under grants CNS-1824518 and ECCS-2203214. (*Corresponding author: Richeng Jin.*)

M. F. Pervej was with the Department of Electrical and Computer Engineering, North Carolina State University, Raleigh, NC 27695, USA, and now is with the Ming Hsieh Department of Electrical and Computer Engineering, University of Southern California, Los Angeles, CA 90089, USA (e-mail: pervej@usc.edu).

H. Dai is with the Department of Electrical and Computer Engineering, North Carolina State University, Raleigh, NC 27695, USA (e-mail: hdai@ncsu.edu).

R. Jin is with the College of Information Science and Electronic Engineering, Zhejiang University, the Zhejiang–Singapore Innovation and AI Joint Research Lab, and the Zhejiang Provincial Key Lab of Information Processing, Communication and Networking (IPCAN), Hangzhou, China, 310000 (e-mail: richengjin@zju.edu.cn).

©2024 IEEE. Personal use of this material is permitted. Permission from IEEE must be obtained for all other uses, in any current or future media, including reprinting/republishing this material for advertising or promotional purposes, creating new collective works, for resale or redistribution to servers or lists, or reuse of any copyrighted component of this work in other works.

arises from the clients' diverse computation powers [15]. Recently, some works have been proposed to deal with system heterogeneity. For example, FedProx [16], anarchic federated averaging (AFA) [17] and federated normalized averaging algorithm (FedNova) [18], to name a few, considered different local rounds for different clients to address the system heterogeneity. More specifically, FedProx adds a proximal term to the client's local objective function to handle heterogeneity. AFA and FedNova present different ways to aggregate clients trained models' weights at the server to tackle this system heterogeneity. However, these algorithms still assume that the client has and trains the original ML model, i.e., neither the computation time for the client's local training nor the communication overhead for offloading the trained model to the server is considered in system design.

Model pruning has attracted research interest recently [19], [20]. It makes the over-parameterized model sparser, which allows the less computationally capable clients to perform local training more efficiently without sacrificing much of the test accuracy. Besides, since the trained model contains fewer non-zero entries, the communication overhead over the unreliable wireless link between the client and the associated base station (BS) also dramatically reduces. However, pruning generally introduces errors that only partially vanish, causing the pruned model to converge only to a neighborhood of the optimal solution [19]. Besides, unlike the traditional FL, where the model averaging happens only at the central server, HFL has multiple hierarchical levels that may adopt their own aggregation strategy. Therefore, model pruning at the local client level leads to additional errors in the available models at different levels, eventually contributing to the global model. As such, more in-depth study is in need to understand the full benefit of model pruning in hierarchical networks.

A. Related Work

Some recent works studied HFL [9]–[14] and model pruning-based traditional single server based FL [20]–[24] separately. In [9], Xu *et al.* proposed an adaptive HFL scheme, where they optimized edge aggregation intervals and bandwidth allocation to minimize a weighted combination of the model training delay and training loss. Liu *et al.* proposed network-assisted HFL in [10], where they optimized wireless resource allocation and user associations to minimize 1) learning latency for independent identically distributed (IID) data distribution and 2) weighted sum of the total data distance and learning latency for the non-IID data distribution. Similar to [9], [10], Luo *et al.* jointly optimized the wireless network parameters in order to minimize the weighted combination of the total energy consumption and delay during the training process in [11]. Besides, [12] also proposed an HFL algorithm based on federated averaging (FedAvg) [1]. In [13], Feng *et al.* proposed a mobility-aware clustered FL algorithm owing to user mobility. More specifically, assuming that all users had an equal probability of staying at a cluster, the authors derived an upper bound of the convergence rate to capture the impact of user mobility, data heterogeneity and network heterogeneity. Abad *et al.* also optimized wireless resources to reduce the communication latency and facilitate HFL in [14].

On the model pruning side, Jiang *et al.* considered two-stage distributed model pruning in [20] with traditional single server based FL setting without any wireless network aspects. In a similar setting, Zhu *et al.* proposed a layer-wise pruning mechanism in [21]. Liu *et al.* optimized the pruning ratio and time allocation in [22] in order to maximize the convergence rate in a time division multiple access operated small BS (sBS). The idea was extended to joint client selection, pruning ratio optimization and time allocation in [23]. Using a similar network model, Ren *et al.* optimized pruning ratios and bandwidth allocations jointly to minimize a weighted combination of the FL training time and pruning error in [24]. These works [22]–[24] decomposed the original problem into different sub-problems that they solved iteratively in an attempt to solve the original problem sub-optimally. Moreover, [22]–[24] considered a simple network system model with a single BS serving the distributed clients with the wireless links.

B. Our Contributions

While the studies mentioned above shed some light on HFL and model pruning in the traditional single server based FL, the impact of pruning on HFL in resource-constrained wireless HetNet is yet to be explored. On the one hand, the clients need to train the original model for a few local episodes to determine the neurons they shall prune, which adds additional time and energy costs. On the other hand, pruning adds errors to the learning performance. Therefore, it is necessary to theoretically and empirically study these errors from different levels in HFL. Moreover, it is also crucial to justify how and when one should adopt model pruning in practical wireless HetNets. Motivated by these, in this work, we present our pruning-enabled HFL (PHFL) framework with the following major contributions:

- Considering a practical wireless HetNet, we propose a PHFL solution in which the clients perform local training on the initial models to determine the neurons to prune, perform extensive training on the pruned models, and offload the trained models under strict delay and energy constraints.
- We theoretically analyze how pruning introduces errors in different levels under resource constraints in wireless HetNets by deriving a convergence bound that captures the impact of the wireless links between the clients and server and the pruning ratios. More specifically, the proposed solution converges to the neighborhood of a stationary point of traditional HFL with a convergence rate of $\mathcal{O}(1/\sqrt{UT}) + \mathcal{O}(\beta^2 D^2 \delta^{\text{th}})$, where U is the total number of clients, T is the total local iterations, β quantifies smoothness of the loss function, D^2 is an upper bound of the L_2 norm of the model weights, and $0 < \delta^{\text{th}} < 1$ is the maximum allowable pruning ratio.
- Then, we formulate an optimization problem to maximize the convergence rate by jointly configuring wireless resources and system parameters. To tackle the non-convexity of the original problem, we use a successive convex approximation (SCA) algorithm to solve the relaxed convex problem efficiently.

TABLE I: Important Notations

Notation	Description
$u; b; l$	u^{th} user; b^{th} sBS; l^{th} mBS
$\mathcal{B}_l; k$	sBS set under the l^{th} mBS; k^{th} sBS in \mathcal{B}_l
$\mathcal{V}_{k,l}; j$	VC set of sBS k under the l^{th} mBS; j^{th} VC of sBS k
$\mathcal{U}_{j,k,l}; i$	Client set of the j^{th} VC of l^{th} sBS under the l^{th} mBS; i^{th} client in $\mathcal{U}_{j,k,l}$
$z; \mathcal{Z}$	z^{th} pRB; pRB set
\mathbf{P}_i^t	Client i 's transmission power during t
$\mathbf{w}; \mathbf{m}; \tilde{\mathbf{w}}$	Original model; binary mask; pruned model
$\mathbf{w}_i; \mathbf{w}_j; \mathbf{w}_k; \mathbf{w}_l$	Local model of the client, VC, sBS, and mBS
$f_i(\cdot); f_j(\cdot); f_k(\cdot); f_l(\cdot); f(\cdot)$	Loss function of the client, VC, sBS, mBS, and central server, respectively
$\nabla f_i(\cdot); g(\cdot); \eta$	True gradient; stochastic gradient; learning rate
$d; d_p$	Total & pruned parameters of the ML model
$\delta_i^t; \delta^{\text{th}}$	Pruning ratio of client i during t ; max pruning ratio
$\alpha_i; \alpha_j; \alpha_k; \alpha_l$	Weight of i^{th} client, j^{th} VC, k^{th} sBS, and l^{th} mBS
ρ	Number of SGD rounds on \mathbf{w} to get winning ticket
$\kappa_0; \kappa_1; \kappa_2; \kappa_3$	Number of local, VC, sBS, and mBS rounds
$\mathbf{1}_i^t; p_i^t$	Binary indicator function to define if sBS receives i^{th} client's trained model; probability that $\mathbf{1}_i^t = 1$
β	Smoothness of the loss functions
σ^2	Bounded variance of the gradients
ε^2	Bounded divergence of the loss functions of two inter-connected tiers
$G^2; D^2$	Upper bound of the L_2 -norm of stochastic gradients and model weights, respectively
$f_i^t; f_i^{\text{max}}$	CPU clock cycle of i during t ; max CPU cycle of i
b, n	Batch size; number of mini-batch
$c_i; D_i$	Required number of CPU cycle of i to process 1-bit data; each data sample size in bits
FPP	Floating point precision
$t_i^{\text{cpd}}; e_i^{\text{cpd}}$	Time and energy overheads to get the lottery ticket
$t_i^{\text{cps}}; e_i^{\text{cps}}$	Time and energy overheads to compute κ_0 local SGD rounds with the pruned model
$t_i^{\text{up}}; e_i^{\text{up}}$	Time and energy overheads for offloading client i 's trained model
$t_i^{\text{tot}}; e_i^{\text{tot}}$	Client i 's total time and energy overheads to finish one VC round
$t_i^{\text{th}}; e_i^{\text{th}}$	Time and energy budgets to finish one VC round

- Finally, using extensive simulation on two popular datasets and three popular ML models, we show the effectiveness of our proposed solution in terms of test accuracy, training time, energy consumption and bandwidth requirement.

The rest of the paper is organized as follows: Section II introduces our system model. Detailed theoretical analysis is performed in Section III, followed by our joint problem formulation and solution in Section IV. Based on our extensive simulation, we discuss the results in Section V. Finally, Section VI concludes the paper. Moreover, Table I summarizes the important notations used in the paper.

II. SYSTEM MODEL

A. Wireless Network Model

We consider a generic heterogeneous network (HetNet) consisting of some UEs, sBSs and macro BSs (mBSs), as shown in Fig. 1. Denote the UE, sBS and mBS sets by $\mathcal{U} := \{u\}_{u=1}^U$, $\mathcal{B} := \{b\}_{b=1}^B$ and $\mathcal{L} := \{l\}_{l=1}^L$, respectively. Each UE and sBS are connected to one sBS and mBS, respectively. The mBSs are connected to the central server. While the UEs communicate over wireless links with the sBS, the connections between the sBS and mBS and between the mBS and central server are wired. Moreover, due to UEs' system heterogeneity, we consider that the sBS groups UEs with similar computation and battery powers into a virtual cluster (VC).

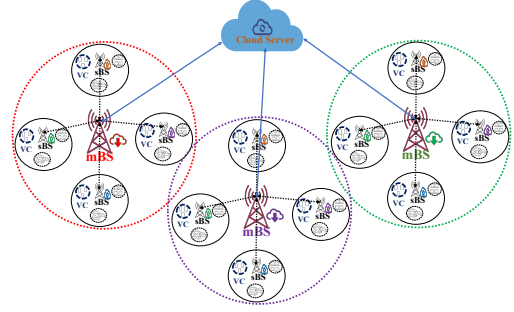


Fig. 1: Pruning-enabled hierarchical FL system model

We can benefit from the VC since it enables one additional aggregation tier. Besides, thanks to the recent progress of the proximity-services in practical networks [25], one can also select a cluster head and leverage device-to-device communication to receive and distribute the models to the UEs in the same VC. However, in this work, we assume that the sBS creates the VC and also manages it. We use the notation $\mathcal{B}_l := \{k\}_{k=1}^{B_l}$, $\mathcal{V}_{k,l} := \{j\}_{j=1}^{V_{k,l}}$ and $\mathcal{U}_{j,k,l} := \{i\}_{i=1}^{U_{j,k,l}}$ to represent the sBS set associated to mBS l , VC set of sBS $k \in \mathcal{B}_l$ and UE set of VC $j \in \mathcal{V}_{k,l}$, respectively. Moreover, denote the UEs associated with sBS k , mBS l by $\mathcal{U}_{k,l} = \bigcup_{j=1}^{V_{k,l}} \mathcal{U}_{j,k,l}$ and $\mathcal{U}_l = \bigcup_{k=1}^{B_l} \mathcal{U}_{k,l}$, respectively. Finally, $\mathcal{U} = \bigcup_{l=1}^L \mathcal{U}_l$. Note that we consider that these associations are known and provided by the network administrator. The network has a fixed bandwidth divided into orthogonal physical resource blocks (pRBs) for performing the FL task. Denote the pRB set by $\mathcal{Z} := \{z\}_{z=1}^Z$. Each mBS reuses the same pRB set, i.e., the frequency reuse factor is 1. Besides, each mBS allocates dedicated pRBs to its associated sBSs. Each sBS further uses dedicated pRBs to communicate with the associated UEs. As such, there is no intra-tier interference in the system.

To this end, denote the distance between UE i and the sBS k by $d_{i,k}$. The wireless fading channel between the UE and sBS follows Rayleigh distribution², and is denoted by $h_{i,k}^t$. The transmission power of UE is denoted by P_i^t . As such, the uplink signal-to-noise-plus-interference ratio (SINR) is expressed as

$$\gamma_{i,k}^t = P_i^t h_{i,k}^t d_{i,k}^{-\alpha} / (\omega \zeta^2 + I_{i,k}^t), \quad (3)$$

where α is the path loss exponent, ζ^2 is the variance of the circularly symmetric zero-mean Gaussian distributed random noise and ω is the pRB size. Moreover, $I_{i,k}^t = \sum_{l=1}^L \sum_{k'=1, k \neq k'}^{B_l} \sum_{j'=1}^{V_{k',l}} \sum_{i' \in \mathcal{U}_{j',k',l}} P_{i'}^t h_{i',k'}^t d_{i',k'}^{-\alpha}$ is the inter-cell interference. Thus, the data rate

$$r_i^t = \omega \log_2 [1 + \gamma_{i,k}^t]. \quad (4)$$

B. Pruning-Enabled Hierarchical Federated Learning (PHFL)

In this work, we consider that each client uses mini-batch stochastic gradient descent (SGD) to minimize (2) over n mini-batches since the gradient descent over the entire dataset is time-consuming. Denote the stochastic gradient $g(\mathbf{w})$ such that $\mathbb{E}_{\xi_n \sim \mathcal{D}_i} [g(\mathbf{w})] := \nabla f_i(\mathbf{w})$, where ξ_n is a randomly sampled

²Rayleigh distribution is widely used for its simplicity. Other distributions are not precluded.

batch from dataset \mathcal{D}_i . However, computation with the original model $\mathbf{w} \in \mathbb{R}^d$ is still costly and may significantly extend the training time of a computationally limited client. To alleviate this, the UE trains a pruned model by removing some of the weights of the original model \mathbf{w} [19].

Denote a binary mask by $\mathbf{m}_i \in \mathbb{R}^d$ and the pruned model by $\tilde{\mathbf{w}}_i := \mathbf{w}_i \odot \mathbf{m}_i$, where \odot means element-wise multiplication. Note that training the pruned model $\tilde{\mathbf{w}}_i$ is computationally less expensive as it has fewer parameters than the original model. It is worth pointing out that the UE utilizes the state-of-the-art lottery ticket hypothesis [26] to find the winning ticket $\tilde{\mathbf{w}}_i$ and the corresponding mask with the following key steps. Denote the number of parameters required to be pruned by d_p . The UE performs ρ local iterations on the original model \mathbf{w}_i as

$$\mathbf{w}_i^\rho = \mathbf{w}_i - \eta \sum_{\bar{\rho}=1}^{\rho} g(\mathbf{w}_i^{\bar{\rho}}), \quad (5)$$

where η is the step size. The UE then prunes d_p entries of $\mathbf{w}_i^\rho \in \mathbb{R}^d$ with the smallest magnitudes³ and generates a binary mask $\mathbf{m}_i \in \{0, 1\}^d$. To that end, the client obtains the winning ticket $\tilde{\mathbf{w}}_i$ by retaining the original weights of the corresponding nonzero entries of the mask \mathbf{m}_i from the original initial model \mathbf{w}_i [26]. Note that other pruning techniques can also be adopted. Moreover, we denote the pruning ratio by [23]

$$\delta_i := d_p/d. \quad (6)$$

Given the pruned model $\tilde{\mathbf{w}}_i^{t,0} := \mathbf{w}_i^t \odot \mathbf{m}_i^t$, the loss function of the UE is rewritten as

$$f_i(\tilde{\mathbf{w}}_i^{t,0}) := [1/|\mathcal{D}_i|] \sum_{(\mathbf{x}_a, \mathbf{y}_a) \in \mathcal{D}_i} f(\tilde{\mathbf{w}}_i^{t,0}, \mathbf{x}_a, \mathbf{y}_a), \quad (7)$$

Each UE updates its pruned model as

$$\tilde{\mathbf{w}}_i^{t+1} := \tilde{\mathbf{w}}_i^{t,0} - \eta g(\tilde{\mathbf{w}}_i^{t,0}) \odot \mathbf{m}_i^t. \quad (8)$$

As such, we denote the loss functions of the j^{th} VC, k^{th} sBS, l^{th} mBS and central server as $f_j(\mathbf{w}_j) := \sum_{i=1}^{U_{j,k,l}} \alpha_i f_i(\tilde{\mathbf{w}}_i)$, $f_k(\mathbf{w}_k) := \sum_{j=1}^{V_{k,l}} \alpha_j f_j(\mathbf{w}_j)$, $f_l(\mathbf{w}_l) := \sum_{k=1}^{B_l} \alpha_k f_k(\mathbf{w}_k)$, and $f(\mathbf{w}) := \sum_{l=1}^L \alpha_l f_l(\mathbf{w}_l)$, respectively. Note that for simplicity, we consider identical weights, i.e., $\alpha_i = 1/U_{j,k,l}$, $\alpha_j = 1/V_{k,l}$, $\alpha_k = 1/B_l$ and $\alpha_l = 1/L$, which can be easily adjusted for other weighting strategies. Besides, since aggregation happens at different times and different levels, we need to capture the time indices explicitly. Let each UE perform κ_0 local iterations before sending the updated model to the associated VC. It is worth noting that the winning ticket and the corresponding binary mask are only obtained before these κ_0 local rounds begin. Besides, since training the original model is costly, it is reasonable to consider $\rho \ll \kappa_0$ ⁴. Moreover, although the sBS-mBS and mBS-central server links are wired, communication and computation at these nodes incur additional burdens. As such, we assume that each VC, sBS and mBS perform κ_1 , κ_2 and κ_3 rounds, respectively, before sending the trained model

to the respective upper layers. Denote the indices of the current global round, mBS round, sBS round, VC round and UE's local round by m , t_3 , t_2 , t_1 and t_0 , respectively. Besides, similar to [9], [13], let $t := [\{(m\kappa_3 + t_3)\kappa_2 + t_2\}\kappa_1 + t_1]\kappa_0 + t_0$ denote the index of local update iterations.

If $t \bmod \kappa_0 = 0$, the UE receives the latest available model of its associated VC, i.e.,

$$\tilde{\mathbf{w}}_i^{\bar{t}_0} \leftarrow \tilde{\mathbf{w}}_i^{\bar{t}_0}, \quad (9)$$

where $\bar{t}_0 = [\{(m\kappa_3 + t_3)\kappa_2 + t_2\}\kappa_1 + t_1]\kappa_0$. The UE then computes the pruned model $\tilde{\mathbf{w}}_i^{\bar{t}_0,0}$ and the binary mask $\mathbf{m}_i^{\bar{t}_0}$. It then performs κ_0 local SGD rounds as

$$\tilde{\mathbf{w}}_i^{\bar{t}_0+\kappa_0} = \tilde{\mathbf{w}}_i^{\bar{t}_0,0} - \eta \sum_{t_0=1}^{\kappa_0} g(\tilde{\mathbf{w}}_i^{\bar{t}_0+t_0,0}) \odot \mathbf{m}_i^{\bar{t}_0}. \quad (10)$$

Each VC j performs $t_1 = 0, \dots, \kappa_1 - 1$ local rounds. When $(t_1 + 1) \bmod \kappa_1 = 0$, the VC's model gets updated by the latest available sBS model, i.e.,

$$\tilde{\mathbf{w}}_j^{\bar{t}_1} \leftarrow \tilde{\mathbf{w}}_j^{\bar{t}_1}, \quad (11)$$

where $\bar{t}_1 = \{(m\kappa_3 + t_3)\kappa_2 + t_2\}\kappa_1 \kappa_0$. Besides, between two VC rounds, the local model of the VC is updated as

$$\begin{aligned} \tilde{\mathbf{w}}_j^{\bar{t}_1+(t_1+1)\kappa_0} &= \sum_{i=1}^{U_{j,k,l}} \alpha_i \tilde{\mathbf{w}}_i^{\bar{t}_1+(t_1+1)\kappa_0} = \tilde{\mathbf{w}}_j^{\bar{t}_1+t_1\kappa_0,0} - \\ &\eta \sum_{i=1}^{U_{j,k,l}} [\mathbf{1}_i^{\bar{t}_1+t_1\kappa_0}/p_i^{\bar{t}_1+t_1\kappa_0}] \alpha_i \sum_{t_0=1}^{\kappa_0} g(\tilde{\mathbf{w}}_i^{\bar{t}_1+t_1\kappa_0+t_0,0}) \odot \mathbf{m}_i^{\bar{t}_1+t_1\kappa_0}, \end{aligned} \quad (12)$$

where $\tilde{\mathbf{w}}_j^{\bar{t}_1+t_1\kappa_0,0} := \sum_{i=1}^{U_{j,k,l}} \alpha_i \tilde{\mathbf{w}}_i^{\bar{t}_1+t_1\kappa_0,0}$ and $\mathbf{1}_i^{\bar{t}_1+t_1\kappa_0}$ is a binary indicator function that indicates whether the sBS receives the trained model of i during the VC aggregation round $\bar{t}_1 + (t_1 + 1)\kappa_0$ or not, and is defined as follows:

$$\mathbf{1}_i^{\bar{t}_1+t_1\kappa_0} := \begin{cases} 1, & \text{with probability } p_i^{\bar{t}_1+t_1\kappa_0}, \\ 0, & \text{otherwise,} \end{cases} \quad (13)$$

where $p_i^{\bar{t}_1+t_1\kappa_0}$ is the probability of receiving the trained model over the wireless link and is calculated in the subsequent section (c.f. (42)). Note that since the sBS has to receive the gradient over the wireless link, we use the binary indicator function $\mathbf{1}_i^{\bar{t}_1+t_1\kappa_0}$ in (12) as a common practice [13], [27].

The sBS performs $t_2=0, \dots, \kappa_2-1$ local rounds before updating its model. When $(t_2 + 1) \bmod \kappa_2 = 0$, the sBS updates its local model with the latest available model at its associated mBS, i.e.,

$$\tilde{\mathbf{w}}_k^{\bar{t}_2} \leftarrow \tilde{\mathbf{w}}_k^{\bar{t}_2}, \quad (14)$$

where $\bar{t}_2 = (m\kappa_3 + t_3)\kappa_2 \kappa_1 \kappa_0$. In each sBS round t_2 , the sBS updates its model as

$$\begin{aligned} \tilde{\mathbf{w}}_k^{\bar{t}_2+(t_2+1)\kappa_1\kappa_0} &= \sum_{j=1}^{V_{k,l}} \alpha_j \tilde{\mathbf{w}}_j^{\bar{t}_2+(t_2+1)\kappa_1\kappa_0} = \tilde{\mathbf{w}}_k^{\bar{t}_2+t_2\kappa_1\kappa_0,0} - \\ &\eta \sum_{j=1}^{V_{k,l}} \alpha_j \sum_{t_1=0}^{\kappa_1-1} \sum_{i=1}^{U_{j,k,l}} \alpha_i \frac{\mathbf{1}_i^{\bar{t}_2+t_2\kappa_1\kappa_0}}{p_i^{\bar{t}_2+t_2\kappa_1\kappa_0}} \sum_{t_0=1}^{\kappa_0} g(\tilde{\mathbf{w}}_i^{\bar{t}_2+t_2\kappa_1\kappa_0+t_0,0}) \odot \mathbf{m}_i^{\bar{t}_2+t_2\kappa_1\kappa_0}, \end{aligned} \quad (15)$$

where $\tilde{\mathbf{w}}_k^{\bar{t}_2+t_2\kappa_1\kappa_0,0} := \sum_{j=1}^{V_{k,l}} \alpha_j \tilde{\mathbf{w}}_j^{\bar{t}_2+t_2\kappa_1\kappa_0,0}$ and $\bar{t}_2 = (t_2 \kappa_1 + t_1) \kappa_0$. Similarly, the mBS performs $t_3 = 0, \dots, \kappa_3 - 1$ local rounds before updating its local model with the latest available global model when $(t_3 + 1) \bmod \kappa_3 = 0$, i.e.,

$$\tilde{\mathbf{w}}_l^{m\kappa_3\kappa_2\kappa_1\kappa_0} \leftarrow \tilde{\mathbf{w}}_l^{m\kappa_3\kappa_2\kappa_1\kappa_0}. \quad (16)$$

³The time complexity to sort the d parameters and then prune the d_p smallest ones depends on the sorting technique. Many sorting algorithms have logarithmic time complexity, which can be computed quickly in modern graphical processing units. Following the common practice in literature [22]–[24], the overhead for pruning is ignored in this work. Moreover, the proposed method can be readily extended to incorporate the time overhead for pruning.

⁴In our simulation, we considered $\rho < \kappa_0$ and observed that even $\rho = 1$ with $\kappa_0 \geq 5$ performed well.

Algorithm 1: Pruning-Enabled Hierarchical FL

Input: Total global round M , initial model \mathbf{w}^0

- 1 Synchronize all edge devices with the initial model \mathbf{w}^0
- 2 **for** All global rounds $m = 0$ to $M-1$ **do**
- 3 **for** All mBS rounds $t_3 = 0, 1, \dots, \kappa_3 - 1$ **do**
- 4 **for** All sBS rounds $t_2 = 0, 1, \dots, \kappa_2 - 1$ **do**
- 5 **for** All VC rounds $t_1 = 0, 1, \dots, \kappa_1 - 1$ **do**
- 6 **for** $i \in \mathcal{U}_{j,k,l}$ in parallel **do**
- 7 UE receives the latest available model from the associated VC
- 8 Compute binary mask and get the winning ticket using lottery ticket hypothesis
- 9 **for** All local rounds $t_0 = 1, 2, \dots, \kappa_0$ **do**
- 10 $t \leftarrow \lceil \{(m\kappa_3 + t_3)\kappa_2 + t_2\}\kappa_1 + t_1 \rceil \kappa_0 + t_0$
- 11 UE updates local model using (8)
- 12 **end**
- 13 **end**
- 14 sBS updates VC model using (11) and (12)
- 15 **end**
- 16 sBS update local cell model using (14) and (15)
- 17 **end**
- 18 mBS updates local cell model using (16) and (17)
- 19 **end**
- 20 Central server updates global model using (18)
- 21 **end**

Output: Global ML model \mathbf{w}^{M-1}

Moreover, between two mBS rounds, we can write

$$\mathbf{w}_l^{(m\kappa_3 + (t_3+1))\kappa_2\kappa_1\kappa_0} = \mathbf{w}_l^{(m\kappa_3 + t_3)\kappa_2\kappa_1\kappa_0, 0} - \eta \sum_{k=1}^{B_l} \alpha_k \sum_{t_2=0}^{\kappa_2-1} \sum_{j=1}^{V_{k,l}} \alpha_j \sum_{t_1=0}^{\kappa_1-1} \sum_{i=1}^{U_{j,k,l}} \alpha_i \frac{1}{p_i} \sum_{t_0=1}^{\tilde{t}_3} g(\tilde{\mathbf{w}}_i^{\tilde{t}_3+t_0,0}) \odot \mathbf{m}_i^{\tilde{t}_3}, \quad (17)$$

where $\tilde{\mathbf{w}}_l^{(m\kappa_3 + t_3)\kappa_2\kappa_1\kappa_0, 0} := \sum_{k=1}^{B_l} \alpha_k \tilde{\mathbf{w}}_k^{(m\kappa_3 + t_3)\kappa_2\kappa_1\kappa_0, 0}$ and $\tilde{t}_3 = \lceil ((m\kappa_3 + t_3)\kappa_2 + t_2)\kappa_1 + t_1 \rceil \kappa_0$. Finally, the central server performs global aggregation by collecting the updated models from all mBSs as follows:

$$\mathbf{w}^{(m+1)\Pi_{z=0}^3 \kappa_z} = \tilde{\mathbf{w}}^m \Pi_{z=0}^3 \kappa_z, 0 - \eta \sum_{l=1}^L \alpha_l \sum_{t_3=0}^{\kappa_3-1} \sum_{k=1}^{B_l} \alpha_k \sum_{t_2=0}^{\kappa_2-1} \sum_{j=1}^{V_{k,l}} \alpha_j \sum_{t_1=0}^{\kappa_1-1} \sum_{i=1}^{U_{j,k,l}} \alpha_i \frac{1}{p_i} \sum_{t_0=1}^{\tilde{t}_3} g(\tilde{\mathbf{w}}_i^{\tilde{t}_3+t_0,0}) \odot \mathbf{m}_i^{\tilde{t}_3}, \quad (18)$$

where $\tilde{\mathbf{w}}^m \Pi_{z=0}^3 \kappa_z, 0 := \sum_{l=1}^L \alpha_l \tilde{\mathbf{w}}_l^m \Pi_{z=0}^3 \kappa_z, 0$.

The proposed PHFL process is summarized in Algorithm 1.

III. PHFL: CONVERGENCE ANALYSIS

A. Assumptions

We make the following standard assumptions [7], [13], [20], [23], [28]:

- 1) The loss functions are lower-bounded, i.e., $f(\mathbf{w}) \geq f_{\inf}$.
- 2) The loss functions are β -smooth, i.e., $\|\nabla f_i(\mathbf{w}) - \nabla f_i(\mathbf{w}')\| \leq \beta \|\mathbf{w} - \mathbf{w}'\|$.
- 3) Mini-batch gradients are unbiased $\mathbb{E}_{\tilde{\mathbf{g}} \sim \mathcal{D}_i} [g(\tilde{\mathbf{w}}_i)] = \nabla f_i(\tilde{\mathbf{w}}_i)$. Besides, the variance of the gradients is bounded, i.e., $\|g(\tilde{\mathbf{w}}_i) - \nabla f_i(\tilde{\mathbf{w}}_i)\|^2 \leq \sigma^2$.
- 4) The divergence of the local, VC, sBS, mBS and global loss functions are bounded for all i, j, k, l and \mathbf{w} , i.e.,

$$\begin{aligned} \sum_{i=1}^{U_{j,k,l}} \alpha_i \|\nabla f_i(\mathbf{w}) - \nabla f_j(\mathbf{w})\|^2 &\leq \varepsilon_{\text{vc}}^2, \\ \sum_{j=1}^{V_{k,l}} \alpha_j \|\nabla f_j(\mathbf{w}) - \nabla f_k(\mathbf{w})\|^2 &\leq \varepsilon_{\text{sbs}}^2, \\ \sum_{k=1}^{B_l} \alpha_k \|\nabla f_k(\mathbf{w}) - \nabla f_l(\mathbf{w})\|^2 &\leq \varepsilon_{\text{mbs}}^2, \end{aligned}$$

$$\sum_{l=1}^L \alpha_l \|\nabla f_l(\mathbf{w}) - \nabla f(\mathbf{w})\|^2 \leq \varepsilon^2.$$

- 5) The stochastic gradients are independent of each other in different iterations.
- 6) The stochastic gradients are bounded, i.e., $\mathbb{E} \|g(\mathbf{w}_i)\|^2 \leq G^2$.
- 7) The model weights are bounded, i.e., $\mathbb{E} \|\mathbf{w}_i\|^2 \leq D^2$.
- 8) The pruning ratio $\delta_i^t \in [0, \delta^{\text{th}}]$, in which $0 < \delta^{\text{th}} < 1$ and δ^{th} is the maximum allowable pruning ratio, follows

$$\delta_i^t \geq \|\mathbf{w}_i^t - \tilde{\mathbf{w}}_i^{t,0}\|^2 / \|\mathbf{w}_i^t\|^2. \quad (19)$$

Since the updated global, mBS, sBS and VC models are not available in each local iteration t , similar to standard practice [7], [9], [13], we assume the virtual copies of these models, denoted by $\tilde{\mathbf{w}}^t$, $\tilde{\mathbf{w}}_l^t$, $\tilde{\mathbf{w}}_k^t$ and $\tilde{\mathbf{w}}_j^t$, respectively, are available. Besides, we assume that the bounded divergence assumptions amongst the above loss functions also hold for these virtual models. Moreover, analogous to our previous notations, we express $\tilde{\mathbf{w}}^{t,0} := \sum_{l=1}^L \alpha_l \sum_{k=1}^{B_l} \alpha_k \sum_{j=1}^{V_{k,l}} \alpha_j \sum_{i=1}^{U_{j,k,l}} \alpha_i \tilde{\mathbf{w}}_i^{t,0} = \sum_{u=1}^U \alpha_u \tilde{\mathbf{w}}_u^{t,0}$ and $\tilde{\mathbf{w}}^0 := \tilde{\mathbf{w}}^{0,0}$.

B. Convergence Analysis

Similar to existing literature [7], [9], [13], [20], we consider the average global gradient norm as the indicator of the proposed PHFL algorithm's convergence. As such, in the following, we seek an θ_{PHFL} -suboptimal solution such that $\frac{1}{T} \sum_{t=0}^{T-1} \|\sum_{u=1}^U \alpha_u \nabla f_u(\tilde{\mathbf{w}}^{t,0}) \odot \mathbf{m}_u^t\|^2 \leq \theta_{\text{PHFL}}$ and $\theta_{\text{PHFL}} \geq 0$. Particularly, we start with Theorem 1 that requires bounding the differences amongst the models in different hierarchical levels. These differences are first calculated in Lemma 1 to Lemma 4 and then plugged into Theorem 1 to get the θ_{PHFL} -suboptimal bound in Corollary 1.

Theorem 1. When the assumptions in Section III-A hold and $\eta \leq 1/\beta$, we have

$$\begin{aligned} \theta_{\text{PHFL}} &\leq \underbrace{\mathcal{O}\left(\frac{f(\tilde{\mathbf{w}}^0) - f_{\inf}}{\eta T}\right)}_{\text{wireless factor}} + \underbrace{\mathcal{O}\left(\frac{\beta \eta \sigma^2}{U}\right)}_{\text{pruning error}} + \underbrace{\mathcal{O}(\delta^{\text{th}} \beta^2 D^2)}_{\text{pruning error}} + \\ &\quad \underbrace{\mathcal{O}(\beta \eta G^2 \cdot \varphi_{\mathbf{w},0}(\boldsymbol{\delta}, \mathbf{f}, \mathbf{P}))}_{\text{wireless factor}} + \mathcal{O}(\beta^2 [L_1 + L_2 + L_3 + L_4]), \quad (20) \end{aligned}$$

where $\boldsymbol{\delta} = \{\delta_1^t, \dots, \delta_U^t\}_{t=0}^{T-1}$, $\mathbf{f} = \{f_1^t, \dots, f_U^t\}_{t=0}^{T-1}$, $\mathbf{P} = \{P_1^t, \dots, P_U^t\}_{t=0}^{T-1}$ and f_i^t is the i^{th} client's central processing unit (CPU) frequency in the wireless factor. Besides, the terms L_1 , L_2 , L_3 and L_4 are

$$\varphi_{\mathbf{w},0}(\boldsymbol{\delta}, \mathbf{f}, \mathbf{P}) = \frac{1}{T} \sum_{t=0}^{T-1} \sum_{l=1}^L \alpha_l^2 \sum_{k=1}^{B_l} \alpha_k^2 \sum_{j=1}^{V_{k,l}} \alpha_j^2 \sum_{i=1}^{U_{j,k,l}} \alpha_i^2 \left[\frac{1}{p_i} - 1 \right], \quad (21)$$

$$L_1 = \frac{1}{T} \sum_{t=0}^{T-1} \sum_{l=1}^L \alpha_l \sum_{k=1}^{B_l} \alpha_k \sum_{j=1}^{V_{k,l}} \alpha_j \sum_{i=1}^{U_{j,k,l}} \alpha_i \mathbb{E} \|\tilde{\mathbf{w}}_j^t - \tilde{\mathbf{w}}_i^t\|^2, \quad (22)$$

$$L_2 = [1/T] \sum_{t=0}^{T-1} \sum_{l=1}^L \alpha_l \sum_{k=1}^{B_l} \alpha_k \sum_{j=1}^{V_{k,l}} \alpha_j \mathbb{E} \|\tilde{\mathbf{w}}_k^t - \tilde{\mathbf{w}}_j^t\|^2, \quad (23)$$

$$L_3 = [1/T] \sum_{t=0}^{T-1} \sum_{l=1}^L \alpha_l \sum_{k=1}^{B_l} \alpha_k \mathbb{E} \|\tilde{\mathbf{w}}_l^t - \tilde{\mathbf{w}}_k^t\|^2, \quad (24)$$

$$L_4 = [1/T] \sum_{t=0}^{T-1} \sum_{l=1}^L \alpha_l \mathbb{E} \|\tilde{\mathbf{w}}^t - \tilde{\mathbf{w}}_l^t\|^2. \quad (25)$$

The proof of Theorem 1 and the subsequent Lemmas are left in the supplementary materials.

Remark 1. The first term in (20) is what we get for centralized learning, while the second term arises from the randomness of the mini-batch gradients [29]. The third term appears from model pruning. Besides, the fourth term arises from the wireless links among the sBS and UEs. It is worth noting that $\varphi_{w,0}(\mathbf{f}, \mathbf{P}) = 0$ when all p_i^t 's are 1's. Finally, the last term is due to the difference among the VC-local, sBS-VC, sBS-mBS and mBS-global model parameters, respectively, which are derived in the following.

Remark 2. When the system has no pruning, i.e., all UEs use the original models, all $\delta_i^t = 0$. Besides, under the perfect communication among the sBS and UEs, we have $p_i^t = 1$. In such cases, the θ_{PHFL} -suboptimal bound boils down to

$$\theta_{\text{PHFL}} \leq \mathcal{O}((f(\tilde{\mathbf{w}}^0) - f_{\text{inf}})/[\eta T]) + \mathcal{O}(\beta \eta \sigma^2/U) + \mathcal{O}(\beta^2[L_1 + L_2 + L_3 + L_4]). \quad (26)$$

Besides, the last term in (26) appears from the four hierarchical levels. When $U = 1$ and there are no levels, i.e., $L_1 = L_2 = L_3 = L_4 = 0$, the convergence bound is exactly the same as the original SGD with non-convex loss function [7].

To that end, we calculate the divergence among the local, VC, sBS, mBS and global model parameters, and derive the corresponding pruning errors in each level in what follows.

Lemma 1. When $\eta \leq 1/[2\sqrt{10}\kappa_0\beta]$, the average difference between the VC and local model parameters, i.e., the L_1 term of (20), is upper bounded as

$$\frac{\beta^2}{T} \sum_{t=0}^{T-1} \sum_{l=1}^L \alpha_l \sum_{k=1}^{B_l} \alpha_k \sum_{j=1}^{V_{k,l}} \alpha_j \sum_{i=1}^{U_{j,k,l}} \alpha_i \mathbb{E} \|\tilde{\mathbf{w}}_j^t - \tilde{\mathbf{w}}_i^t\|^2 \leq \mathcal{O}(\kappa_0 \eta^2 \beta^2 \sigma^2) + \mathcal{O}(\kappa_0^2 \eta^2 \beta^2 \varepsilon_{\text{vc}}^2) + \mathcal{O}(\delta^{\text{th}} \beta^2 D^2) + \mathcal{O}(\kappa_0 \eta^2 \beta^2 G^2 \cdot \varphi_{w,L_1}), \quad (27)$$

$$\text{where } \varphi_{w,L_1} = \frac{1}{T} \sum_{l=1}^L \alpha_l \sum_{k=1}^{B_l} \alpha_k \sum_{j=1}^{V_{k,l}} \alpha_j \sum_{i=1}^{U_{j,k,l}} \alpha_i \sum_{t=0}^{T-1} (1/p_i^t - 1).$$

Remark 3. In (27), the first term comes from the statistical data heterogeneity, while the second term arises from the divergence between the local and VC loss functions. The third term emanates from model pruning. Finally, the fourth term stems from the wireless links among the UEs and sBS.

Lemma 2. When $\eta \leq 1/[2\sqrt{10}\kappa_0\kappa_1\beta]$, the difference between the sBS model parameters and VC model parameters, i.e., the L_2 term of (20), is upper bounded as

$$\frac{\beta^2}{T} \sum_{t=0}^{T-1} \sum_{l=1}^L \alpha_l \sum_{k=1}^{B_l} \alpha_k \sum_{j=1}^{V_{k,l}} \alpha_j \mathbb{E} \|\tilde{\mathbf{w}}_k^t - \tilde{\mathbf{w}}_j^t\|^2 \leq \mathcal{O}(\beta^4 \kappa_0^4 \kappa_1^4 \eta^4 \varepsilon_{\text{vc}}^2) + \mathcal{O}(\kappa_0^2 \kappa_1^2 \eta^2 \beta^2 \varepsilon_{\text{sbs}}^2) + \mathcal{O}(\kappa_0 \kappa_1 \eta^2 \sigma^2 \beta^2) + \mathcal{O}(\delta^{\text{th}} \beta^2 D^2) + \mathcal{O}(\kappa_0^3 \kappa_1^3 \beta^4 \eta^4 G^2 \varphi_{w,L_1}) + \mathcal{O}(\kappa_0 \kappa_1 \beta^2 \eta^2 \varphi_{w,L_2}), \quad (28)$$

$$\text{where } \varphi_{w,L_2} = \frac{1}{T} \sum_{t=0}^{T-1} \sum_{l=1}^L \alpha_l \sum_{k=1}^{B_l} \alpha_k \sum_{j=1}^{V_{k,l}} \alpha_j \sum_{i=1}^{U_{j,k,l}} \alpha_i^2 (1/p_i^t - 1).$$

Remark 4. The first term in (28) appears from the divergence of the loss functions of the clients and VC, while the second term stems from the divergence between the loss function of the VC and sBS. The rest of the terms are due to the statistical data heterogeneity, model pruning and wireless links, respectively.

Lemma 3. When $\eta \leq 1/[2\sqrt{14}\kappa_0\kappa_1\kappa_2\beta]$, the average difference between the sBS and mBS model parameters, i.e., the L_3 term of (20), is upper bounded as

$$\begin{aligned} & [\beta^2/T] \sum_{t=0}^{T-1} \sum_{l=1}^L \alpha_l \sum_{k=1}^{B_l} \alpha_k \mathbb{E} \|\tilde{\mathbf{w}}_l^t - \tilde{\mathbf{w}}_k^t\|^2 \\ & \leq \mathcal{O}(\kappa_0^3 \kappa_1^3 \kappa_2^3 \eta^4 \beta^4 \varepsilon_{\text{vc}}^2) + \mathcal{O}(\kappa_0^4 \kappa_1^4 \kappa_2^4 \eta^4 \beta^4 \varepsilon_{\text{sbs}}^2) + \\ & \mathcal{O}(\kappa_0^2 \kappa_1^2 \kappa_2^2 \eta^2 \beta^4 \varepsilon_{\text{mbs}}^2) + \mathcal{O}(\kappa_0 \kappa_1 \kappa_2 \eta^2 \beta^2 \sigma^2) + \\ & \mathcal{O}(\delta^{\text{th}} \beta^2 D^2) + \mathcal{O}(\kappa_0^3 \kappa_1^3 \kappa_2^3 \eta^4 \beta^4 G^2 \cdot \varphi_{w,L_1}) + \\ & \mathcal{O}(\kappa_0^2 \kappa_1^2 \kappa_2^2 \beta^4 \eta^4 \cdot \varphi_{w,L_2}) + \mathcal{O}(\kappa_0 \kappa_1 \kappa_2 \eta^2 \beta^2 G^2 \cdot \varphi_{w,L_3}). \end{aligned} \quad (29)$$

$$\text{where } \varphi_{w,L_3} = \frac{1}{T} \sum_{l=1}^L \alpha_l \sum_{k=1}^{B_l} \alpha_k \sum_{j=1}^{V_{k,l}} \alpha_j^2 \sum_{i=1}^{U_{j,k,l}} \alpha_i^2 \sum_{t=0}^{T-1} (1/p_i^t - 1).$$

Lemma 4. When $\eta \leq 1/[6\sqrt{2}\kappa_0\kappa_1\kappa_2\kappa_3\beta]$, the average difference between the global and the mBS models, i.e., the L_4 term, is bounded as follows:

$$\begin{aligned} & [\beta^2/T] \sum_{t=0}^{T-1} \sum_{l=1}^L \alpha_l \mathbb{E} \|\tilde{\mathbf{w}}^t - \tilde{\mathbf{w}}_l^t\|^2 \leq \mathcal{O}(\kappa_0^4 \kappa_1^4 \kappa_2^4 \kappa_3^4 \eta^4 \beta^4 \varepsilon_{\text{vc}}^2) + \\ & \mathcal{O}(\kappa_0^4 \kappa_1^4 \kappa_2^4 \kappa_3^4 \eta^4 \beta^4 \varepsilon_{\text{sbs}}^2) + \mathcal{O}(\kappa_0^4 \kappa_1^4 \kappa_2^4 \kappa_3^4 \eta^4 \beta^6 \varepsilon_{\text{mbs}}^2) + \\ & \mathcal{O}(\kappa_0^2 \kappa_1^2 \kappa_2^2 \kappa_3^2 \eta^2 \varepsilon^2) + \mathcal{O}(\kappa_0 \kappa_1 \kappa_2 \kappa_3 \beta^2 \eta^2 \sigma^2) + \mathcal{O}(\delta^{\text{th}} \beta^2 D^2) + \\ & \mathcal{O}(\kappa_0^3 \kappa_1^3 \kappa_2^3 \kappa_3^3 \eta^4 \beta^4 G^2 \varphi_{w,L_1}) + \mathcal{O}(\kappa_0^3 \kappa_1^3 \kappa_2^3 \kappa_3^3 \beta^4 \eta^4 \varphi_{w,L_2}) + \\ & \mathcal{O}(\kappa_0^3 \kappa_1^3 \kappa_2^3 \kappa_3^3 \eta^4 \beta^4 G^2 \varphi_{w,L_3}) + \mathcal{O}(\kappa_0 \kappa_1 \kappa_2 \kappa_3 \beta^2 \eta^2 G^2 \varphi_{w,L_4}), \end{aligned} \quad (30)$$

$$\text{where } \varphi_{w,L_4} = \frac{1}{T} \sum_{l=1}^L \alpha_l \sum_{k=1}^{B_l} \alpha_k^2 \sum_{j=1}^{V_{k,l}} \alpha_j^2 \sum_{i=1}^{U_{j,k,l}} \alpha_i^2 \sum_{t=0}^{T-1} (1/p_i^t - 1).$$

Note that we have similar observations for (29) and (30) as in Remark 4. Now, using the above Lemmas, we find the final convergence rate in Corollary 1.

Corollary 1. When $\eta \leq 1/[6\sqrt{2}\kappa_0\kappa_1\kappa_2\kappa_3\beta]$, the θ_{PHFL} bound of Theorem 1 boils down to

$$\begin{aligned} \theta_{\text{PHFL}} & \leq \mathcal{O}([f(\tilde{\mathbf{w}}^0) - f_{\text{inf}}]/[\eta T]) + \mathcal{O}(\beta \eta \sigma^2/U) + \\ & \mathcal{O}(\kappa_0^2 \eta^2 \beta^2 \varepsilon_{\text{vc}}^2) + \mathcal{O}(\kappa_0^2 \kappa_1^2 \eta^2 \beta^2 \varepsilon_{\text{sbs}}^2) + \\ & \mathcal{O}(\kappa_0^2 \kappa_1^2 \kappa_2^2 \eta^2 \beta^4 \varepsilon_{\text{mbs}}^2) + \mathcal{O}(\kappa_0^2 \kappa_1^2 \kappa_2^2 \kappa_3^2 \beta^4 \eta^2 \varepsilon^2) + \\ & \underbrace{\mathcal{O}(\delta^{\text{th}} \beta^2 D^2)}_{\text{pruning error}} + \underbrace{\mathcal{O}(\beta \eta G^2 \cdot \varphi_{w,0}(\mathbf{f}, \mathbf{P}))}_{\text{wireless factor}}. \end{aligned} \quad (31)$$

Remark 5. In (31), the third, fourth, fifth and sixth terms appear from the divergence between client-VC, VC-sBS, sBS-mBS and mBS-global loss functions, respectively.

Remark 6. In typical HFL with no model pruning, i.e., $\delta_u^t = 0$, $\forall u \in \mathcal{U}$, $\mathcal{O}(\delta^{\text{th}} \beta^2 D^2) = 0$. Besides, when the wireless links are ignored, the last term in (31) becomes zero. In such a special case, Corollary 1 boils down to

$$\begin{aligned} \theta_{\text{PHFL}} & \leq \mathcal{O}([f(\tilde{\mathbf{w}}^0) - f_{\text{inf}}]/[\eta T]) + \mathcal{O}(\beta \eta \sigma^2/U) + \\ & \mathcal{O}(\kappa_0^2 \eta^2 \beta^2 \varepsilon_{\text{vc}}^2) + \mathcal{O}(\kappa_0^2 \kappa_1^2 \eta^2 \beta^2 \varepsilon_{\text{sbs}}^2) + \\ & \mathcal{O}(\kappa_0^2 \kappa_1^2 \kappa_2^2 \eta^2 \beta^4 \varepsilon_{\text{mbs}}^2) + \mathcal{O}(\kappa_0^2 \kappa_1^2 \kappa_2^2 \kappa_3^2 \beta^4 \eta^2 \varepsilon^2). \end{aligned} \quad (32)$$

Remark 7. When $\eta = \sqrt{U/T}$, we have $T \geq 1/[72U\kappa_0^2\kappa_1^2\kappa_2^2\kappa_3^2\beta^2]$. With a sufficiently large T , when the trained model reception success probability is 1 for all users in all time steps, we have $\theta_{\text{PHFL}} \approx \mathcal{O}(1/\sqrt{UT}) + \mathcal{O}(\delta^{\text{th}} \beta^2 D^2)$, where the second term comes from the pruning error. Therefore, the proposed PHFL solution converges to the neighborhood of a stationary point of traditional HFL.

IV. JOINT PROBLEM FORMULATION AND SOLUTION

Similar to existing literature [3], [4], [8], [27], we ignore the downlink delay in this paper since the sBS can utilize the higher spectrum and transmission power to broadcast the updated model. Moreover, since the sBS-mBS and mBS-cloud server links are wired, we ignore the transmission delays for these links⁵. Furthermore, since the sBS, mBS and the cloud server usually have high computation power, we also ignore the model aggregation and processing delays⁶. Therefore, at the beginning of each VC round, i.e., $t \div (m \prod_{z=0}^{\kappa_0} + t_0) \bmod \kappa_0 = 0$, we first calculate the required computation time for finding the lottery ticket as

$$t_i^{\text{cpd}} = \rho \times (bnc_i D_i / f_i^t), \quad (33)$$

where b is the batch size, n is the number of batches, c_i is the CPU cycles to process 1-bit data, D_i is UE u_i 's each data sample's size in bits and f_i^t is the CPU frequency. Upon finding the pruned model, each client performs κ_0 local iterations, which require the following computation time [23]

$$t_i^{\text{cps}} = \kappa_0 \times (bn(1 - \delta_i^t) c_i D_i / f_i^t). \quad (34)$$

To that end, the UE only offloads the non-zero weights along with the binary mask to the sBS. As such, we calculate the uplink payload size of UE i as follows⁷:

$$s_i \leq d[1 - \delta_i^t](\text{FPP} + 1) + d, \quad (35)$$

where FPP is the floating point precision. Note that, in (35), we need 1 bit to represent the sign of the entry. Therefore, we calculate the uplink payload offloading delay as follows:

$$t_i^{\text{up}} \leq d[(1 - \delta_i^t)(\text{FPP} + 1) + 1] / r_i^t. \quad (36)$$

As such, UE i 's total duration for local computing and trained model offloading is

$$t_i^{\text{tot}} \leq t_i^{\text{cpd}} + t_i^{\text{cps}} + t_i^{\text{up}}. \quad (37)$$

We now calculate the energy consumption for performing the model training, followed by the required energy for offloading the trained models. First, let us calculate the energy consumption to get the lottery ticket as

$$e_i^{\text{cpd}} = \rho \times 0.5\xi bnc_i D_i (f_i^t)^2, \quad (38)$$

where 0.5ξ is the effective capacitance of UE's CPU chip. Similarly, we calculate the energy consumption to train κ_0 local iterations using the pruned model as

$$e_i^{\text{cps}} = \kappa_0 \times 0.5\xi bn(1 - \delta_i^t) c_i D_i (f_i^t)^2. \quad (39)$$

⁵The transmissions over the wired sBS-mBS and mBS-cloud server links happen in the backhaul, and the corresponding delays are quite small. In order to calculate these delays, one should also consider the overall network loads, which are beyond the scope of this paper.

⁶The addition of d parameters and then taking the average have a time complexity of $\mathcal{O}(d+1)$. With highly capable CPUs at the sBS, mBS, and central server, the corresponding time delays for parameter aggregation are usually small and therefore ignored in the literature [9], [10], [23].

⁷Note that one may send the non-pruned weights and the corresponding indices, which are unknown until the original initial model is trained for ρ iterations. We consider an upper bound for the uplink payload, which will be used during the joint parameters optimization phase.

Moreover, we calculate the uplink payload offloading energy consumption as follows:

$$e_i^{\text{up}} \leq d[(1 - \delta_i^t)(\text{FPP} + 1) + 1] P_i^t / r_i. \quad (40)$$

Therefore, the total energy consumption is calculated as

$$e_i^{\text{tot}} \leq e_i^{\text{cpd}} + e_i^{\text{cps}} + e_i^{\text{up}}. \quad (41)$$

A. Problem Formulation

Denote the duration between VC aggregation t^{th} . Then, we calculate the probability of successful reception of UE's trained model as follows:

$$\begin{aligned} p_i^t &= \Pr\{t_i^{\text{tot}} \leq t^{\text{th}}\} = \Pr\{s_i \leq r_i^t [t^{\text{th}} - t_i^{\text{cpd}} - t_i^{\text{cps}}]\} \\ &= \Pr\{h_{i,k}^t \geq [(2\chi_i^t - 1)(\omega\zeta^2 + I_{i,k}^t) / (P_i^t d_{i,k}^{-\alpha})]\} \\ &\stackrel{(a)}{=} \exp[-(2\chi_i^t - 1)(\omega\zeta^2 + I_{i,k}^t) / (P_i^t d_{i,k}^{-\alpha})], \end{aligned} \quad (42)$$

where $\chi_i^t = \frac{d f_i^t [(1 - \delta_i^t)(\text{FPP} + 1) + 1]}{\omega [f_i^t t^{\text{th}} - bnc_i D_i (\rho + \kappa_0(1 - \delta_i^t))]}$ and (a) follows from the Rayleigh fading channels between the UE and the sBS.

Notice that the pruning ratio δ_i^t , CPU frequency f_i^t , transmission power P_i^t and the probability of successful model reception p_i^t are intertwined. More specifically, p_i^t depends on δ_i^t , f_i^t and P_i^t , given that the other parameters remain fixed. As such, we aim to optimize these parameters jointly by considering the controllable terms in our convergence bound in Corollary 1. Therefore, we focus on each VC round, i.e., the local iteration round t at which $t \bmod \kappa_0 = 0$. Specifically, we focus on minimizing the error terms due to pruning and wireless links, which are given by

$$\mathcal{O}(\delta^{\text{th}} \beta^2 D^2) + \mathcal{O}(\beta \eta G^2 \cdot \phi_{w,0}(\boldsymbol{\delta}, \mathbf{f}, \mathbf{P})). \quad (43)$$

Remark 8. In the above expression, the first term appears from the pruning error $\frac{12\beta^2}{T} \sum_{t=0}^{T-1} \sum_{l=1}^L \alpha_l \sum_{k=1}^{B_l} \alpha_k \sum_{j=1}^{V_{k,l}} \alpha_j \sum_{i=1}^{U_{j,k,l}} \alpha_i (1 + 2\{\alpha_i [1 + \alpha_j (1 + \alpha_k \{1 + \alpha_l\})]\}) \delta_i^t \|\mathbf{w}_i^t\|^2 \leq \mathcal{O}(\delta^{\text{th}} \beta^2 D^2)$, while the second term comes from the wireless factor $\frac{2\beta\eta}{T} \sum_{l=1}^L \alpha_l^2 \sum_{k=1}^{B_l} \alpha_k^2 \sum_{j=1}^{V_{k,l}} \alpha_j^2 \sum_{i=1}^{U_{j,k,l}} \alpha_i^2 \sum_{t=0}^{T-1} (1/p_i^t - 1) \mathbb{E}[\|\tilde{\mathbf{g}}(\tilde{\mathbf{w}}_i^{t,0})\|^2] \leq \mathcal{O}(\frac{\beta\eta G^2}{T} \sum_{l=1}^L \alpha_l^2 \sum_{k=1}^{B_l} \alpha_k^2 \sum_{j=1}^{V_{k,l}} \alpha_j^2 \sum_{i=1}^{U_{j,k,l}} \alpha_i^2 \sum_{t=0}^{T-1} (1/p_i^t - 1))$.

Based on the above observations, we consider a weighted combination of these two terms as our objective function to minimize the bound in (43). Using (42) in the wireless factor, we, therefore, consider the following objective function.

$$\begin{aligned} \phi^t(\boldsymbol{\delta}^t, \mathbf{f}^t, \mathbf{P}^t) &= \phi_1 \sum_{l=1}^L \alpha_l \sum_{k=1}^{B_l} \alpha_k \sum_{j=1}^{V_{k,l}} \alpha_j \sum_{i=1}^{U_{j,k,l}} \alpha_i \delta_i^t + \\ &\phi_2 \sum_{l=1}^L \alpha_l \sum_{k=1}^{B_l} \alpha_k \sum_{j=1}^{V_{k,l}} \alpha_j \sum_{i=1}^{U_{j,k,l}} \alpha_i \left[\exp\left(\frac{(2\chi_i^t - 1)(\omega\zeta^2 + I_{i,k}^t)}{P_i^t d_{i,k}^{-\alpha}}\right) - 1 \right], \end{aligned} \quad (44)$$

where ϕ_1 and ϕ_2 are two weights to strike the balance between the terms. Note that the wireless factor is multiplied by the learning rate and gradient in (43). Typically, the learning rate is small. Besides, the gradient becomes smaller as the training progresses. As such, the wireless factor term is relatively small when $p_i^t > 0$ for all UEs and VC aggregation rounds. The model weights are non-negative. Furthermore, a larger pruning ratio δ_i^t can dramatically reduce the computation and

offloading time, making the wireless factor 0. However, as a higher pruning ratio means more model parameters are pruned, we wish to avoid making the δ_i^t 's large to reduce the pruning-induced errors. The above facts suggest we put more weight on the pruning error term to penalize more for the δ_i^t 's. As such, we consider $\phi_1 \gg \phi_2$. However, in our resource-constrained setting, a small δ_i^t can prolong the training and offloading time, leading p_i^t to be 0, i.e., the sBS will not receive the local trained model. Therefore, although ϕ_2 is small, we keep the wireless factor to ensure p_i^t is never 0.

Therefore, we pose the following optimization problem to configure the parameters jointly.

$$\underset{\delta^t, \mathbf{f}, \mathbf{P}^t}{\text{minimize}} \quad \varphi^t(\delta^t, \mathbf{f}, \mathbf{P}^t), \quad (45)$$

$$\text{s.t. (C1)} \quad t_i^{\text{tot}} \leq t^{\text{th}}, \quad \forall i, \quad (45a)$$

$$\text{(C2)} \quad e_i^{\text{tot}} \leq e_i^{\text{th}}, \quad \forall i, \quad (45b)$$

$$\text{(C3)} \quad 0 \leq f_i^t \leq f_i^{\text{max}}, \quad \forall i, \quad (45c)$$

$$\text{(C4)} \quad 0 \leq P_i^t \leq P_i^{\text{max}}, \quad \forall i, \quad (45d)$$

$$\text{(C5)} \quad 0 \leq \delta_i^t \leq \delta^{\text{th}}, \quad \forall i, \quad (45e)$$

where constraint (C1) ensures that the completion of one VC round is within the required deadline. Constraint (C2) controls the energy expense to be within the allowable budget. Besides, (C3) and (C4) restrict us from choosing the CPU frequency and transmission power within the UE's minimum and maximum CPU cycles and transmission power, respectively. Finally, constraint (C5) ensures the pruning ratio to be within a tolerable limit δ^{th} .

Remark 9. We assume that clients' system configurations remain unchanged over time, while the channel state information (CSI) is dynamic and known at the sBS. The clients share their system configurations with their associated sBS. The sBSs share their respective users' system configurations and CSI with the central server. As such, problem (45) is solved centrally, and the optimized parameters are broadcasted to the clients. Besides, problem (45) is non-convex with the multiplications and divisions of the optimization variables in the second term. Moreover, constraints (C1) and (C2) are not convex. Therefore, it is not desirable to minimize this original problem directly. In the following, we transform the problem into an approximate convex problem that can be solved efficiently.

B. Problem Transformation

Let us define $A(\delta_i^t, f_i, P_i) := \exp[(2\chi_i^t - 1)(\omega\zeta^2 + I_{i,k}^t)/(P_i^t d_{i,k}^{-\alpha})]$. Given an initial feasible point set $(\delta_i^{t,q}, f_i^{t,q}, P_i^{t,q})$, we perform a linear approximation of this non-convex expression as follows:

$$\begin{aligned} A(\delta_i^t, f_i, P_i) &\approx A(\delta_i^{t,q}, f_i^{t,q}, P_i^{t,q}) + \nabla_{\delta_i^t} [A(\delta_i^{t,q}, f_i^{t,q}, P_i^{t,q})] (\delta_i^t - \delta_i^{t,q}) \\ &\quad + \nabla_{f_i^t} [A(\delta_i^{t,q}, f_i^{t,q}, P_i^{t,q})] (f_i^t - f_i^{t,q}) + \\ &\quad \nabla_{P_i^t} [A(\delta_i^{t,q}, f_i^{t,q}, P_i^{t,q})] (P_i^t - P_i^{t,q}) := \tilde{A}(\delta_i^t, f_i^t, P_i^t), \end{aligned} \quad (46)$$

where $A(\delta_i^{t,q}, f_i^{t,q}, P_i^{t,q}) = \exp[(2\chi_i^{t,q} - 1)(\omega\zeta^2 + \tilde{I}_{i,k}^t)/(P_i^{t,q} d_{i,k}^{-\alpha})]$, $\chi_i^{t,q} = \frac{d_{i,k}^{t,q}[(1-\delta_i^t)(\text{FPP}+1)+1]}{\omega[f_i^{t,q} t^{\text{th}} - \text{bnc}_i D_i (\rho + \kappa_0(1-\delta_i^{t,q})]}$ and

Algorithm 2: Iterative Joint Pruning Ratio, CPU Frequency and Transmission Power Selection Process

Input: Initial feasible set $(\delta^{t,0}, \mathbf{f}^{t,0}, \mathbf{P}^{t,0})$, maximum iteration Q , precision level ϵ^{prec} ; set $q = 0$

2 Repeat:

3 Solve (55) using $(\delta^{t,q}, \mathbf{f}^{t,q}, \mathbf{P}^{t,q})$ to get the optimized $(\delta^t, \mathbf{f}, \mathbf{P}^t)$

4 $q \leftarrow q + 1$; $\delta^{t,q} \leftarrow \delta^t$; $\mathbf{f}^{t,q} \leftarrow \mathbf{f}$; $\mathbf{P}^{t,q} \leftarrow \mathbf{P}^t$

5 **Until** converge with ϵ^{prec} precision or $q = Q$

Output: Optimal $(\delta^t, \mathbf{f}, \mathbf{P}^t)$

$\tilde{I}_{i,k}^t = \sum_{l=1}^L \sum_{k'=1, k \neq k'}^K \sum_{j'=1}^{J_{k',l}} \sum_{u_j' \in \mathcal{U}_{j',k',l}} P_{i'}^{t,q} h_{i',k'} d_{i',k'}^{-\alpha}$. Moreover, $\nabla_{\delta_i^t} [A(\delta_i^{t,q}, f_i^{t,q}, P_i^{t,q})]$, $\nabla_{f_i^t} [A(\delta_i^{t,q}, f_i^{t,q}, P_i^{t,q})]$ and $\nabla_{P_i^t} [A(\delta_i^{t,q}, f_i^{t,q}, P_i^{t,q})]$ are calculated in (47), (48) and (49), respectively.

As such, we approximate (44) as follows:

$$\tilde{\varphi}^t(\delta^t, \mathbf{f}, \mathbf{P}^t) = \sum_{l=1}^L \alpha_l \sum_{k=1}^{B_l} \alpha_k \sum_{j=1}^{V_{k,l}} \alpha_j \sum_{i=1}^{U_{j,k,l}} \alpha_i (\phi_1 \delta_i^t + \phi_2 [\tilde{A}(\delta_i^t, f_i^t, P_i^t) - 1]), \quad (52)$$

where $\tilde{A}(\delta_i^t, f_i^t, P_i^t)$ is calculated in (46).

We now focus on the non-convex constraints. First, let us approximate the local pruned model computation time as

$$t_i^{\text{cps}} \approx [\kappa_0 \text{bnc}_i D_i / f_i^{t,q}] (1 - \delta_i^t - (1 - \delta_i^{t,q})(f_i^t - f_i^{t,q}) / f_i^{t,q}) = \tilde{t}_i^{\text{cps}}. \quad (53)$$

Then, we approximate the non-convex uplink model offloading delay as shown in (50). Using a similar treatment, we write

$$\begin{aligned} e_i^{\text{cps}} &\approx \kappa_0 \xi \text{bnc}_i D_i f_i^{t,q} [(\delta_i^{t,q} - 0.5) f_i^{t,q} - 0.5 f_i^{t,q} \delta_i^t + \\ &\quad (1 - \delta_i^{t,q}) f_i^t] := \tilde{e}_i^{\text{cps}}. \end{aligned} \quad (54)$$

Similarly, we approximate the energy consumption for model offloading as shown in (51).

Therefore, we pose the following transformed problem

$$\underset{\delta^t, \mathbf{f}, \mathbf{P}^t}{\text{minimize}} \quad \tilde{\varphi}^t(\delta^t, \mathbf{f}, \mathbf{P}^t), \quad (55)$$

$$\text{s.t. (C1)} \quad \tilde{t}_i^{\text{cpsd}} + \tilde{t}_i^{\text{cps}} + \tilde{t}_i^{\text{up}} \leq t^{\text{th}}, \quad (55a)$$

$$\text{(C2)} \quad \tilde{e}_i^{\text{cpsd}} + \tilde{e}_i^{\text{cps}} + \tilde{e}_i^{\text{up}} \leq e_i^{\text{th}}, \quad (55b)$$

$$(45c), (45d), (45e), \quad (55c)$$

where the constraints are taken for the same reasons as in the original problem. Besides, $\tilde{t}_i^{\text{cpsd}} = 2p \text{bnc}_i D_i / f_i^{t,q} - p \text{bnc}_i D_i f_i^t / (f_i^{t,q})^2$.

Note that problem (55) is now convex and can be solved iteratively using existing solvers such as CVX [30]. The key steps of our iterative solution are summarized in Algorithm 2. Moreover, as (55) has 3U decision variables and 5U constraints, the time complexity of running Algorithm 2 for Q iterations is $\mathcal{O}(Q \times [(3U)^3 \times 5U])$ [31]. While Algorithm 2 yields a suboptimal solution and converges to a local stationary solution set of the original problem (45), SCA-based solutions are well-known for fast convergence [32]. Moreover, our extensive empirical study in the sequel suggests that the proposed PHFL solution with Algorithm 2 delivers nearly identical performance to the upper bounded performance.

$$\nabla_{\delta_i^t} [A(\delta_i^{t,q}, \mathbf{f}_i^{t,q}, \mathbf{P}_i^{t,q})] = \{\ln(2)2^{\chi_i^{t,q}} d\mathbf{f}_i^{t,q} A(\delta_i^{t,q}, \mathbf{f}_i^{t,q}, \mathbf{P}_i^{t,q})(\omega\zeta^2 + \tilde{l}_{i,k})[bnc_i D_i(\rho(\text{FPP} + 1) - \kappa_0) - \mathbf{f}_i^{t,q} t^{\text{th}}(\text{FPP} + 1)]\} / \{\omega \mathbf{P}_i^{t,q} d_{i,k}^{-\alpha} \times [\mathbf{f}_i^{t,q} t^{\text{th}} - bnc_i D_i(\rho + \kappa_0(1 - \delta_i^{t,q}))]^2\}. \quad (47)$$

$$\nabla_{\mathbf{f}_i^t} [A(\delta_i^{t,q}, \mathbf{f}_i^{t,q}, \mathbf{P}_i^{t,q})] = \{-\ln(2)2^{\chi_i^{t,q}} bnc_i dD_i A(\delta_i^{t,q}, \mathbf{f}_i^{t,q}, \mathbf{P}_i^{t,q})(\omega\zeta^2 + \tilde{l}_{i,k})[(1 - \delta_i^{t,q})(\text{FPP} + 1) + 1] \times (\rho + \kappa_0[1 - \delta_i^{t,q}])\} / \{\omega \mathbf{P}_i^{t,q} d_{i,k}^{-\alpha} \times [\mathbf{f}_i^{t,q} t^{\text{th}} - bnc_i D_i(\rho + \kappa_0(1 - \delta_i^{t,q}))]^2\}. \quad (48)$$

$$\nabla_{\mathbf{P}_i^t} [A(\delta_i^{t,q}, \mathbf{f}_i^{t,q}, \mathbf{P}_i^{t,q})] = -A(\delta_i^{t,q}, \mathbf{f}_i^{t,q}, \mathbf{P}_i^{t,q})(2^{\chi_i^{t,q}} - 1)(\omega\zeta^2 + \tilde{l}_{i,k}) / [(\mathbf{P}_i^{t,q})^2 d_{i,k}^{-\alpha}]. \quad (49)$$

$$t_i^{\text{up}} \approx \frac{d(2 + \text{FPP} - (1 + \text{FPP})\delta_i^t)}{\omega \log_2(1 + \mathbf{P}_i^{t,q} h_{i,k} d_{i,k}^{-\alpha} / [\omega\zeta^2 + \tilde{l}_{i,k}])} + \frac{-\ln(2) d h_{i,k} d_{i,k}^{-\alpha} [(1 - \delta_i^{t,q})(\text{FPP} + 1) + 1] \times (\mathbf{P}_i^t - \mathbf{P}_i^{t,q})}{\omega \{\ln(1 + [\mathbf{P}_i^{t,q} h_{i,k} d_{i,k}^{-\alpha}] / [\omega\zeta^2 + \tilde{l}_{i,k}])\}^2 (\omega\zeta^2 + \tilde{l}_{i,k} + \mathbf{P}_i^{t,q} h_{i,k} d_{i,k}^{-\alpha})} := \tilde{t}_i^{\text{up}}. \quad (50)$$

$$e_i^{\text{up}} \approx \{d\mathbf{P}_i^{t,q}[(\text{FPP} + 2) - (\text{FPP} + 1)\delta_i^t] / \{\omega \log_2(1 + \mathbf{P}_i^{t,q} h_{i,k} d_{i,k}^{-\alpha} / (\omega\zeta^2 + \tilde{l}_{i,k}))\} + \frac{d[(1 - \delta_i^{t,q})(\text{FPP} + 1) + 1] \left[\log_2 \left(1 + \frac{\mathbf{P}_i^{t,q} h_{i,k} d_{i,k}^{-\alpha}}{\omega\zeta^2 + \tilde{l}_{i,k}} \right) - \frac{\mathbf{P}_i^{t,q} h_{i,k} d_{i,k}^{-\alpha}}{\ln(2)(\omega\zeta^2 + \tilde{l}_{i,k} + \mathbf{P}_i^{t,q} h_{i,k} d_{i,k}^{-\alpha})} \right]}{\omega \{\log_2(1 + \mathbf{P}_i^{t,q} h_{i,k} d_{i,k}^{-\alpha} / (\omega\zeta^2 + \tilde{l}_{i,k}))\}^2} (\mathbf{P}_i^t - \mathbf{P}_i^{t,q}) = \tilde{e}_i^{\text{up}}. \quad (51)$$

V. SIMULATION RESULTS AND DISCUSSIONS

A. Simulation Setting

For the performance evaluation, we consider $L = 2$, $B = 4$ and $U = 48$. We let each sBS maintain 2 VCs, where each VC has 6 UEs. In other words, we have $U_{j,k,l} = 6, \forall j, k$ and l , $V_{k,l} = 2, \forall k$ and l , and $B_l = 2, \forall l$. We assume $\omega = 1$ megahertz (MHz). We randomly generate maximum transmission power P^{max} , energy budget for each VC aggregation round e^{th} , CPU frequency f^{max} and required CPU cycle to process per-bit data c , respectively, from [23, 30] dBm, [10, 13] Joules, [1.8, 2.8] gigahertz (GHz) and [20, 25] for these two VCs. Therefore, all UEs in a VC have the above randomly generated system configurations⁸. Moreover, as described earlier in Section II, our proposed PHFL has 4 tiers, namely (1) UE-VC, (2) VC-sBS, (3) sBS-mBS, and (4) mBS-central server.

For our ML task, we use image classification with the popular CIFAR-10 and CIFAR-100 datasets [33] for performance evaluation. We use symmetric Dirichlet distribution $\text{Dir}(\bar{\alpha})$ with concentration parameter $\bar{\alpha}$ for the non-IID data distribution as commonly used in literature [4], [27]. Besides, we use 1) convolutional neural network (CNN), 2) residual network (ResNet)-18 [34] and 3) ResNet-34 [34]. The CNN model has the following architecture: Conv2d(3, 128), MaxPool2d, Conv2d(128, 64), MaxPool2d, Linear(256, 256), Linear(256, #Labels), whereas the ResNets have a similar architecture as in the original paper [34]. Moreover, the total number of trainable parameters depends on various configurations, such as the input/output shapes, kernel sizes, strides, etc. In our implementation, the original CNN, ResNet-18 and ResNet-34 models, respectively, have 151,882; 6,992,138 and 12,614,794 trainable parameters on CIFAR-10, and 175,012; 7,038,308 and 12,660,964 trainable parameters on CIFAR-100. Besides, with $\text{FPP} = 32$, we have a wireless payload of about 5.01

megabits (Mbs), 230.7 Mbs and 416.3 Mbs for CIFAR-10, and 5.8 Mbs, 232.3 Mbs and 417.8 Mbs for CIFAR-100 datasets for the respective three original models.

B. Performance Study

First, we investigate the pruning ratios δ_i^t 's in different VCs. When the system configurations remain the same, the pruning ratio depends on the deadline threshold t^{th} . More specifically, a larger deadline allows the client to prune fewer model parameters, given that the energy constraint is satisfied. Intuitively, less pruning leads to a bulky model that takes longer training time. The CNN model is shallower compared to the ResNets. More specifically, the original non-pruned ResNet-18 and ResNet-34 models have about 46 times and 83 times the trainable parameters of the CNN model, respectively, on CIFAR-10. Therefore, the clients require a larger t^{th} to perform their local training and trained model offloading as the trainable parameters increase.

Intuitively, given a fixed t^{th} , the clients need to prune more model parameters for a bulky model in order to meet the deadline and energy constraints. Our simulation results also show that this general intuition holds in determining the δ_i^t 's, as shown in Fig. 2, which show the cumulative distribution function (CDF) of the δ_i^t 's in different VCs. It is worth noting that the pruning ratios δ_i^t 's in each VC aggregation rounds are not deterministic due to the randomness of the wireless channels. We know the optimal variables once we solve the optimization problem in (55), which depends on the realizations of the wireless channels. Then, for a given VC j , we generate the plot by calculating $\frac{\sum_{l=1}^L \sum_{k=1}^{B_l} \sum_{i=1}^{U_{j,k,l}} \mathbf{1}(\delta_i^t \leq \delta)}{\sum_{l=1}^L \sum_{k=1}^{B_l} \sum_{i=1}^{U_{j,k,l}} 1}$,

where $\mathbf{1}(\delta_i^t \leq \delta)$ is an indicator function that takes value 1 if $\delta_i^t \leq \delta$ and 0 otherwise. With the CNN model, about 50% clients have a δ_i^t less than 0.23, 0.43, 0.58 and 0.72 in VC-0 in all cells, for 1.3s, 1s, 0.8s and 0.6s deadline thresholds, respectively, in Fig. 2a. Note that we use $\delta^{\text{th}} = 0.9$, i.e., the clients can prune up to 90% of the neurons. Moreover, we consider $t^{\text{th}} = 4\text{s}$ and $t^{\text{th}} = 6\text{s}$, to make the problem feasible

⁸Our approach can easily be extended where all clients can have random $\mathbf{f}_i^{\text{max}}$'s, e_i^{th} 's and P_i^{max} 's. Our approach is practical since these parameters depend on the clients' manufacturers and their specific models.

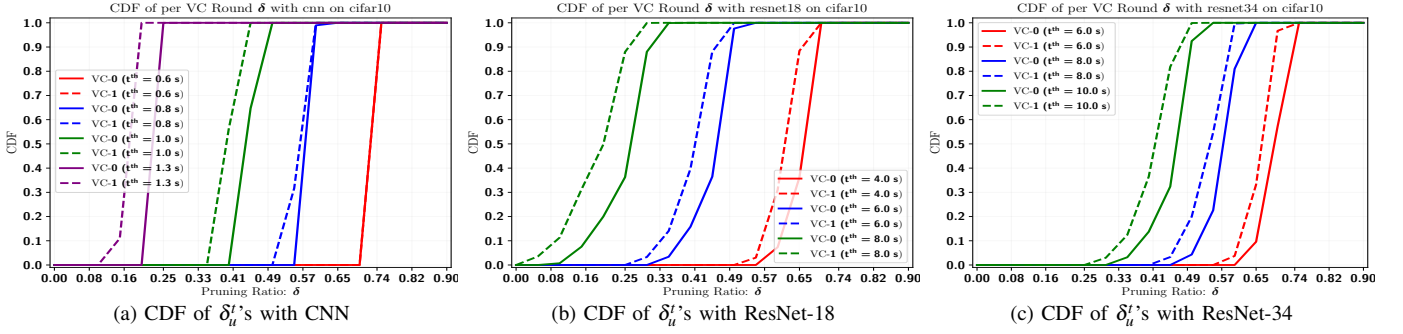


Fig. 2: CDF of clients' pruning ratios in different VCs for different t^{th} with different ML models

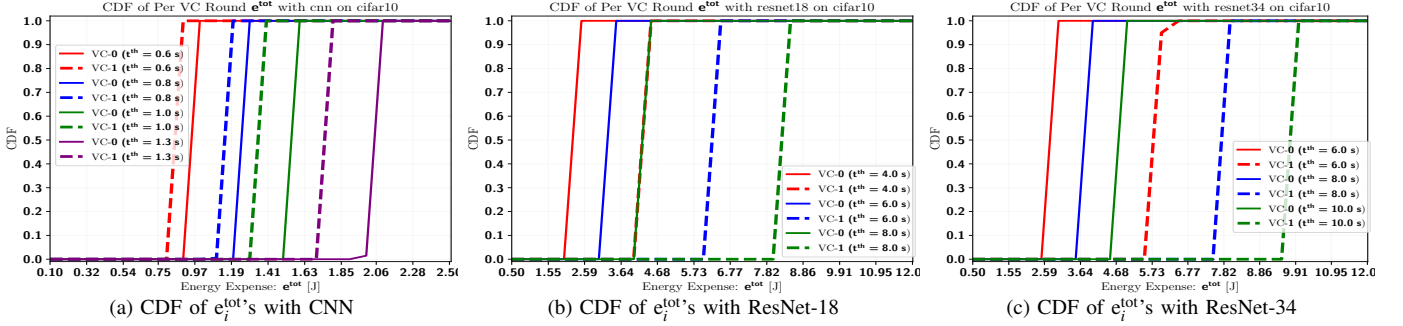


Fig. 3: CDF of clients' e_i^{tot} 's in different VCs for different t^{th} with different ML models

for all clients for the ResNet-18 and ResNet-34 models, respectively. Furthermore, from Fig. 2a - Fig. 2c, it is quite clear that the UEs in VC-1 have to prune slightly lesser model parameters than the UEs in VC-0, even though the maximum CPU frequency f_i^{max} of the UEs in VC-0 is 2.58 GHz, which is about 6.22% higher than the UEs in VC-1. However, due to the wireless payloads in the offloading phase, the transmission powers of the clients can also influence the δ_i^t 's. In our setting, the UEs' maximum transmission powers are 0.35 Watt and 0.95 Watt, respectively, in VC-0 and VC-1. As such, with a similar wireless channel, the UEs in VC-1 can offload much faster than the UEs in VC-0. The above observations, thus, point out that trained model offloading time t_i^{up} dominates the total time to finish one VC round t_i^{tot} .

When it comes to energy expense, from (39) and (40), it is quite obvious that a high δ_i^t shall lead to less energy consumption for both the training and offloading. However, the total energy expense of the clients boils down to the dominating factor between the required energy for computation and trained model offloading due to the interplay between the wireless and the learning parameters. Particularly, with $\omega = 1$ MHz, the clients can offload the CNN model fast, leading the computational energy consumption to be the dominating factor. The ResNets, on the other hand, have huge wireless overheads, leading the offloading time and energy be the dominating factors. This is also observed in our results in Fig. 3, which is the CDF plot of the energy expense e_i^{tot} , calculated in (41), of the clients in each VC and is generated following a similar strategy as in Fig. 2. When the CNN model is used, the total energy cost of the clients in VC-0 is larger, even though they prune more parameters, compared to the clients in VC-1 since larger f_i^{max} 's of the clients in VC-0 leads to a higher

computational energy cost. This, however, changes for the ResNets since the wireless communication burden dominates the computation burden. The clients in VC-1 can use their higher P_i^{max} 's for the offloading time reduction when they determine the pruning ratios δ_i^t 's. As such, the total energy expenses of the clients in VC-1 are much larger than the ones in VC-0. Our simulation results in Fig. 3a and Figs. 3b-3c also reveal the same trends.

Now, we observe the impact of δ_i^t 's on the test accuracies and required bandwidth for trained model offloading. Intuitively, if the model is shallow, pruning further makes it shallower. Therefore, the test performance can exacerbate if δ_i^t 's increases for a shallow model. On the other hand, for a bulky model, pruning may have a less severe effect. Specifically, under the deadline and energy constraints, pruning may eventually help because pruning a few neurons leads to a shallower but still reasonably well-constructed model that can be trained more efficiently. Moreover, our convergence bound in (31) clearly shows that the increasing δ_i^t 's decreases the convergence speed. However, the wireless payload is directly related to δ_i^t 's as shown in (35). Particularly, the wireless payload is an increasing function of the δ_i^t 's. As such, increasing the deadline threshold t^{th} should decrease the δ_i^t 's but significantly increase the wireless payload size.

Our simulation results also reveal the above trends in Fig. 4. Note that, in Fig. 4 and the subsequent figures, the (solid/dashed) lines are the average of 4 independent simulation trials using the configurations mentioned in Section V-A, while the shaded strips show the corresponding standard deviations. Particularly, we observe that the CNN model is largely affected by a small t^{th} because that leads to a large δ_i^t , which eventually prunes more neurons of the already shallow

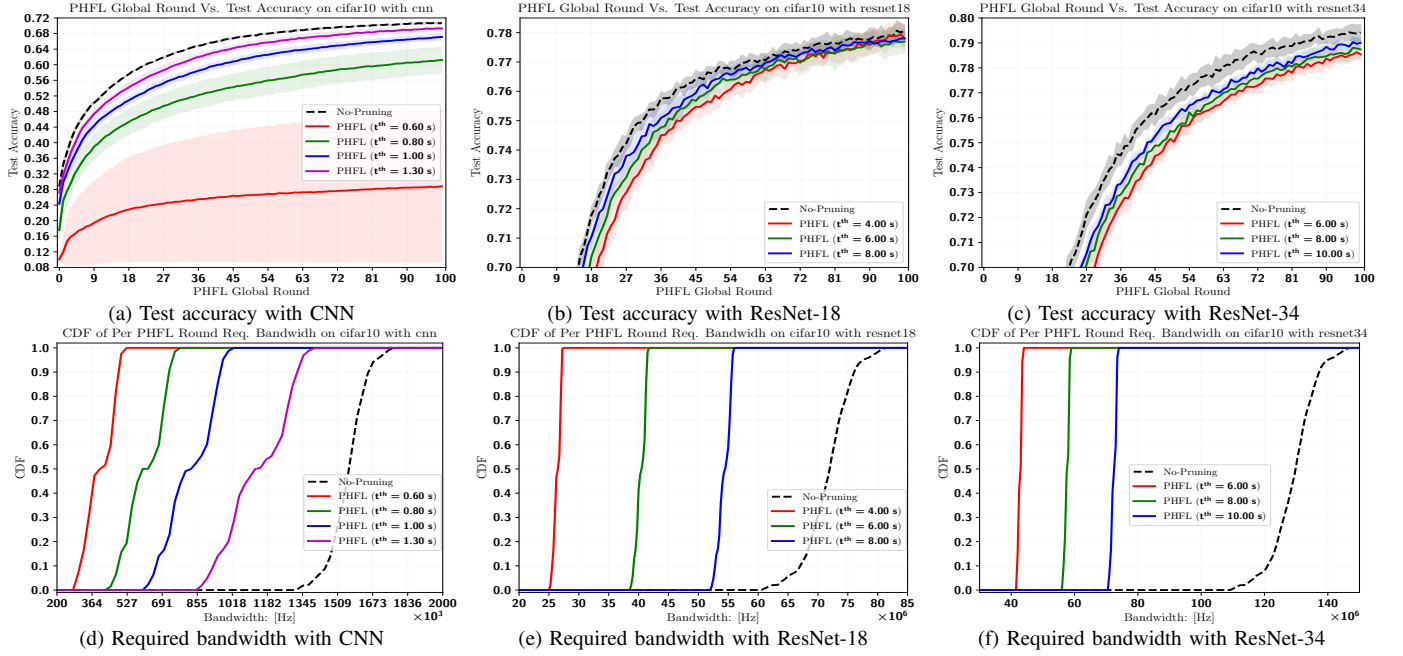


Fig. 4: Trade-offs between test accuracies and required bandwidth for different t^{th} 's with different ML models

model. On the other hand, the bulky ResNets exhibit small performance degradation when t^{th} decreases. Moreover, compared to the original non-pruned counterparts, the performance difference is small if t^{th} is selected appropriately, as shown in Fig. 4a to Fig. 4c. However, even a slight increase in d_p shall reduce the wireless payload size, which can significantly save a large portion of the bandwidth, as observed in Fig. 4d to Fig. 4f. For example, if the CNN model is used, with $t^{\text{th}} = 1.3\text{s}$, the performance degradation on test accuracy is about 1.92% after 100 PHFL round, while the per PHFL round bandwidth saving for at least 70% of the clients is about 20.84%. Similarly, if $t^{\text{th}} = 6\text{s}$, the test accuracy degradation is about 0.47% and 1.11% after 100 global rounds, while the per PHFL round bandwidth saving for at least 70% of the clients are about 33.12% and 81.26%, for ResNet-18 and ResNet-34, respectively.

C. Baseline Comparisons

We now focus on performance comparisons. First, we consider the existing HFL [9], [10] algorithm that does not consider model pruning or any energy constraints. Besides, [9], [10] only considered two levels, UE-BS and BS-cloud/server. For a fair comparison, we adapt HFL into three levels 1) UE-sBS, 2) sBS-mBS and 3) mBS-cloud/server. Furthermore, we enforce the energy and deadline constraints in each UE-sBS aggregation round and name this baseline HFL with constraints (HFL-WC). Moreover, since [9], [10] did not have any VC and we have κ_1 VC aggregation rounds before the sBS aggregation round, we have adapted the deadline accordingly for HFL-WC to make our comparison fair. Furthermore, we consider a random PHFL (R-PHFL) scheme, which has the same system model as ours and allows model pruning. In R-PHFL, the pruning ratios, δ_i^t 's, are randomly selected between 0 and δ^{th} to satisfy constraint (45e). Moreover, in both HFL-

WC and R-PHFL, a common κ_0 that satisfies both deadline and energy constraints for all clients in all VCs leads to poor test accuracy. As such, we determine the local iterations of the UEs within a VC by selecting the maximum possible number of iterations that all clients within that VC can perform without violating the delay and energy constraints. For our proposed PHFL, we choose $\kappa_0 = 5$ and $\kappa_1 = 2$. Moreover, we let $\kappa_2 = \kappa_3 = 2$ for both HFL-WC and PHFL. We also consider centralized SGD to show the performance gap of PHFL with the ideal case where all training data samples are available centrally.

From our above discussion, it is expected that pruning will likely not have the edge over the HFL-WC with a shallow model. Moreover, one may not need pruning for a shallow model in the first place. However, for a bulky model, due to a large number of training parameters and a huge wireless payload, pruning can be a necessity under extreme resource constraints. Furthermore, it is crucial to jointly optimize δ_i^t 's, f_i^t 's and P_i^t 's in order to increase the test accuracy. The simulation results in Fig. 5 also validate these claims. We observe that when the t^{th} increases, HFL-WC's performance improves with the CNN model. Moreover, when HFL-WC has κ_1 times the deadline of PHFL, the performance is comparable, as shown in Fig. 5a and Fig. 5d. More specifically, the maximum performance degradation of the proposed PHFL algorithm is about 1.88% on CIFAR-10 when HFL-WC has 2.31 times the deadline of PHFL. However, for the ResNets model, HFL-WC requires a significantly longer deadline threshold to make the problem feasible. Particularly, with ResNet-18, $t^{\text{th}} \leq 6\text{s}$ does not allow the UEs to perform even a single local iteration, leading to the same initial model weights and, thus, the same test accuracy in HFL-WC. Moreover, when the deadline threshold is κ_1 times the t^{th} of the PHFL, HFL-WC's test accuracy significantly lags, as shown in Fig. 5b and Fig.

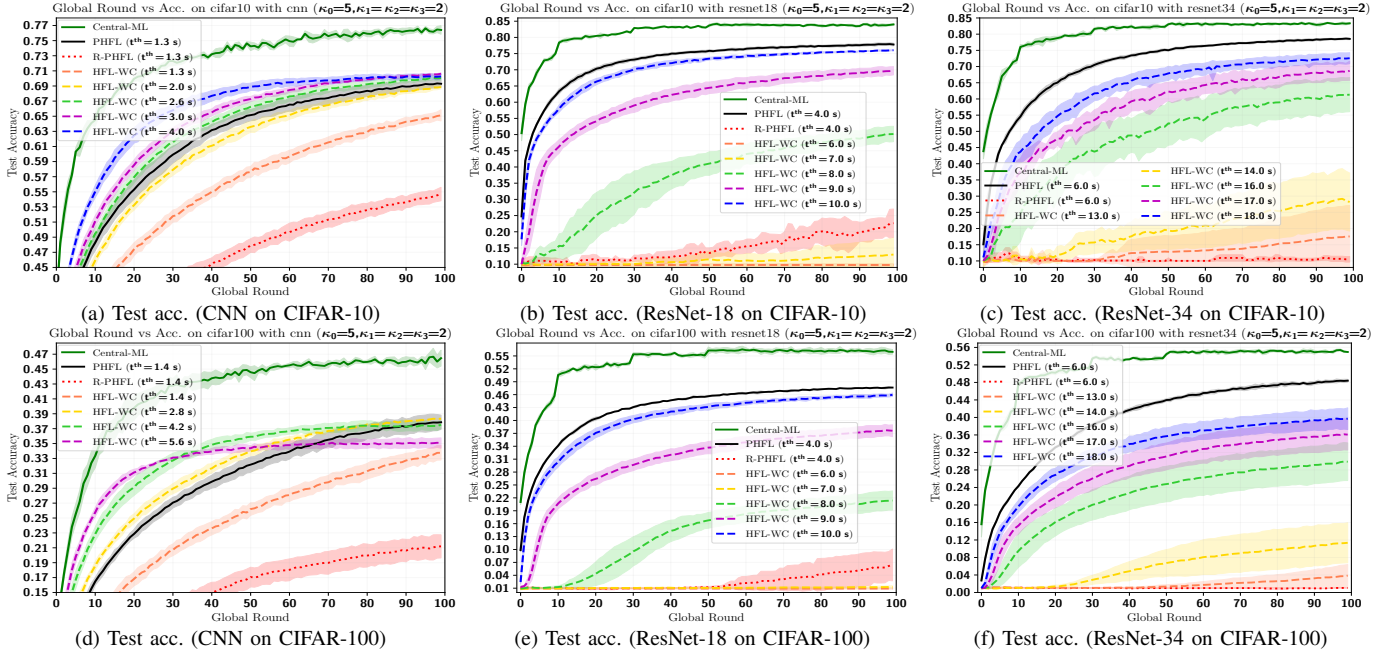


Fig. 5: Test accuracies for different t^{th} 's with different ML models on different datasets

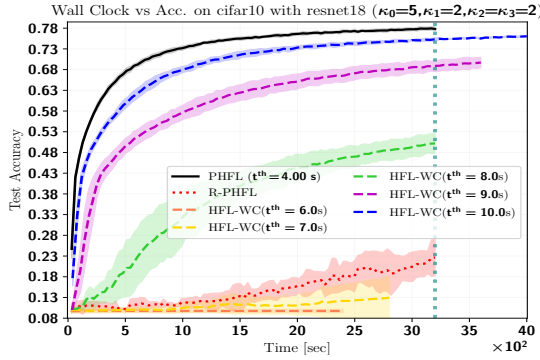


Fig. 6: Wall clock vs test accuracy on CIFAR-10 with ResNet-18

5e. Particularly, after $T = 100$ rounds, our proposed solution with $t^{\text{th}} = 4\text{s}$ provides about 55.06%, 11.62% and 2.33%, and about 122.8%, 26.7% and 3.62% better test accuracy on CIFAR-10 and on CIFAR-100, respectively, than the HFL-WC with $t^{\text{th}} = 8\text{s}$, $t^{\text{th}} = 9\text{s}$ and $t^{\text{th}} = 10\text{s}$. For the ResNet-34 model, the clients require $t^{\text{th}} \geq 13\text{s}$ for performing some local training in HFL-WC, whereas our proposed solution can achieve significantly better performance with only $t^{\text{th}} = 6\text{s}$. For example, our proposed solution with $t^{\text{th}} = 6\text{s}$ yields about 28.09%, 14.34% and 8.22%, and about 61.97%, 34.19% and 21.86% better test accuracy than the HFL-WC with $t^{\text{th}} = 16\text{s}$, $t^{\text{th}} = 17\text{s}$ and $t^{\text{th}} = 18\text{s}$ on CIFAR-10 and CIFAR-100, respectively. Moreover, our proposed solution provides about 243.47% and 643.29% and about 648.36% and 4542.45% better test accuracy than R-PHFL on CIFAR-10 and CIFAR-100 with the ResNet-18 and ResNet-34 models, respectively. The gap with the ideal centralized ML is also expected since FL suffers from data and system heterogeneity.

We also examine the performance of the proposed method in terms of wall clock time. Since HFL-WC does not have

the VC tier, the wall clock time to run M global rounds for HFL-WC with a deadline smaller than $\kappa_1 \times t^{\text{th}}$ will be lower than the proposed PHFL's wall clock time to run the same number of global rounds. However, that does not necessarily guarantee a higher test accuracy than our PHFL since training and offloading the original bulky model may take a long time, allowing only a few local SGD rounds of the clients. Besides, any deadline greater than $\kappa_1 \times t^{\text{th}}$ for the HFL-WC will require a longer wall clock time than our proposed PHFL solution. Our simulation results in Fig. 6 clearly shows these trends. We observe that when HFL-WC has a deadline $\kappa_1 \times t^{\text{th}}$, i.e., $2 \times 4\text{s} = 8\text{s}$, the test accuracies are about 42.52% and 76.24%, respectively, for HFL-WC and PHFL when the wall clock reaches 1800 seconds. Even with $t^{\text{th}} > 4\kappa_1$ seconds, the HFL-WC algorithm performs worse than our proposed PHFL solution.

From the above results and discussion, it is quite clear that R-PHFL yields poor test accuracy due to the random selection of δ_i^t 's. Besides, HFL-WC cannot deliver reasonable performance when the model has a large number of training parameters. Furthermore, our proposed PHFL's performance is comparable to the non-pruned HFL-WC performance with the shallow model. As such, in the following, we only consider the upper bound (UB) of the HFL baseline, which does not consider the constraints. Moreover, to show how pruning degrades test accuracy, we also consider the UB, called HFL-VC-UB, by inheriting the same system model described in Section II, but without the model pruning and the constraints. In other words, we inherit the same underlying four levels, UE-VC, VC-sBS, sBS-mBS and mBS-cloud/server aggregation policy with the original non-pruned model.

First, we illustrate the required computation time and the corresponding energy expenses for the baselines and our proposed PHFL solution with different deadline thresholds.

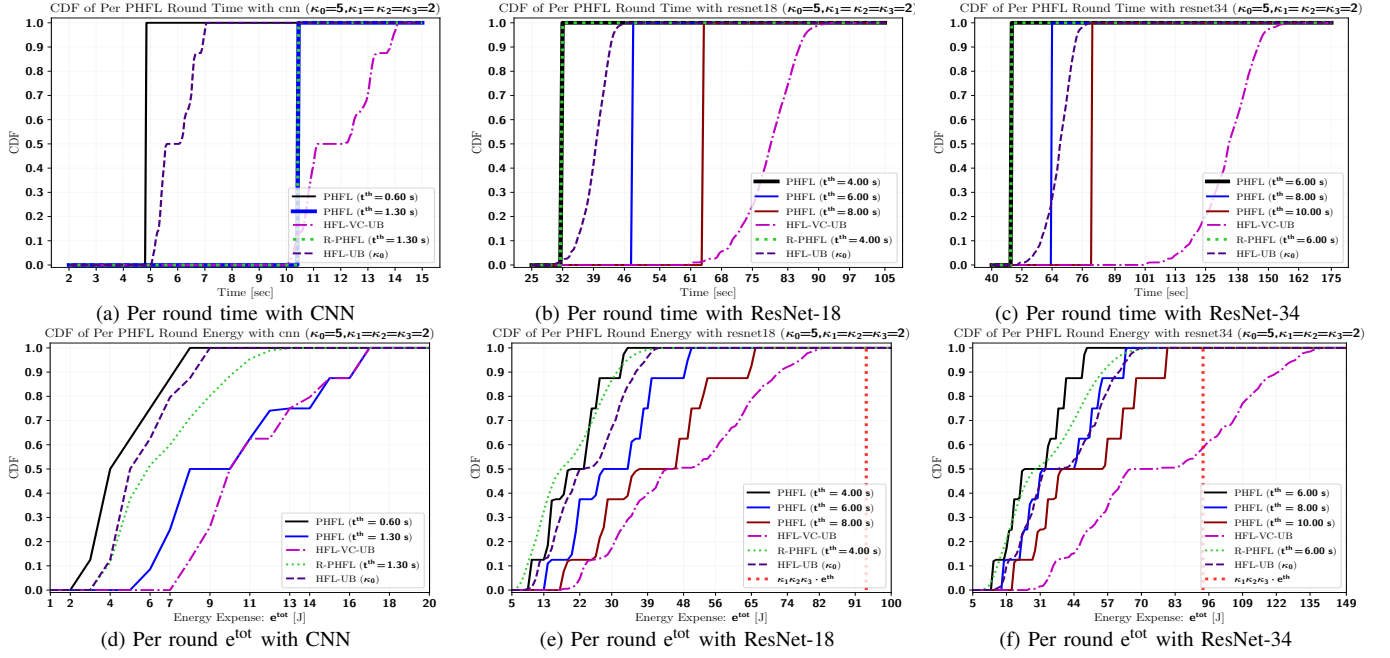


Fig. 7: CDF of per PHFL round time and energy consumption with different ML models on CIFAR-10

TABLE II: Test Accuracy with Trained \mathbf{w}^T on CIFAR-10 dataset with $\kappa_0 = 5, \kappa_1 = \kappa_2 = \kappa_3 = 2$ and $T = 100$

Methods	Dir($\hat{\alpha}$)	With CNN Model			With ResNet-18 Model			With ResNet-34 Model		
		Acc	Req T [s]	Req E [J]	Acc	Req T [s]	Req E [J]	Acc	Req T [s]	Req E [J]
PHFL (Ours)	0.5	0.6791 \pm 0.0049	1040	48355 \pm 14664	0.7613 \pm 0.0026	3200	98122 \pm 15878	0.7677 \pm 0.0017	4800	140469 \pm 20993
	0.9	0.6930 \pm 0.0049		48355 \pm 14663	0.7780 \pm 0.0043		98122 \pm 15878	0.7854 \pm 0.0026		140469 \pm 20993
	10	0.7091 \pm 0.0022		48355 \pm 14663	0.7899 \pm 0.0020		98122 \pm 15878	0.7994 \pm 0.0010		140469 \pm 20994
HFL-VC (UB) (Ours)	0.5	0.6971 \pm 0.0037	1293 \pm 110	53041 \pm 12377	0.7689 \pm 0.0054	8985 \pm 182	231634 \pm 32761	0.7789 \pm 0.0030	15370 \pm 269	378436 \pm 51167
	0.9	0.7066 \pm 0.0017	1293 \pm 110	53041 \pm 12377	0.7807 \pm 0.0019	8985 \pm 182	231634 \pm 32761	0.7942 \pm 0.0033	15370 \pm 269	378436 \pm 51167
	10	0.7211 \pm 0.0010	1293 \pm 110	53041 \pm 12377	0.7920 \pm 0.0037	8985 \pm 182	231634 \pm 32761	0.8031 \pm 0.0027	15370 \pm 269	378436 \pm 51167
R-PHFL (Ours)	0.5	0.5346 \pm 0.0074	1040	31483 \pm 9454	0.2447 \pm 0.0161	3200	92529 \pm 12400	0.1112 \pm 0.0193	4800	158622 \pm 20589
	0.9	0.5471 \pm 0.0089		31467 \pm 9427	0.2265 \pm 0.0439		92495 \pm 12356	0.1049 \pm 0.0086		158827 \pm 20834
	10	0.5847 \pm 0.0164		31455 \pm 9406	0.3265 \pm 0.0273		92441 \pm 12287	0.1096 \pm 0.0108		158651 \pm 20624
HFL (UB) - κ_0	0.5	0.6624 \pm 0.0021	646 \pm 55	26520 \pm 6188	0.7539 \pm 0.0044	4493 \pm 90	115810 \pm 16379	0.7445 \pm 0.0049	7686 \pm 132	189207 \pm 25580
	0.9	0.6752 \pm 0.0018	646 \pm 55	26520 \pm 6188	0.7695 \pm 0.0014	4493 \pm 90	115810 \pm 16379	0.7664 \pm 0.0045	7686 \pm 132	189207 \pm 25580
	10	0.6934 \pm 0.0012	646 \pm 55	26520 \pm 6188	0.7833 \pm 0.0032	4493 \pm 90	115810 \pm 16379	0.7844 \pm 0.0013	7686 \pm 132	189207 \pm 25580

TABLE III: Test Accuracy with Trained \mathbf{w}^T on CIFAR-10 dataset with $\kappa_0 = 10, \kappa_1 = \kappa_2 = \kappa_3 = 2$ and $T = 100$

Methods	Dir($\hat{\alpha}$)	With CNN Model			With ResNet-18 Model			With ResNet-34 Model		
		Acc	Req T [s]	Req E [J]	Acc	Req T [s]	Req E [J]	Acc	Req T [s]	Req E [J]
PHFL (Ours)	0.5	0.6859 \pm 0.0037	1600	76084 \pm 23665	0.7668 \pm 0.0016	3200	103997 \pm 18692	0.7774 \pm 0.0016	4800	146238 \pm 23406
	0.9	0.6966 \pm 0.0034		76084 \pm 23665	0.7804 \pm 0.0014		103998 \pm 18693	0.7948 \pm 0.0023		146239 \pm 23408
	10	0.7093 \pm 0.0024		76083 \pm 23664	0.7935 \pm 0.0015		103999 \pm 18695	0.8092 \pm 0.0019		146238 \pm 23407
HFL-VC (UB) (Ours)	0.5	0.6932 \pm 0.0021	2417 \pm 221	102117 \pm 24405	0.7704 \pm 0.0042	10052 \pm 267	280710 \pm 43428	0.7825 \pm 0.0033	16416 \pm 346	427512 \pm 61116
	0.9	0.7070 \pm 0.0024	2417 \pm 221	102117 \pm 24405	0.7866 \pm 0.0016	10052 \pm 267	280710 \pm 43428	0.7975 \pm 0.0025	16416 \pm 346	427512 \pm 61116
	10	0.7164 \pm 0.0042	2417 \pm 221	102117 \pm 24405	0.7936 \pm 0.0009	10052 \pm 267	280710 \pm 43428	0.8102 \pm 0.0018	16416 \pm 346	427512 \pm 61116
HFL (UB) - κ_0	0.5	0.6934 \pm 0.0030	1208 \pm 110	51058 \pm 12202	0.7634 \pm 0.0017	5026 \pm 132	140349 \pm 21712	0.7726 \pm 0.0014	8209 \pm 171	213745 \pm 30554
	0.9	0.7033 \pm 0.0031	1208 \pm 110	51058 \pm 12202	0.7769 \pm 0.0060	5026 \pm 132	140349 \pm 21712	0.7847 \pm 0.0014	8209 \pm 171	213745 \pm 30554
	10	0.7208 \pm 0.0018	1208 \pm 110	51058 \pm 12202	0.7895 \pm 0.0023	5026 \pm 132	140349 \pm 21712	0.8004 \pm 0.0016	8209 \pm 171	213745 \pm 30554

Naturally, if we increase the t^{th} for each VC aggregation round, our proposed solution will take longer time and energy to perform $T = 100$ global rounds. Moreover, since there are κ_1 VC aggregation rounds in our proposed system model, the original model training and offloading with HFL-VC-UB is expected to take significantly longer and consume more energy than the HFL-UB baseline. Therefore, the effectiveness, in terms of time and energy consumption, of PHFL is largely dependent upon the deadline threshold t^{th} . While R-PHFL requires the same time as our proposed PHFL, the energy requirements for R-PHFL can vary significantly due to the random selection of the δ_i^t 's that lead to different model sizes and different local training episodes in different VCs.

Our results in Figs. 7a-7c and Figs. 7d-7f clearly show these trade-offs with time and energy consumption, respectively, for the three models. It is worth pointing out that we adopted the popular lottery ticket hypothesis [26] for finding the winning ticket that requires performing p iterations on the initial model with full parameter space as described in Section II-B. This incurs additional t_i^{cpd} time and e_i^{cpd} energy overheads, as calculated in (33) and (38), respectively. As such, when the t^{th} is large, if the UEs have sufficient energy budgets, they can prune only a few neurons. Therefore, the total time and energy consumption for the original model computation for getting the winning ticket, training the pruned model and offloading the trained pruned model parameters can become slightly larger

TABLE IV: Test Accuracy with Trained \mathbf{w}^T on CIFAR-10 dataset with $\kappa_0 = 5, \kappa_1 = 4, \kappa_2 = \kappa_3 = 2$ and $T = 100$

Methods	Dir(α)	With CNN Model			With ResNet-18 Model			With ResNet-34 Model		
		Acc	Req T [s]	Req E [J]	Acc	Req T [s]	Req E [J]	Acc	Req T [s]	Req E [J]
PHFL (Ours)	0.5	0.6950 \pm 0.0047	2080	96710 \pm 29327	0.7699 \pm 0.0016	6400	196244 \pm 31755	0.7826 \pm 0.0023	9600	280939 \pm 41988
	0.9	0.7060 \pm 0.0026		96710 \pm 29327	0.7828 \pm 0.0018		196245 \pm 31757	0.8010 \pm 0.0033		280938 \pm 41986
	10	0.7136 \pm 0.0043		96710 \pm 29327	0.7945 \pm 0.0014		196244 \pm 31756	0.8111 \pm 0.0014		280938 \pm 41987
HFL-VC (UB) (Ours)	0.5	0.7052 \pm 0.0038	2587 \pm 220	106082 \pm 24755	0.7726 \pm 0.0057	17969 \pm 364	463257 \pm 65516	0.7881 \pm 0.0028	30737 \pm 534	756853 \pm 102321
	0.9	0.7122 \pm 0.0016	2587 \pm 220	106082 \pm 24755	0.7874 \pm 0.0015	17969 \pm 364	463257 \pm 65516	0.8012 \pm 0.0009	30737 \pm 534	756853 \pm 102321
	10	0.7195 \pm 0.0015	2587 \pm 220	106082 \pm 24755	0.7961 \pm 0.0028	17969 \pm 364	463257 \pm 65516	0.8117 \pm 0.0031	30737 \pm 534	756853 \pm 102321
R-PHFL	0.5	0.5813 \pm 0.0146	2080	62927 \pm 18914	0.3863 \pm 0.0408	6400	184493 \pm 24419	0.1042 \pm 0.0069	9600	316985 \pm 41406
	0.9	0.6013 \pm 0.0164		62933 \pm 18924	0.4010 \pm 0.0208		184766 \pm 24766	0.1157 \pm 0.0137		316870 \pm 41267
	10	0.6360 \pm 0.0082		62849 \pm 18781	0.4648 \pm 0.0352		184617 \pm 24577	0.1111 \pm 0.0078		317122 \pm 41570

TABLE V: Test Accuracy with Trained \mathbf{w}^T on CIFAR-100 dataset with $\kappa_0 = 5, \kappa_1 = \kappa_2 = \kappa_3 = 2$ and $T = 100$

Methods	Dir(α)	With CNN Model			With ResNet-18 Model			With ResNet-34 Model		
		Acc	Req T [s]	Req E [J]	Acc	Req T [s]	Req E [J]	Acc	Req T [s]	Req E [J]
PHFL (Ours)	0.5	0.3723 \pm 0.0101	1120	51667 \pm 15530	0.4725 \pm 0.0032	3200	98074 \pm 15856	0.4770 \pm 0.0032	4800	140445 \pm 20984
	0.9	0.3786 \pm 0.0096		51667 \pm 15531	0.4765 \pm 0.0003		98075 \pm 15857	0.4840 \pm 0.0032		140444 \pm 20983
	10	0.3795 \pm 0.0084		51667 \pm 15531	0.4811 \pm 0.0024		98075 \pm 15857	0.4834 \pm 0.0023		140444 \pm 20984
HFL-VC (UB) (Ours)	0.5	0.3962 \pm 0.0030	1319 \pm 109	53645 \pm 12431	0.4805 \pm 0.0022	9038 \pm 183	232839 \pm 32910	0.4909 \pm 0.0017	15422 \pm 270	379641 \pm 51319
	0.9	0.3956 \pm 0.0030	1319 \pm 109	53645 \pm 12431	0.4832 \pm 0.0034	9038 \pm 183	232839 \pm 32910	0.4922 \pm 0.0019	15422 \pm 270	379641 \pm 51319
	10	0.4004 \pm 0.0042	1319 \pm 109	53645 \pm 12431	0.4800 \pm 0.0019	9038 \pm 183	232839 \pm 32910	0.4895 \pm 0.0024	15422 \pm 270	379641 \pm 51319
R-PHFL	0.5	0.1994 \pm 0.0075	1120	33751 \pm 10069	0.0587 \pm 0.0212	3200	92996 \pm 12374	0.0123 \pm 0.0028	4800	159083 \pm 20562
	0.9	0.2119 \pm 0.0156		33763 \pm 10089	0.0641 \pm 0.0371		92893 \pm 12245	0.0104 \pm 0.0007		159122 \pm 20608
	10	0.2165 \pm 0.0057		33733 \pm 10040	0.0728 \pm 0.0427		92893 \pm 12245	0.0109 \pm 0.0011		159175 \pm 20671
HFL (UB) - κ_0	0.5	0.3509 \pm 0.0023	659 \pm 54	26822 \pm 6215	0.4730 \pm 0.0025	4519 \pm 90	116413 \pm 16453	0.4663 \pm 0.0018	7712 \pm 133	189809 \pm 25656
	0.9	0.3524 \pm 0.0029	659 \pm 54	26822 \pm 6215	0.4768 \pm 0.0047	4519 \pm 90	116413 \pm 16453	0.4756 \pm 0.0021	7712 \pm 133	189809 \pm 25656
	10	0.3590 \pm 0.0019	659 \pm 54	26822 \pm 6215	0.4841 \pm 0.0057	4519 \pm 90	116413 \pm 16453	0.4776 \pm 0.0035	7712 \pm 133	189809 \pm 25656

TABLE VI: Test Accuracy with Trained \mathbf{w}^T on CIFAR-100 dataset with $\kappa_0 = 10, \kappa_1 = \kappa_2 = \kappa_3 = 2$ and $T = 100$

Methods	Dir(α)	With CNN Model			With ResNet-18 Model			With ResNet-34 Model		
		Acc	Req T [s]	Req E [J]	Acc	Req T [s]	Req E [J]	Acc	Req T [s]	Req E [J]
PHFL (Ours)	0.5	0.3700 \pm 0.0035	2000	94632 \pm 29277	0.4654 \pm 0.0035	3200	103923 \pm 18656	0.4801 \pm 0.0009	4800	146195 \pm 23388
	0.9	0.3648 \pm 0.0044		94632 \pm 29277	0.4699 \pm 0.0026		103923 \pm 18655	0.4810 \pm 0.0047		146196 \pm 23388
	10	0.3634 \pm 0.0039		94632 \pm 29277	0.4763 \pm 0.0019		103922 \pm 18655	0.4780 \pm 0.0018		146195 \pm 23388
HFL-VC (UB) (Ours)	0.5	0.3756 \pm 0.0041	2443 \pm 220	102721 \pm 24458	0.4720 \pm 0.0020	10104 \pm 268	281915 \pm 43569	0.4877 \pm 0.0058	16469 \pm 346	428717 \pm 61264
	0.9	0.3754 \pm 0.0053	2443 \pm 220	102721 \pm 24458	0.4701 \pm 0.0043	10104 \pm 268	281915 \pm 43569	0.4895 \pm 0.0015	16469 \pm 346	428717 \pm 61264
	10	0.3794 \pm 0.0025	2443 \pm 220	102721 \pm 24458	0.4736 \pm 0.0012	10104 \pm 268	281915 \pm 43569	0.4736 \pm 0.0012	10104 \pm 268	281915 \pm 43569
HFL (UB) - κ_0	0.5	0.3877 \pm 0.0031	1221 \pm 110	51360 \pm 12228	0.4713 \pm 0.0052	5052 \pm 132	140951 \pm 21783	0.4806 \pm 0.0058	8235 \pm 171	214347 \pm 30628
	0.9	0.3877 \pm 0.0024	1221 \pm 110	51360 \pm 12228	0.4731 \pm 0.0020	5052 \pm 132	140951 \pm 21783	0.4855 \pm 0.0011	8235 \pm 171	214347 \pm 30628
	10	0.3922 \pm 0.0042	1221 \pm 110	51360 \pm 12228	0.4772 \pm 0.0047	5052 \pm 132	140951 \pm 21783	0.4844 \pm 0.0031	8235 \pm 171	214347 \pm 30628

TABLE VII: Test Accuracy with Trained \mathbf{w}^T on CIFAR-100 dataset with $\kappa_0 = 5, \kappa_1 = 4, \kappa_2 = \kappa_3 = 2$ and $T = 100$

Methods	Dir(α)	With CNN Model			With ResNet-18 Model			With ResNet-34 Model		
		Acc	Req T [s]	Req E [J]	Acc	Req T [s]	Req E [J]	Acc	Req T [s]	Req E [J]
PHFL (Ours)	0.5	0.3817 \pm 0.0053	2240	103334 \pm 31061	0.4712 \pm 0.0043	6400	196151 \pm 31714	0.4932 \pm 0.0039	9600	280889 \pm 41968
	0.9	0.3782 \pm 0.0022		103335 \pm 31061	0.4815 \pm 0.0049		196151 \pm 31714	0.4928 \pm 0.0029		280889 \pm 41968
	10	0.3853 \pm 0.0035		103335 \pm 31061	0.4806 \pm 0.0035		196150 \pm 31714	0.4935 \pm 0.0037		280889 \pm 41968
HFL-VC (UB) (Ours)	0.5	0.3924 \pm 0.0055	2638 \pm 219	107290 \pm 24863	0.4780 \pm 0.0043	18074 \pm 365	465668 \pm 65814	0.4974 \pm 0.0032	30841 \pm 535	759264 \pm 102626
	0.9	0.3871 \pm 0.0063	2638 \pm 219	107290 \pm 24863	0.4819 \pm 0.0012	18074 \pm 365	465668 \pm 65814	0.4992 \pm 0.0022	30841 \pm 535	759264 \pm 102626
	10	0.3934 \pm 0.0048	2638 \pm 219	107290 \pm 24863	0.4824 \pm 0.0035	18074 \pm 365	465668 \pm 65814	0.4954 \pm 0.0058	30841 \pm 535	759264 \pm 102626
R-PHFL	0.5	0.2338 \pm 0.0047	2240	67480 \pm 20211	0.1562 \pm 0.0181	6400	185662 \pm 24670	0.0153 \pm 0.0032	9600	318013 \pm 41476
	0.9	0.2282 \pm 0.0092		67530 \pm 20296	0.1706 \pm 0.0180		185738 \pm 24765	0.0149 \pm 0.0011		318004 \pm 41465
	10	0.2398 \pm 0.0085		67535 \pm 20304	0.1837 \pm 0.0220		185639 \pm 24640	0.0144 \pm 0.0036		317815 \pm 41240

than the HFL-VC-UB. This is observed in Fig. 7a and Fig. 7d for CNN model when $t^{\text{th}} = 1.3\text{s}$, and also in Fig. 7b and Fig. 7e when $t^{\text{th}} = 8\text{s}$ for the ResNet-18 model. Besides, the dashed vertical lines in Fig. 7e and Fig. 7f show the mean energy budget of the clients for each PHFL global round. While all UEs are able to perform the learning and offloading within this mean energy budget with CNN and ResNet-18 models, clearly, when the ResNet-34 model is used, more than 57% of the clients will fail to perform the HFL-VC-UB due to their limited energy budgets.

Finally, we show the impact of κ_0 and κ_1 for different dataset heterogeneity levels on CIFAR-10 dataset in Table II - Table IV, where $t^{\text{th}} = 4\text{s}$ and $t^{\text{th}} = 6\text{s}$ is used in our proposed PHFL algorithms for ResNet-18 and ResNet-34 models, respectively. Besides, for the CNN model, we used $t^{\text{th}} = 1.3\text{s}$ and 2s , respectively, in our PHFL algorithm when $\kappa_0 = 5$ and $\kappa_0 = 10$, respectively, due to the facts that pruning

exacerbates test performance for a shallow model and computational time dominates the offloading delay. Similarly, we considered $t^{\text{th}} = 1.4\text{s}$ and $t^{\text{th}} = 2.5\text{s}$, respectively, for $\kappa_0 = 5$ and $\kappa_0 = 10$ on CIFAR-100 datasets for the CNN model. The performance comparisons for different α 's are shown in Table V - Table VII. From the tables, it is quite clear that pruning helps with negligible performance deviation from its original non-pruned counterparts. Besides, for the shallow CNN model, the performance gain, in terms of test accuracy, of our proposed PHFL is insignificant compared to the bulky ResNets. Moreover, increasing κ_0 or κ_1 generally improves the test accuracy. However, if the same t^{th} is to be used, it is beneficial to increase κ_0 compared to increasing κ_1 .

VI. CONCLUSION

This work proposed a model pruning solution to alleviate bandwidth scarcity and limited computational capacity of

wireless clients in heterogeneous networks. Using the convergence upper-bound, pruning ratio, computation frequency and transmission power of the clients were jointly optimized to maximize the convergence rate. The performances were evaluated on two popular datasets using three popular machine learning models of different total training parameter sizes. The results suggest that pruning can significantly reduce training time, energy expense and bandwidth requirement while incurring negligible test performance.

REFERENCES

- [1] B. McMahan, E. Moore, D. Ramage, S. Hampson, and B. A. y Arcas, "Communication-efficient learning of deep networks from decentralized data," in *Proc. AISTATS*, 2017.
- [2] N. H. Tran, W. Bao, A. Zomaya, M. N. H. Nguyen, and C. S. Hong, "Federated learning over wireless networks: Optimization model design and analysis," in *Proc. IEEE INFOCOM*, 2019.
- [3] Z. Yang, M. Chen, W. Saad, C. S. Hong, and M. Shikh-Bahaei, "Energy efficient federated learning over wireless communication networks," *IEEE Trans. Wireless Commun.*, vol. 20, no. 3, pp. 1935–1949, 2020.
- [4] R. Jin, X. He, and H. Dai, "Communication efficient federated learning with energy awareness over wireless networks," *IEEE Trans. Wireless Commun.*, vol. 21, no. 7, pp. 5204–5219, Jan. 2022.
- [5] Z. Chen, W. Yi, and A. Nallanathan, "Exploring representativity in device scheduling for wireless federated learning," *IEEE Trans. Wireless Commun.*, pp. 1–1, 2023.
- [6] T. Zhang, K.-Y. Lam, J. Zhao, and J. Feng, "Joint device scheduling and bandwidth allocation for federated learning over wireless networks," *IEEE Trans. Wireless Commun.*, pp. 1–1, 2023.
- [7] J. Wang, S. Wang, R.-R. Chen, and M. Ji, "Demystifying why local aggregation helps: Convergence analysis of hierarchical sgd," in *Proc. AAAI*, 2022.
- [8] S. Hosseinalipour, S. S. Azam, C. G. Brinton, N. Michelusi, V. Aggarwal, D. J. Love, and H. Dai, "Multi-stage hybrid federated learning over large-scale d2d-enabled fog networks," *IEEE/ACM Trans. Network.*, vol. 30, no. 4, pp. 1569–1584, 2022.
- [9] B. Xu, W. Xia, W. Wen, P. Liu, H. Zhao, and H. Zhu, "Adaptive hierarchical federated learning over wireless networks," *IEEE Trans. Vehicular Technol.*, vol. 71, no. 2, pp. 2070–2083, 2021.
- [10] S. Liu, G. Yu, X. Chen, and M. Bennis, "Joint user association and resource allocation for wireless hierarchical federated learning with iid and non-iid data," *IEEE Trans. Wireless Commun.*, vol. 21, no. 10, pp. 7852–7866, 2022.
- [11] S. Luo, X. Chen, Q. Wu, Z. Zhou, and S. Yu, "Hfel: Joint edge association and resource allocation for cost-efficient hierarchical federated edge learning," *IEEE Trans. Wireless Commun.*, vol. 19, no. 10, pp. 6535–6548, 2020.
- [12] L. Liu, J. Zhang, S. Song, and K. B. Letaief, "Client-edge-cloud hierarchical federated learning," in *Proc. IEEE ICC*, 2020.
- [13] C. Feng, H. H. Yang, D. Hu, Z. Zhao, T. Q. S. Quek, and G. Min, "Mobility-aware cluster federated learning in hierarchical wireless networks," *IEEE Trans. Wireless Commun.*, vol. 21, no. 10, pp. 8441–8458, Oct. 2022.
- [14] M. S. H. Abad, E. Ozfatura, D. Gunduz, and O. Ercetin, "Hierarchical federated learning across heterogeneous cellular networks," in *Proc. ICASSP*. IEEE, 2020.
- [15] P. Kairouz, H. B. McMahan, B. Avent, A. Bellet, M. Bennis, A. N. Bhagoji, K. Bonawitz, Z. Charles, G. Cormode, R. Cummings *et al.*, "Advances and open problems in federated learning," *Foundations and Trends® in Machine Learning*, vol. 14, no. 1–2, pp. 1–210, 2021.
- [16] T. Li, A. K. Sahu, M. Zaheer, M. Sanjabi, A. Talwalkar, and V. Smith, "Federated optimization in heterogeneous networks," *Proc. MLSys*, vol. 2, pp. 429–450, 2020.
- [17] H. Yang, X. Zhang, P. Khanduri, and J. Liu, "Anarchic federated learning," in *Proc. ICML*. PMLR, 2022, pp. 25 331–25 363.
- [18] J. Wang, Q. Liu, H. Liang, G. Joshi, and H. V. Poor, "Tackling the objective inconsistency problem in heterogeneous federated optimization," *Proc. NeurIPS*, vol. 33, pp. 7611–7623, 2020.
- [19] T. Lin, S. U. Stich, L. Barba, D. Dmitriev, and M. Jaggi, "Dynamic model pruning with feedback," in *Proc. ICLR*, 2020.
- [20] Y. Jiang, S. Wang, V. Valls, B. J. Ko, W.-H. Lee, K. K. Leung, and L. Tassiulas, "Model pruning enables efficient federated learning on edge devices," *IEEE Trans. Neural Netw. Learn. Syst.*, pp. 1–13, Apr. 2022.
- [21] Z. Zhu, Y. Shi, J. Luo, F. Wang, C. Peng, P. Fan, and K. B. Letaief, "Fedlp: Layer-wise pruning mechanism for communication-computation efficient federated learning," *arXiv preprint arXiv:2303.06360*, 2023.
- [22] S. Liu, G. Yu, R. Yin, and J. Yuan, "Adaptive network pruning for wireless federated learning," *IEEE Wireless Commun. Lett.*, vol. 10, no. 7, pp. 1572–1576, 2021.
- [23] S. Liu, G. Yu, R. Yin, J. Yuan, L. Shen, and C. Liu, "Joint model pruning and device selection for communication-efficient federated edge learning," *IEEE Trans. Commun.*, vol. 70, no. 1, pp. 231–244, Jan. 2022.
- [24] J. Ren, W. Ni, and H. Tian, "Toward communication-learning trade-off for federated learning at the network edge," *IEEE Commun. Lett.*, vol. 26, no. 8, pp. 1858–1862, Aug. 2022.
- [25] "3rd Generation Partnership Project; Technical Specification Group Core Network and Terminals; Proximity-services in 5G System protocol aspects; Stage 3," 3GPP TS 24.554 V18.0.0, Rel. 18, Mar. 2023.
- [26] J. Frankle and M. Carbin, "The lottery ticket hypothesis: Finding sparse, trainable neural networks," in *Proc. ICLR*, 2019.
- [27] M. F. Pervej, R. Jin, and H. Dai, "Resource constrained vehicular edge federated learning with highly mobile connected vehicles," *IEEE J. Sel. Areas Commun.*, vol. 41, no. 6, pp. 1825–1844, June 2023.
- [28] S. U. Stich, J.-B. Cordonnier, and M. Jaggi, "Sparsified sgd with memory," in *Proc. NeurIPS*, 2018.
- [29] L. Bottou, F. E. Curtis, and J. Nocedal, "Optimization methods for large-scale machine learning," *Siam Review*, vol. 60, no. 2, pp. 223–311, 2018.
- [30] S. Diamond and S. Boyd, "Cvxpy: A python-embedded modeling language for convex optimization," *J. Mach. Learn. Res.*, vol. 17, no. 1, pp. 2909–2913, 2016.
- [31] E. Che, H. D. Tuan, and H. H. Nguyen, "Joint optimization of cooperative beamforming and relay assignment in multi-user wireless relay networks," *IEEE Trans. Wireless Comm.*, vol. 13, no. 10, pp. 5481–5495, 2014.
- [32] Y. Sun, D. Xu, D. W. K. Ng, L. Dai, and R. Schober, "Optimal 3d-trajectory design and resource allocation for solar-powered uav communication systems," *IEEE Trans. Commun.*, vol. 67, no. 6, pp. 4281–4298, 2019.
- [33] A. Krizhevsky, "Learning multiple layers of features from tiny images," Apr. 2009. [Online]. Available: <https://www.cs.toronto.edu/~kriz/learning-features-2009-TR.pdf>
- [34] K. He, X. Zhang, S. Ren, and J. Sun, "Deep residual learning for image recognition," in *Proc. IEEE CVPR*, 2016.



Md Ferdous Pervej (M'23) received the B.Sc. degree in electronics and telecommunication engineering from the Rajshahi University of Engineering and Technology, Rajshahi, Bangladesh, in 2014, and the M.S. and Ph.D. degrees in electrical engineering from Utah State University, Logan, UT, USA, in 2019 and North Carolina State University, Raleigh, NC, USA, in 2023, respectively.

He was with Mitsubishi Electric Research Laboratories, Cambridge, MA, in summer 2021, and with Futurewei Wireless Research and Standards, Schaumburg, IL from May to December 2022. He is currently a Postdoctoral Scholar – Research Associate in the Ming Hsieh Department of Electrical and Computer Engineering at the University of Southern California, Los Angeles, CA, USA. His primary research interests are wireless networks, distributed machine learning, vehicle-to-everything communication, edge caching/computing, and machine learning for wireless networks.



Richeng Jin (M'21) received the B.S. degree in information and communication engineering from Zhejiang University, Hangzhou, China, in 2015, and the Ph.D. degree in electrical engineering from North Carolina State University, Raleigh, NC, USA, in 2020.

He was a Postdoctoral Researcher in electrical and computer engineering at North Carolina State University, Raleigh, NC, USA, from 2021 to 2022. He is currently a faculty member of the department of information and communication engineering with Zhejiang University, Hangzhou, China. His research interests are in the general area of wireless AI, game theory, and security and privacy in machine learning/artificial intelligence and wireless networks.



Huaiyu Dai (F'17) received the B.E. and M.S. degrees in electrical engineering from Tsinghua University, Beijing, China, in 1996 and 1998, respectively, and the Ph.D. degree in electrical engineering from Princeton University, Princeton, NJ in 2002.

He was with Bell Labs, Lucent Technologies, Holmdel, NJ, in summer 2000, and with AT&T Labs-Research, Middletown, NJ, in summer 2001. He is currently a Professor of Electrical and Computer Engineering with NC State University, Raleigh, holding the title of University Faculty Scholar. His research interests are in the general areas of communications, signal processing, networking, and computing. His current research focuses on machine learning and artificial intelligence for communications and networking, multilayer and interdependent networks, dynamic spectrum access and sharing, as well as security and privacy issues in the above systems.

He has served as an area editor for IEEE Transactions on Communications, a member of the Executive Editorial Committee for IEEE Transactions on Wireless Communications, and an editor for IEEE Transactions on Signal Processing. Currently he serves as an area editor for IEEE Transactions on Wireless Communications. He was a co-recipient of best paper awards at 2010 IEEE International Conference on Mobile Ad-hoc and Sensor Systems (MASS 2010), 2016 IEEE INFOCOM BIGSECURITY Workshop, and 2017 IEEE International Conference on Communications (ICC 2017). He received Qualcomm Faculty Award in 2019.

SUPPLEMENTARY MATERIALS

Additional Notations: Analogous to our previous notations, we express the pruned virtual models at different hierarchy levels as $\tilde{\mathbf{w}}_j^{t,0} := \sum_{i=1}^{U_{j,k,l}} \alpha_i \tilde{\mathbf{w}}_i^{t,0}$, $\tilde{\mathbf{w}}_k^{t,0} := \sum_{j=1}^{V_{k,l}} \alpha_j \sum_{i=1}^{U_{j,k,l}} \alpha_i \tilde{\mathbf{w}}_i^{t,0} = \sum_{j=1}^{V_{k,l}} \alpha_j \tilde{\mathbf{w}}_j^{t,0}$, $\tilde{\mathbf{w}}_l^{t,0} := \sum_{k=1}^{B_l} \alpha_k \sum_{j=1}^{V_{k,l}} \alpha_j \sum_{i=1}^{U_{j,k,l}} \alpha_i \tilde{\mathbf{w}}_i^{t,0} = \sum_{k=1}^{B_l} \alpha_k \tilde{\mathbf{w}}_k^{t,0}$ and $\tilde{\mathbf{w}}^{t,0} := \sum_{l=1}^L \alpha_l \tilde{\mathbf{w}}_l^{t,0} = \sum_{u=1}^U \alpha_u \tilde{\mathbf{w}}_u^{t,0}$. Moreover, $\tilde{g}(\tilde{\mathbf{w}}_i^{t,0}) := g(\tilde{\mathbf{w}}_i^{t,0}) \odot \mathbf{m}_i^t$, $\nabla \tilde{f}_i(\tilde{\mathbf{w}}_i^{t,0}) := \nabla f_i(\tilde{\mathbf{w}}_i^{t,0}) \odot \mathbf{m}_i^t$ and $\nabla \tilde{f}(\tilde{\mathbf{w}}^{t,0}) = \sum_{u=1}^U \alpha_u \nabla \tilde{f}_u(\tilde{\mathbf{w}}_u^{t,0})$. **Additional Assumptions:** Since the element-wise mask operation is equivalent to replacing a subset of the actual entries with zero, similar to [20], [22], we also assume that the assumptions made in Section III-A hold if we apply the binary masks to all gradients.

APPENDIX A
PROOF OF THEOREM 1

Theorem 1. When the assumptions in Section III-A hold and $\eta \leq 1/\beta$, we have

$$\theta_{\text{PHFL}} \leq \mathcal{O}([f(\tilde{\mathbf{w}}^0) - f_{\text{inf}}]/[\eta T]) + \underbrace{\mathcal{O}(\beta \eta \sigma^2/U)}_{\text{pruning error}} + \underbrace{\mathcal{O}(\delta^{\text{th}} \beta^2 D^2)}_{\text{wireless factor}} + \mathcal{O}(\beta \eta G^2 \cdot \varphi_{w,0}(\boldsymbol{\delta}, \mathbf{f}, \mathbf{P})) + \mathcal{O}(\beta^2 [L_1 + L_2 + L_3 + L_4]), \quad (56)$$

where $\boldsymbol{\delta} = \{\delta_1^t, \dots, \delta_U^t\}_{t=0}^{T-1}$, $\mathbf{f} = \{f_1^t, \dots, f_U^t\}_{t=0}^{T-1}$, $\mathbf{P} = \{P_1^t, \dots, P_U^t\}_{t=0}^{T-1}$ and f_i^t is the i^{th} client's CPU frequency in the wireless factors. Besides, the terms L_1 , L_2 , L_3 and L_4 are

$$\varphi_{w,0}(\boldsymbol{\delta}, \mathbf{f}, \mathbf{P}) = [1/T] \sum_{t=0}^{T-1} \sum_{l=1}^L \alpha_l^2 \sum_{k=1}^{B_l} \alpha_k^2 \sum_{j=1}^{V_{k,l}} \alpha_j^2 \sum_{i=1}^{U_{j,k,l}} \alpha_i^2 [1/p_i^t - 1], \quad (57)$$

$$L_1 = [1/T] \sum_{t=0}^{T-1} \sum_{l=1}^L \alpha_l \sum_{k=1}^{B_l} \alpha_k \sum_{j=1}^{V_{k,l}} \alpha_j \sum_{i=1}^{U_{j,k,l}} \alpha_i \mathbb{E} \|\tilde{\mathbf{w}}_j^t - \tilde{\mathbf{w}}_i^t\|^2, \quad (58)$$

$$L_2 = [1/T] \sum_{t=0}^{T-1} \sum_{l=1}^L \alpha_l \sum_{k=1}^{B_l} \alpha_k \sum_{j=1}^{V_{k,l}} \alpha_j \mathbb{E} \|\tilde{\mathbf{w}}_k^t - \tilde{\mathbf{w}}_j^t\|^2, \quad (59)$$

$$L_3 = [1/T] \sum_{t=0}^{T-1} \sum_{l=1}^L \alpha_l \sum_{k=1}^{B_l} \alpha_k \mathbb{E} \|\tilde{\mathbf{w}}_l^t - \tilde{\mathbf{w}}_k^t\|^2, \quad (60)$$

$$L_4 = [1/T] \sum_{t=0}^{T-1} \sum_{l=1}^L \alpha_l \mathbb{E} \|\tilde{\mathbf{w}}^t - \tilde{\mathbf{w}}_l^t\|^2. \quad (61)$$

Proof. Since there are U clients and we consider the virtual models at different hierarchy levels, we start the convergence proof assuming the global model is the weighted combination of all these U clients. After that, we break down our derivations for different hierarchy levels based on our proposed PHFL algorithm. Note that this is also a standard practice in the literature [9], [13].

First, let us write the update rule for the global model as

$$\tilde{\mathbf{w}}^{t+1} = \sum_{u=1}^U \alpha_u \tilde{\mathbf{w}}_u^{t+1} = \sum_{u=1}^U \alpha_u \left(\tilde{\mathbf{w}}_u^{t,0} - \eta \tilde{g}(\tilde{\mathbf{w}}_u^{t,0}) \frac{\mathbf{1}_u^t}{P_u^t} \right) = \tilde{\mathbf{w}}^{t,0} - \eta \sum_{u=1}^U \alpha_u \tilde{g}(\tilde{\mathbf{w}}_u^{t,0}) \frac{\mathbf{1}_u^t}{P_u^t}, \quad (62)$$

where $\tilde{\mathbf{w}}^{t,0} := \sum_{u=1}^U \alpha_u \tilde{\mathbf{w}}_u^{t,0}$. As such, we write

$$f(\tilde{\mathbf{w}}^{t+1}) = f(\tilde{\mathbf{w}}^{t,0} - \eta \sum_{u=1}^U \alpha_u \tilde{g}(\tilde{\mathbf{w}}_u^{t,0}) \frac{\mathbf{1}_u^t}{P_u^t}), \stackrel{(a)}{\leq} f(\tilde{\mathbf{w}}^{t,0}) + \left\langle \nabla f(\tilde{\mathbf{w}}^{t,0}), -\eta \sum_{u=1}^U \alpha_u \tilde{g}(\tilde{\mathbf{w}}_u^{t,0}) \frac{\mathbf{1}_u^t}{P_u^t} \right\rangle + \frac{\beta \eta^2}{2} \left\| \sum_{u=1}^U \alpha_u \tilde{g}(\tilde{\mathbf{w}}_u^{t,0}) \frac{\mathbf{1}_u^t}{P_u^t} \right\|^2, \quad (63)$$

where (a) stems from β -smoothness assumption. For the third term in (63), we can write

$$\begin{aligned} \left\langle \nabla f(\tilde{\mathbf{w}}^{t,0}), -\eta \sum_{u=1}^U \alpha_u \tilde{g}(\tilde{\mathbf{w}}_u^{t,0}) \frac{\mathbf{1}_u^t}{P_u^t} \right\rangle &= -\eta \left\langle \sum_{u=1}^U \alpha_u \nabla f_u(\tilde{\mathbf{w}}^{t,0}), \sum_{u=1}^U \alpha_u \tilde{g}(\tilde{\mathbf{w}}_u^{t,0}) \frac{\mathbf{1}_u^t}{P_u^t} \right\rangle \\ &= -\eta \sum_{u=1}^U \alpha_u \left\langle \nabla f_u(\tilde{\mathbf{w}}^{t,0}) \odot \mathbf{m}_u^t, (\tilde{g}(\tilde{\mathbf{w}}_u^{t,0}) \odot \mathbf{m}_u^t) \frac{\mathbf{1}_u^t}{P_u^t} \right\rangle = -\eta \sum_{u=1}^U \alpha_u \left\langle \nabla \tilde{f}_u(\tilde{\mathbf{w}}_u^{t,0}), \tilde{g}(\tilde{\mathbf{w}}_u^{t,0}) \frac{\mathbf{1}_u^t}{P_u^t} \right\rangle, \end{aligned} \quad (64)$$

where $\nabla \tilde{f}_u(\tilde{\mathbf{w}}_u^{t,0}) := \nabla f_u(\tilde{\mathbf{w}}^{t,0}) \odot \mathbf{m}_u^t$.

Plugging (64) into (63) and taking expectation over both sides, we get

$$\mathbb{E}[f(\tilde{\mathbf{w}}^{t+1})] \leq f(\tilde{\mathbf{w}}^{t,0}) - \eta \sum_{u=1}^U \alpha_u \mathbb{E} \left[\left\langle \nabla \tilde{f}_u(\tilde{\mathbf{w}}_u^{t,0}), \tilde{g}(\tilde{\mathbf{w}}_u^{t,0}) \frac{\mathbf{1}_u^t}{P_u^t} \right\rangle \right] + \frac{\beta \eta^2}{2} \mathbb{E} \left[\left\| \sum_{u=1}^U \alpha_u \tilde{g}(\tilde{\mathbf{w}}_u^{t,0}) \frac{\mathbf{1}_u^t}{P_u^t} \right\|^2 \right], \quad (65)$$

We simply the third term in (65) as follows:

$$\begin{aligned} -\eta \sum_{u=1}^U \alpha_u \mathbb{E} \left[\left\langle \nabla \tilde{f}_u(\tilde{\mathbf{w}}_u^{t,0}), \tilde{g}(\tilde{\mathbf{w}}_u^{t,0}) \frac{\mathbf{1}_u^t}{P_u^t} \right\rangle \right] &\stackrel{(a)}{=} -\eta \sum_{u=1}^U \alpha_u \left\langle \nabla \tilde{f}_u(\tilde{\mathbf{w}}_u^{t,0}), \mathbb{E}[\tilde{g}(\tilde{\mathbf{w}}_u^{t,0})] \mathbb{E} \left[\frac{\mathbf{1}_u^t}{P_u^t} \right] \right\rangle, \\ &= -\eta \sum_{u=1}^U \alpha_u \langle \nabla \tilde{f}_u(\tilde{\mathbf{w}}_u^{t,0}), \nabla \tilde{f}_u(\tilde{\mathbf{w}}_u^{t,0}) \rangle, \end{aligned}$$

$$\begin{aligned}
&= -\frac{\eta}{2} \sum_{u=1}^U \alpha_u \left\{ \|\nabla \tilde{f}_u(\tilde{\mathbf{w}}^{t,0})\|^2 + \|\nabla \tilde{f}_u(\tilde{\mathbf{w}}_u^{t,0})\|^2 - \|\nabla \tilde{f}_u(\tilde{\mathbf{w}}^{t,0}) - \nabla \tilde{f}_u(\tilde{\mathbf{w}}_u^{t,0})\|^2 \right\}, \\
&= \frac{\eta}{2} \sum_{u=1}^U \alpha_u \left\{ \|\nabla \tilde{f}_u(\tilde{\mathbf{w}}^{t,0}) - \nabla \tilde{f}_u(\tilde{\mathbf{w}}_u^{t,0})\|^2 - \|\nabla \tilde{f}_u(\tilde{\mathbf{w}}^{t,0})\|^2 - \|\nabla \tilde{f}_u(\tilde{\mathbf{w}}_u^{t,0})\|^2 \right\}, \\
&= \frac{\eta}{2} \sum_{u=1}^U \alpha_u \left\{ \|\nabla \tilde{f}_u(\tilde{\mathbf{w}}^{t,0}) - \nabla \tilde{f}_u(\tilde{\mathbf{w}}_u^{t,0})\|^2 - \|\nabla \tilde{f}_u(\tilde{\mathbf{w}}_u^{t,0})\|^2 \right\} - \frac{\eta}{2} \sum_{u=1}^U \alpha_u \|\nabla \tilde{f}_u(\tilde{\mathbf{w}}^{t,0})\|^2, \\
&\leq \frac{\eta}{2} \sum_{u=1}^U \alpha_u \left\{ \|\nabla \tilde{f}_u(\tilde{\mathbf{w}}^{t,0}) - \nabla \tilde{f}_u(\tilde{\mathbf{w}}_u^{t,0})\|^2 - \|\nabla \tilde{f}_u(\tilde{\mathbf{w}}_u^{t,0})\|^2 \right\} - \frac{\eta}{2} \left\| \sum_{u=1}^U \alpha_u \nabla \tilde{f}_u(\tilde{\mathbf{w}}^{t,0}) \right\|^2, \\
&\stackrel{(b)}{=} \frac{\eta}{2} \sum_{u=1}^U \alpha_u \left\{ \|\nabla \tilde{f}_u(\tilde{\mathbf{w}}^{t,0}) - \nabla \tilde{f}_u(\tilde{\mathbf{w}}_u^{t,0})\|^2 - \|\nabla \tilde{f}_u(\tilde{\mathbf{w}}_u^{t,0})\|^2 \right\} - \frac{\eta}{2} \|\nabla \tilde{f}(\tilde{\mathbf{w}}^{t,0})\|^2,
\end{aligned} \tag{66}$$

where (a) follows from the independence of client selection and SGD. Besides, we define $\|\nabla \tilde{f}(\tilde{\mathbf{w}}^{t,0})\|^2 := \|\sum_{u=1}^U \alpha_u \nabla \tilde{f}_u(\tilde{\mathbf{w}}^{t,0})\|^2 = \|\sum_{u=1}^U \alpha_u \nabla f_u(\tilde{\mathbf{w}}^{t,0}) \odot \mathbf{m}_u^t\|^2$ in (b).

The second term in (65) can be simplified as follows:

$$\begin{aligned}
&\mathbb{E} \left[\left\| \sum_{u=1}^U \alpha_u \tilde{g}(\tilde{\mathbf{w}}_u^{t,0}) \frac{\mathbf{1}_u^t}{p_u^t} \right\|^2 \right] \\
&\stackrel{(a)}{=} \mathbb{E} \left[\left\| \sum_{u=1}^U \alpha_u \tilde{g}(\tilde{\mathbf{w}}_u^{t,0}) \frac{\mathbf{1}_u^t}{p_u^t} - \mathbb{E} \left[\sum_{u=1}^U \alpha_u \tilde{g}(\tilde{\mathbf{w}}_u^{t,0}) \frac{\mathbf{1}_u^t}{p_u^t} \right] \right\|^2 \right] + \left(\mathbb{E} \left[\sum_{u=1}^U \alpha_u \tilde{g}(\tilde{\mathbf{w}}_u^{t,0}) \frac{\mathbf{1}_u^t}{p_u^t} \right] \right)^2, \\
&= \mathbb{E} \left[\left\| \sum_{u=1}^U \alpha_u \tilde{g}(\tilde{\mathbf{w}}_u^{t,0}) \frac{\mathbf{1}_u^t}{p_u^t} \pm \sum_{u=1}^U \alpha_u \tilde{g}(\tilde{\mathbf{w}}_u^{t,0}) - \sum_{u=1}^U \alpha_u \nabla \tilde{f}_u(\tilde{\mathbf{w}}_u^{t,0}) \right\|^2 \right] + \left\| \sum_{u=1}^U \alpha_u \nabla \tilde{f}_u(\tilde{\mathbf{w}}_u^{t,0}) \right\|^2, \\
&\stackrel{(b)}{\leq} \mathbb{E} \left[\left\| \sum_{u=1}^U \alpha_u \left(\frac{\mathbf{1}_u^t}{p_u^t} - 1 \right) \tilde{g}(\tilde{\mathbf{w}}_u^{t,0}) + \sum_{u=1}^U \alpha_u (\tilde{g}(\tilde{\mathbf{w}}_u^{t,0}) - \nabla \tilde{f}_u(\tilde{\mathbf{w}}_u^{t,0})) \right\|^2 \right] + \sum_{u=1}^U \alpha_u \|\nabla \tilde{f}_u(\tilde{\mathbf{w}}_u^{t,0})\|^2, \\
&\stackrel{(c)}{\leq} 2\mathbb{E} \left[\left\| \sum_{u=1}^U \alpha_u \left(\frac{\mathbf{1}_u^t}{p_u^t} - 1 \right) \tilde{g}(\tilde{\mathbf{w}}_u^{t,0}) \right\|^2 \right] + 2\mathbb{E} \left[\left\| \sum_{u=1}^U \alpha_u (\tilde{g}(\tilde{\mathbf{w}}_u^{t,0}) - \nabla \tilde{f}_u(\tilde{\mathbf{w}}_u^{t,0})) \right\|^2 \right] + \sum_{u=1}^U \alpha_u \|\nabla \tilde{f}_u(\tilde{\mathbf{w}}_u^{t,0})\|^2, \\
&= 2\mathbb{E} \left[\sum_{u=1}^U \alpha_u^2 \left\| \left(\frac{\mathbf{1}_u^t}{p_u^t} - 1 \right) \tilde{g}(\tilde{\mathbf{w}}_u^{t,0}) \right\|^2 \right] + \sum_{u=1}^U \alpha_u \sum_{u'=1, u' \neq u}^U \alpha_{u'} \left(\frac{\mathbf{1}_u^t}{p_u^t} - 1 \right) \tilde{g}(\tilde{\mathbf{w}}_u^{t,0}) \left(\frac{\mathbf{1}_{u'}^t}{p_{u'}^t} - 1 \right) \tilde{g}(\tilde{\mathbf{w}}_{u'}^{t,0}) + \\
&\quad 2\mathbb{E} \left[\sum_{u=1}^U \alpha_u^2 \left\| (\tilde{g}(\tilde{\mathbf{w}}_u^{t,0}) - \nabla \tilde{f}_u(\tilde{\mathbf{w}}_u^{t,0})) \right\|^2 \right] + \\
&\quad \sum_{u=1}^U \alpha_u \sum_{u'=1, u' \neq u}^U \alpha_{u'} (\tilde{g}(\tilde{\mathbf{w}}_u^{t,0}) - \nabla \tilde{f}_u(\tilde{\mathbf{w}}_u^{t,0})) (\tilde{g}(\tilde{\mathbf{w}}_{u'}^{t,0}) - \nabla \tilde{f}_{u'}(\tilde{\mathbf{w}}_{u'}^{t,0})) + \sum_{u=1}^U \alpha_u \|\nabla \tilde{f}_u(\tilde{\mathbf{w}}_u^{t,0})\|^2, \\
&\stackrel{(d)}{\leq} 2\mathbb{E} \left[\sum_{u=1}^U \alpha_u^2 \left\| \left(\frac{\mathbf{1}_u^t}{p_u^t} - 1 \right) \tilde{g}(\tilde{\mathbf{w}}_u^{t,0}) \right\|^2 \right] + 2\sigma^2 \sum_{u=1}^U \alpha_u^2 + \sum_{u=1}^U \alpha_u \|\nabla \tilde{f}_u(\tilde{\mathbf{w}}_u^{t,0})\|^2, \\
&= 2 \sum_{u=1}^U \alpha_u^2 \left(\frac{1-p_u^t}{p_u^t} \right) \mathbb{E} \|\tilde{g}(\tilde{\mathbf{w}}_u^{t,0})\|^2 + 2\sigma^2 \sum_{u=1}^U \alpha_u^2 + \sum_{u=1}^U \alpha_u \|\nabla \tilde{f}_u(\tilde{\mathbf{w}}_u^{t,0})\|^2,
\end{aligned} \tag{67}$$

where (a) comes from the definition of variance, (b) follows from Jensen inequality, i.e., $\left\| \sum_{u=1}^U \alpha_u \nabla \tilde{f}_u(\tilde{\mathbf{w}}_u^{t,0}) \right\|^2 \leq \sum_{u=1}^U \alpha_u \|\nabla \tilde{f}_u(\tilde{\mathbf{w}}_u^{t,0})\|^2$, (c) stems from the fact that $\|\sum_{i=1}^n \mathbf{a}_i\|^2 \leq n \sum_{i=1}^n \|\mathbf{a}_i\|^2$ and (d) is due to the bounded stochastic gradient assumption.

Plugging (66) and (67) in (65), we get

$$\begin{aligned}
\mathbb{E} [f(\tilde{\mathbf{w}}^{t+1})] &\leq f(\tilde{\mathbf{w}}^{t,0}) + \frac{\eta}{2} \sum_{u=1}^U \alpha_u \left\{ \|\nabla \tilde{f}_u(\tilde{\mathbf{w}}^{t,0}) - \nabla \tilde{f}_u(\tilde{\mathbf{w}}_u^{t,0})\|^2 - \|\nabla \tilde{f}_u(\tilde{\mathbf{w}}_u^{t,0})\|^2 \right\} - \\
&\quad \frac{\eta}{2} \|\nabla \tilde{f}(\tilde{\mathbf{w}}^{t,0})\|^2 + \eta^2 \sum_{u=1}^U \alpha_u^2 \left(\frac{1-p_u^t}{p_u^t} \right) \mathbb{E} \|\tilde{g}(\tilde{\mathbf{w}}_u^{t,0})\|^2 + \beta \eta^2 \sigma^2 \sum_{u=1}^U \alpha_u^2 + \frac{\beta \eta^2}{2} \sum_{u=1}^U \alpha_u \|\nabla \tilde{f}_u(\tilde{\mathbf{w}}_u^{t,0})\|^2, \\
&= f(\tilde{\mathbf{w}}^{t,0}) + \frac{\eta}{2} \sum_{u=1}^U \alpha_u \left\| \nabla \tilde{f}_u(\tilde{\mathbf{w}}^{t,0}) - \nabla \tilde{f}_u(\tilde{\mathbf{w}}_u^{t,0}) \right\|^2 - \frac{\eta}{2} \|\nabla \tilde{f}(\tilde{\mathbf{w}}^{t,0})\|^2 - \frac{\eta}{2} (1-\beta\eta) \sum_{u=1}^U \|\nabla \tilde{f}_u(\tilde{\mathbf{w}}_u^{t,0})\|^2
\end{aligned}$$

$$+ \beta \eta^2 \sum_{u=1}^U \alpha_u^2 \left(\frac{1-p_u^t}{p_u^t} \right) \mathbb{E} \|\tilde{g}(\tilde{\mathbf{w}}_u^{t,0})\|^2 + \beta \eta^2 \sigma^2 \sum_{u=1}^U \alpha_u^2. \quad (68)$$

Note that, when $\eta \leq \frac{1}{\beta}$, $(1-\beta\eta) \geq 0$. Therefore, we can drop the fourth term in (68).

To that end, rearranging the terms in (68), then dividing both sides by $\frac{\eta}{2}$, taking expectations on both sides and averaging over time, we get the following

$$\begin{aligned} \frac{1}{T} \sum_{t=0}^{T-1} \mathbb{E} [\|\nabla \tilde{f}(\tilde{\mathbf{w}}^{t,0})\|^2] &\leq \frac{2(f(\tilde{\mathbf{w}}^0) - \mathbb{E}[f(\tilde{\mathbf{w}}^T)])}{\eta T} + 2\beta\eta\sigma^2 \sum_{u=1}^U \alpha_u^2 + \frac{2\beta\eta G^2}{T} \sum_{t=0}^{T-1} \sum_{u=1}^U \alpha_u^2 \left(\frac{1-p_u^t}{p_u^t} \right) + \\ &\quad \frac{1}{T} \sum_{t=0}^{T-1} \sum_{u=1}^U \alpha_u \mathbb{E} [\|\nabla \tilde{f}_u(\tilde{\mathbf{w}}^{t,0}) - \nabla \tilde{f}_u(\tilde{\mathbf{w}}_u^{t,0})\|^2], \end{aligned} \quad (69)$$

where we use the notation $\tilde{\mathbf{w}}^0$ to represent $\tilde{\mathbf{w}}^{0,0}$ for simplicity.

The last term in (69) can be expanded as follows:

$$\begin{aligned} \frac{1}{T} \sum_{t=0}^{T-1} \sum_{u=1}^U \alpha_u \mathbb{E} [\|\nabla \tilde{f}_u(\tilde{\mathbf{w}}^{t,0}) - \nabla \tilde{f}_u(\tilde{\mathbf{w}}_u^{t,0})\|^2] &= \sum_{u=1}^U \alpha_u \mathbb{E} \left[\left\| \nabla \tilde{f}_u(\tilde{\mathbf{w}}^{t,0}) \pm \nabla \tilde{f}_u(\tilde{\mathbf{w}}_{l,(u)}^{t,0}) \pm \nabla \tilde{f}_u(\tilde{\mathbf{w}}_{k,(u)}^{t,0}) \pm \nabla \tilde{f}_u(\tilde{\mathbf{w}}_{j,(u)}^{t,0}) - \nabla \tilde{f}_u(\tilde{\mathbf{w}}_u^{t,0}) \right\|^2 \right], \\ &\stackrel{(a)}{\leq} \frac{4}{T} \sum_{t=0}^{T-1} \sum_{u=1}^U \alpha_u \mathbb{E} \left[\|\nabla \tilde{f}_u(\tilde{\mathbf{w}}^{t,0}) - \nabla \tilde{f}_u(\tilde{\mathbf{w}}_{l,(u)}^{t,0})\|^2 + \|\nabla \tilde{f}_u(\tilde{\mathbf{w}}_{l,(u)}^{t,0}) - \nabla \tilde{f}_u(\tilde{\mathbf{w}}_{k,(u)}^{t,0})\|^2 + \|\nabla \tilde{f}_u(\tilde{\mathbf{w}}_{k,(u)}^{t,0}) - \nabla \tilde{f}_u(\tilde{\mathbf{w}}_{j,(u)}^{t,0})\|^2 + \right. \\ &\quad \left. \|\nabla \tilde{f}_u(\tilde{\mathbf{w}}_{j,(u)}^{t,0}) - \nabla \tilde{f}_u(\tilde{\mathbf{w}}_u^{t,0})\|^2 \right], \\ &\stackrel{(b)}{\leq} \frac{4\beta^2}{T} \sum_{t=0}^{T-1} \sum_{u=1}^U \alpha_u \left\{ \mathbb{E} [\|\tilde{\mathbf{w}}^{t,0} - \tilde{\mathbf{w}}_{l,(u)}^{t,0}\|^2] + \mathbb{E} [\|\tilde{\mathbf{w}}_{l,(u)}^{t,0} - \tilde{\mathbf{w}}_{k,(u)}^{t,0}\|^2] + \mathbb{E} [\|\tilde{\mathbf{w}}_{k,(u)}^{t,0} - \tilde{\mathbf{w}}_{j,(u)}^{t,0}\|^2] + \mathbb{E} [\|\tilde{\mathbf{w}}_{j,(u)}^{t,0} - \tilde{\mathbf{w}}_u^{t,0}\|^2] \right\}, \\ &= \frac{4\beta^2}{T} \sum_{t=0}^{T-1} \sum_{l=1}^L \alpha_l \sum_{k=1}^{B_l} \alpha_k \sum_{j=1}^{V_{k,l}} \alpha_j \sum_{i=1}^{U_{j,k,l}} \alpha_i \left\{ \mathbb{E} [\|\tilde{\mathbf{w}}^{t,0} - \tilde{\mathbf{w}}_l^{t,0}\|^2] + \mathbb{E} [\|\tilde{\mathbf{w}}_l^{t,0} - \tilde{\mathbf{w}}_k^{t,0}\|^2] + \mathbb{E} [\|\tilde{\mathbf{w}}_k^{t,0} - \tilde{\mathbf{w}}_j^{t,0}\|^2] + \mathbb{E} [\|\tilde{\mathbf{w}}_j^{t,0} - \tilde{\mathbf{w}}_i^{t,0}\|^2] \right\}, \\ &= \frac{4\beta^2}{T} \sum_{t=0}^{T-1} \left\{ \sum_{l=1}^L \alpha_l \mathbb{E} [\|\tilde{\mathbf{w}}^{t,0} - \tilde{\mathbf{w}}_l^{t,0}\|^2] + \sum_{l=1}^L \alpha_l \sum_{k=1}^{B_l} \alpha_k \mathbb{E} [\|\tilde{\mathbf{w}}_l^{t,0} - \tilde{\mathbf{w}}_k^{t,0}\|^2] + \sum_{l=1}^L \alpha_l \sum_{k=1}^{B_l} \alpha_k \sum_{j=1}^{V_{k,l}} \alpha_j \mathbb{E} [\|\tilde{\mathbf{w}}_k^{t,0} - \tilde{\mathbf{w}}_j^{t,0}\|^2] + \right. \\ &\quad \left. \sum_{l=1}^L \alpha_l \sum_{k=1}^{B_l} \alpha_k \sum_{j=1}^{V_{k,l}} \alpha_j \sum_{i=1}^{U_{j,k,l}} \alpha_i \mathbb{E} [\|\tilde{\mathbf{w}}_j^{t,0} - \tilde{\mathbf{w}}_i^{t,0}\|^2] \right\}, \\ &= \frac{4\beta^2}{T} \sum_{t=0}^{T-1} \left\{ \sum_{l=1}^L \alpha_l \mathbb{E} [\|\tilde{\mathbf{w}}^{t,0} \pm \tilde{\mathbf{w}}^t \pm \tilde{\mathbf{w}}_l^t - \tilde{\mathbf{w}}_l^{t,0}\|^2] + \sum_{l=1}^L \alpha_l \sum_{k=1}^{B_l} \alpha_k \mathbb{E} [\|\tilde{\mathbf{w}}_l^{t,0} \pm \tilde{\mathbf{w}}_l^t \pm \tilde{\mathbf{w}}_k^t - \tilde{\mathbf{w}}_k^{t,0}\|^2] + \right. \\ &\quad \left. \sum_{l=1}^L \alpha_l \sum_{k=1}^{B_l} \alpha_k \sum_{j=1}^{V_{k,l}} \alpha_j \mathbb{E} [\|\tilde{\mathbf{w}}_k^{t,0} \pm \tilde{\mathbf{w}}_k^t \pm \tilde{\mathbf{w}}_j^t - \tilde{\mathbf{w}}_j^{t,0}\|^2] + \sum_{l=1}^L \alpha_l \sum_{k=1}^{B_l} \alpha_k \sum_{j=1}^{V_{k,l}} \alpha_j \sum_{i=1}^{U_{j,k,l}} \alpha_i \mathbb{E} [\|\tilde{\mathbf{w}}_j^{t,0} \pm \tilde{\mathbf{w}}_j^t \pm \tilde{\mathbf{w}}_i^t - \tilde{\mathbf{w}}_i^{t,0}\|^2] \right\}, \\ &\stackrel{(c)}{\leq} \frac{12\beta^2}{T} \sum_{t=0}^{T-1} \left\{ \sum_{l=1}^L \alpha_l \mathbb{E} [\|\tilde{\mathbf{w}}^{t,0} - \tilde{\mathbf{w}}^t\|^2 + \|\tilde{\mathbf{w}}_l^t - \tilde{\mathbf{w}}_l^{t,0}\|^2 + \|\tilde{\mathbf{w}}^t - \tilde{\mathbf{w}}_l^t\|^2] + \sum_{l=1}^L \alpha_l \sum_{k=1}^{B_l} \alpha_k \mathbb{E} [\|\tilde{\mathbf{w}}_l^{t,0} - \tilde{\mathbf{w}}_l^t\|^2 + \|\tilde{\mathbf{w}}_k^t - \tilde{\mathbf{w}}_k^{t,0}\|^2 + \|\tilde{\mathbf{w}}_l^t - \tilde{\mathbf{w}}_k^t\|^2] + \right. \\ &\quad \sum_{l=1}^L \alpha_l \sum_{k=1}^{B_l} \alpha_k \sum_{j=1}^{V_{k,l}} \alpha_j \mathbb{E} [\|\tilde{\mathbf{w}}_k^{t,0} - \tilde{\mathbf{w}}_k^t\|^2 + \|\tilde{\mathbf{w}}_j^t - \tilde{\mathbf{w}}_j^{t,0}\|^2 + \|\tilde{\mathbf{w}}_k^t - \tilde{\mathbf{w}}_j^t\|^2] + \\ &\quad \left. \sum_{l=1}^L \alpha_l \sum_{k=1}^{B_l} \alpha_k \sum_{j=1}^{V_{k,l}} \alpha_j \sum_{i=1}^{U_{j,k,l}} \alpha_i \left\{ \mathbb{E} [\|\tilde{\mathbf{w}}_j^{t,0} - \tilde{\mathbf{w}}_j^t\|^2 + \|\tilde{\mathbf{w}}_j^t - \tilde{\mathbf{w}}_i^t\|^2 + \|\tilde{\mathbf{w}}_i^t - \tilde{\mathbf{w}}_i^{t,0}\|^2] \right\} \right\}, \\ &= \frac{12\beta^2}{T} \sum_{t=0}^{T-1} \sum_{l=1}^L \alpha_l \mathbb{E} \|\tilde{\mathbf{w}}^t - \tilde{\mathbf{w}}_l^t\|^2 + \frac{12\beta^2}{T} \sum_{t=0}^{T-1} \sum_{l=1}^L \alpha_l \sum_{k=1}^{B_l} \alpha_k \mathbb{E} \|\tilde{\mathbf{w}}_l^t - \tilde{\mathbf{w}}_k^t\|^2 + \frac{12\beta^2}{T} \sum_{t=0}^{T-1} \sum_{l=1}^L \alpha_l \sum_{k=1}^{B_l} \alpha_k \sum_{j=1}^{V_{k,l}} \alpha_j \mathbb{E} \|\tilde{\mathbf{w}}_k^t - \tilde{\mathbf{w}}_j^t\|^2 + \\ &\quad \underbrace{\frac{12\beta^2}{T} \sum_{t=0}^{T-1} \sum_{l=1}^L \alpha_l \sum_{k=1}^{B_l} \alpha_k \sum_{j=1}^{V_{k,l}} \alpha_j \sum_{i=1}^{U_{j,k,l}} \alpha_i \mathbb{E} \|\tilde{\mathbf{w}}_j^t - \tilde{\mathbf{w}}_i^t\|^2}_{L_1} + \underbrace{\frac{12\beta^2}{T} \sum_{t=0}^{T-1} \mathbb{E} \|\tilde{\mathbf{w}}^t - \tilde{\mathbf{w}}^{t,0}\|^2}_{T_5} + \underbrace{\frac{24\beta^2}{T} \sum_{t=0}^{T-1} \sum_{l=1}^L \alpha_l \mathbb{E} \|\tilde{\mathbf{w}}_l^t - \tilde{\mathbf{w}}_l^{t,0}\|^2}_{T_4} + \\ &\quad \underbrace{\frac{24\beta^2}{T} \sum_{t=0}^{T-1} \sum_{l=1}^L \alpha_l \sum_{k=1}^{B_l} \alpha_k \mathbb{E} \|\tilde{\mathbf{w}}_k^t - \tilde{\mathbf{w}}_k^{t,0}\|^2}_{T_3} + \underbrace{\frac{24\beta^2}{T} \sum_{t=0}^{T-1} \sum_{l=1}^L \alpha_l \sum_{k=1}^{B_l} \alpha_k \sum_{j=1}^{V_{k,l}} \alpha_j \mathbb{E} \|\tilde{\mathbf{w}}_j^t - \tilde{\mathbf{w}}_j^{t,0}\|^2}_{T_2} + \end{aligned}$$

$$\underbrace{\frac{12\beta^2}{T} \sum_{t=0}^{T-1} \sum_{l=1}^L \alpha_l \sum_{k=1}^{B_l} \alpha_k \sum_{j=1}^{V_{k,l}} \alpha_j \sum_{i=1}^{U_{j,k,l}} \mathbb{E} \|\tilde{\mathbf{w}}_i^t - \tilde{\mathbf{w}}_i^{t,0}\|^2}_{T_1}, \quad (70)$$

where we used the notation $\tilde{\mathbf{w}}_{j,(u)}^t, \tilde{\mathbf{w}}_{k,(u)}^t$ and $\tilde{\mathbf{w}}_{l,(u)}^t$ to represent the model of the VC, sBS and mBS, respectively, that UE u is connected to. Furthermore, (a) and (c) stem from the fact that $\|\sum_{i=1}^n \mathbf{a}_i\|^2 \leq n \sum_{i=1}^n \|\mathbf{a}_i\|^2$. Moreover, (b) arises from the β -smoothness and divergence between the loss functions assumptions.

To this end, we bound the terms T_1 to T_5 using our aggregation rules and definitions. First, let us focus on the term T_1

$$\begin{aligned} T_1 &\stackrel{(a)}{=} \frac{12\beta^2}{T} \sum_{l=1}^L \alpha_l \sum_{k=1}^{B_l} \alpha_k \sum_{j=1}^{V_{k,l}} \alpha_j \sum_{i=1}^{U_{j,k,l}} \alpha_i \sum_{t=0}^{T-1} \mathbb{E} \|\mathbf{w}_i^t - \tilde{\mathbf{w}}_i^{t,0}\|^2 \\ &\stackrel{(b)}{\leq} \frac{12\beta^2}{T} \sum_{l=1}^L \alpha_l \sum_{k=1}^{B_l} \alpha_k \sum_{j=1}^{V_{k,l}} \alpha_j \sum_{i=1}^{U_{j,k,l}} \alpha_i \sum_{t=0}^{T-1} \delta_i^t \mathbb{E} \|\mathbf{w}_i^t\|^2, \end{aligned} \quad (71)$$

where in (a), we trace back to the nearest synchronization iteration where $\mathbf{w}_i^t \leftarrow \tilde{\mathbf{w}}_i^t$ and $\tilde{\mathbf{w}}_i^t = \mathbf{w}_i^t$. Besides, we use the definition of pruning ratio in (b).

Now, we calculate the bound for the term T_2 as follows

$$\begin{aligned} T_2 &= \frac{24\beta^2}{T} \sum_{t=0}^{T-1} \sum_{l=1}^L \alpha_l \sum_{k=1}^{B_l} \alpha_k \sum_{j=1}^{V_{k,l}} \alpha_j \sum_{i=1}^{U_{j,k,l}} \alpha_i \mathbb{E} \left\| \sum_{i=1}^{U_{j,k,l}} \alpha_i (\tilde{\mathbf{w}}_i^t - \tilde{\mathbf{w}}_i^{t,0}) \right\|^2 \\ &\stackrel{(a)}{\leq} \frac{24\beta^2}{T} \sum_{t=0}^{T-1} \sum_{l=1}^L \alpha_l \sum_{k=1}^{B_l} \alpha_k \sum_{j=1}^{V_{k,l}} \alpha_j \sum_{i=1}^{U_{j,k,l}} \alpha_i \mathbb{E} \|\tilde{\mathbf{w}}_i^t - \tilde{\mathbf{w}}_i^{t,0}\|^2 \\ &\stackrel{(b)}{\leq} \frac{24\beta^2}{T} \sum_{t=0}^{T-1} \sum_{l=1}^L \alpha_l \sum_{k=1}^{B_l} \alpha_k \sum_{j=1}^{V_{k,l}} \alpha_j \sum_{i=1}^{U_{j,k,l}} \alpha_i \delta_i^t \mathbb{E} \|\mathbf{w}_i^t\|^2, \end{aligned} \quad (72)$$

where (a) arises from Jensen inequality and (b) appears from the same reasoning as in T_1 . Using similar steps, we write the following:

$$T_3 \leq \frac{24\beta^2}{T} \sum_{l=1}^L \alpha_l \sum_{k=1}^{B_l} \alpha_k \sum_{j=1}^{V_{k,l}} \alpha_j \sum_{i=1}^{U_{j,k,l}} \alpha_i \delta_i^t \mathbb{E} \|\mathbf{w}_i^t\|^2, \quad (73)$$

$$T_4 \leq \frac{24\beta^2}{T} \sum_{l=1}^L \alpha_l \sum_{k=1}^{B_l} \alpha_k \sum_{j=1}^{V_{k,l}} \alpha_j \sum_{i=1}^{U_{j,k,l}} \alpha_i \delta_i^t \mathbb{E} \|\mathbf{w}_i^t\|^2, \quad (74)$$

$$T_5 \leq \frac{24\beta^2}{T} \sum_{l=1}^L \alpha_l \sum_{k=1}^{B_l} \alpha_k \sum_{j=1}^{V_{k,l}} \alpha_j \sum_{i=1}^{U_{j,k,l}} \alpha_i \delta_i^t \mathbb{E} \|\mathbf{w}_i^t\|^2. \quad (75)$$

Plugging the above values into (69), we get

$$\begin{aligned} \frac{1}{T} \sum_{t=0}^{T-1} \mathbb{E} [\|\nabla \tilde{f}(\tilde{\mathbf{w}}^{t,0})\|^2] &\leq \frac{2(f(\tilde{\mathbf{w}}^0) - \mathbb{E}[f(\tilde{\mathbf{w}}^T)])}{\eta T} + 2\beta\eta\sigma^2 \sum_{l=1}^L \alpha_l^2 \sum_{k=1}^{B_l} \alpha_k^2 \sum_{j=1}^{V_{k,l}} \alpha_j^2 \sum_{i=1}^{U_{j,k,l}} \alpha_i^2 + \\ &\quad \underbrace{2\beta\eta G^2 \cdot \frac{1}{T} \sum_{t=0}^{T-1} \sum_{l=1}^L \alpha_l^2 \sum_{k=1}^{B_l} \alpha_k^2 \sum_{j=1}^{V_{k,l}} \alpha_j^2 \sum_{i=1}^{U_{j,k,l}} \alpha_i^2 \left(\frac{1-p_i^t}{p_i^t} \right)}_{\phi_{w,0}(\boldsymbol{\delta}, \mathbf{f}, \mathbf{P})} + 12\beta^2 \cdot (\mathbf{L}_1 + 2\{\mathbf{L}_2 + \mathbf{L}_3 + \mathbf{L}_4\}) + \\ &\quad \underbrace{96\beta^2 \cdot \frac{1}{T} \sum_{t=0}^{T-1} \sum_{l=1}^L \alpha_l \sum_{k=1}^{B_l} \alpha_k \sum_{j=1}^{V_{k,l}} \alpha_j \sum_{i=1}^{U_{j,k,l}} \alpha_i \delta_i^t \|\mathbf{w}_i^t\|^2}_{e_0(\boldsymbol{\delta})}. \end{aligned} \quad (76)$$

When $\alpha_i = \frac{1}{U_{j,k,l}}$, $\alpha_j = \frac{1}{V_{k,l}}$, $\alpha_k = \frac{1}{B_l}$ and $\alpha_l = \frac{1}{L}$, we have $\sum_{l=1}^L \alpha_l^2 \sum_{k=1}^{B_l} \alpha_k^2 \sum_{j=1}^{V_{k,l}} \alpha_j^2 \sum_{i=1}^{U_{j,k,l}} \alpha_i^2 = \frac{1}{U}$. As such, using the fact that $f(\tilde{\mathbf{w}}^T) \geq f_{\inf}$ and definition of θ_{PHFL} , we get

$$\theta_{\text{PHFL}} \leq \mathcal{O} \left(\frac{f(\tilde{\mathbf{w}}^0) - f_{\inf}}{\eta T} \right) + \mathcal{O} \left(\frac{\beta\eta\sigma^2}{U} \right) + \mathcal{O}(\delta^{\text{th}} \beta^2 D^2) + \mathcal{O}(\beta\eta G^2 \cdot \phi_{w,0}(\boldsymbol{\delta}, \mathbf{f}, \mathbf{P})) + \mathcal{O}(\beta^2 [\mathbf{L}_1 + \mathbf{L}_2 + \mathbf{L}_3 + \mathbf{L}_4]). \quad (77)$$

■

APPENDIX B
PROOF OF LEMMA 1

Lemma 1. When $\eta \leq 1/[2\sqrt{10}\kappa_0\beta]$, the average difference between the VC and local model parameters, i.e., the L_1 term of (56), is upper bounded as

$$\begin{aligned} & [\beta^2/T] \sum_{t=0}^T \sum_{l=1}^L \alpha_l \sum_{k=1}^{B_l} \alpha_k \sum_{j=1}^{V_{k,l}} \alpha_j \sum_{i=1}^{U_{j,k,l}} \alpha_i \mathbb{E} \|\bar{\mathbf{w}}_j^t - \tilde{\mathbf{w}}_i^t\|^2 \\ & \leq \mathcal{O}(\kappa_0 \eta^2 \beta^2 \sigma^2) + \mathcal{O}(\kappa_0^2 \eta^2 \beta^2 \varepsilon_{\text{vc}}^2) + \mathcal{O}(\kappa_0 \eta^2 \beta^2 G^2 \cdot \varphi_{\text{w},L_1}(\boldsymbol{\delta}, \mathbf{f}, \mathbf{P})) + \mathcal{O}(\delta^{\text{th}} \beta^2 D^2), \end{aligned} \quad (78)$$

where $\varphi_{\text{w},L_1}(\boldsymbol{\delta}, \mathbf{f}, \mathbf{P}) = [1/T] \sum_{l=1}^L \alpha_l \sum_{k=1}^{B_l} \alpha_k \sum_{j=1}^{V_{k,l}} \alpha_j \sum_{i=1}^{U_{j,k,l}} \alpha_i \sum_{t=0}^{T-1} (1/p_i^t - 1)$.

Proof.

$$\begin{aligned} & \frac{1}{T} \sum_{t=0}^{T-1} \sum_{l=1}^L \alpha_l \sum_{k=1}^{B_l} \alpha_k \sum_{j=1}^{V_{k,l}} \alpha_j \sum_{i=1}^{U_{j,k,l}} \alpha_i \mathbb{E} \|\bar{\mathbf{w}}_j^t - \tilde{\mathbf{w}}_i^t\|^2 \\ & = \frac{1}{T} \sum_{t=0}^{T-1} \sum_{l=1}^L \alpha_l \sum_{k=1}^{B_l} \alpha_k \sum_{j=1}^{V_{k,l}} \alpha_j \sum_{i=1}^{U_{j,k,l}} \alpha_i \mathbb{E} \left\| \bar{\mathbf{w}}_j^{\bar{t}_0,0} - \eta \sum_{i'=1}^{U_{j,k,l}} \alpha_{i'} \sum_{\tau=\bar{t}_0}^{t-1} \tilde{g}(\tilde{\mathbf{w}}_{i'}^{\tau,0}) \frac{\mathbf{1}_{i'}^\tau}{p_{i'}^\tau} - \left(\bar{\mathbf{w}}_i^{\bar{t}_0,0} - \eta \sum_{\tau=\bar{t}_0}^{t-1} \tilde{g}(\tilde{\mathbf{w}}_i^{\tau,0}) \frac{\mathbf{1}_i^\tau}{p_i^\tau} \right) \right\|^2, \\ & \stackrel{(a)}{\leq} \frac{2}{T} \sum_{t=0}^{T-1} \sum_{l=1}^L \alpha_l \sum_{k=1}^{B_l} \alpha_k \sum_{j=1}^{V_{k,l}} \alpha_j \sum_{i=1}^{U_{j,k,l}} \alpha_i \mathbb{E} \left\| \bar{\mathbf{w}}_j^{\bar{t}_0,0} - \tilde{\mathbf{w}}_i^{\bar{t}_0,0} \right\|^2 + \\ & \quad \frac{2\eta^2}{T} \sum_{t=0}^{T-1} \sum_{l=1}^L \alpha_l \sum_{k=1}^{B_l} \alpha_k \sum_{j=1}^{V_{k,l}} \alpha_j \sum_{i=1}^{U_{j,k,l}} \alpha_i \mathbb{E} \left\| \sum_{\tau=\bar{t}_0}^{t-1} \tilde{g}(\tilde{\mathbf{w}}_i^{\tau,0}) \frac{\mathbf{1}_i^\tau}{p_i^\tau} - \sum_{i'=1}^{U_{j,k,l}} \alpha_{i'} \sum_{\tau=\bar{t}_0}^{t-1} \tilde{g}(\tilde{\mathbf{w}}_{i'}^{\tau,0}) \frac{\mathbf{1}_{i'}^\tau}{p_{i'}^\tau} \right\|^2, \end{aligned} \quad (79)$$

where $\bar{t}_0 = [\{(m\kappa_3 + t_3)\kappa_2 + t_2\}\kappa_1 + t_1]\kappa_0$ and (a) comes from $\|\sum_{i=1}^n \mathbf{a}_i\|^2 \leq n \sum_{i=1}^n \|\mathbf{a}_i\|^2$.

Note that the first term in (79) comes from the VC receiving a weighted combination of the pruned models of its associated UEs. For this term, we have

$$\begin{aligned} & 2 \sum_{l=1}^L \alpha_l \sum_{k=1}^{B_l} \alpha_k \sum_{j=1}^{V_{k,l}} \alpha_j \sum_{i=1}^{U_{j,k,l}} \alpha_i \mathbb{E} \left\| \bar{\mathbf{w}}_j^{\bar{t}_0,0} - \tilde{\mathbf{w}}_i^{\bar{t}_0,0} \right\|^2, \\ & \stackrel{(a)}{=} 2 \sum_{l=1}^L \alpha_l \sum_{k=1}^{B_l} \alpha_k \sum_{j=1}^{V_{k,l}} \alpha_j \sum_{i=1}^{U_{j,k,l}} \alpha_i \mathbb{E} \left\| \left(\bar{\mathbf{w}}_j^{\bar{t}_0,0} - \mathbf{w}_j^{\bar{t}_0} \right) + \left(\mathbf{w}_i^{\bar{t}_0} - \tilde{\mathbf{w}}_i^{\bar{t}_0,0} \right) \right\|^2, \\ & \stackrel{(b)}{\leq} 4 \sum_{l=1}^L \alpha_l \sum_{k=1}^{B_l} \alpha_k \sum_{j=1}^{V_{k,l}} \alpha_j \sum_{i=1}^{U_{j,k,l}} \alpha_i \mathbb{E} \left\| \bar{\mathbf{w}}_j^{\bar{t}_0,0} - \mathbf{w}_j^{\bar{t}_0} \right\|^2 + 4 \sum_{l=1}^L \alpha_l \sum_{k=1}^{B_l} \alpha_k \sum_{j=1}^{V_{k,l}} \alpha_j \sum_{i=1}^{U_{j,k,l}} \alpha_i \mathbb{E} \left\| \mathbf{w}_i^{\bar{t}_0} - \tilde{\mathbf{w}}_i^{\bar{t}_0,0} \right\|^2, \\ & \leq 4 \sum_{l=1}^L \alpha_l \sum_{k=1}^{B_l} \alpha_k \sum_{j=1}^{V_{k,l}} \alpha_j \left\{ \mathbb{E} \left\| \bar{\mathbf{w}}_j^{\bar{t}_0,0} - \mathbf{w}_j^{\bar{t}_0} \right\|^2 + \sum_{i=1}^{U_{j,k,l}} \alpha_i \delta_i^{\bar{t}_0} \mathbb{E} \left\| \mathbf{w}_i^{\bar{t}_0} \right\|^2 \right\}, \\ & \leq 8 \sum_{l=1}^L \alpha_l \sum_{k=1}^{B_l} \alpha_k \sum_{j=1}^{V_{k,l}} \alpha_j \sum_{i=1}^{U_{j,k,l}} \alpha_i \delta_i^{\bar{t}_0} \mathbb{E} \left\| \mathbf{w}_i^{\bar{t}_0} \right\|^2, \end{aligned} \quad (80)$$

where (a) is true since $\bar{\mathbf{w}}_j^{\bar{t}_0} = \mathbf{w}_j^{\bar{t}_0}$ and (b) comes from $\|\sum_{i=1}^n \mathbf{a}_i\|^2 \leq n \sum_{i=1}^n \|\mathbf{a}_i\|^2$.

As such, the first term is bounded as

$$\frac{2}{T} \sum_{t=0}^{T-1} \sum_{l=1}^L \alpha_l \sum_{k=1}^{B_l} \alpha_k \sum_{j=1}^{V_{k,l}} \alpha_j \sum_{i=1}^{U_{j,k,l}} \alpha_i \mathbb{E} \left\| \bar{\mathbf{w}}_j^{\bar{t}_0,0} - \tilde{\mathbf{w}}_i^{\bar{t}_0,0} \right\|^2 \leq \frac{8}{T} \sum_{t=0}^{T-1} \sum_{l=1}^L \alpha_l \sum_{k=1}^{B_l} \alpha_k \sum_{j=1}^{V_{k,l}} \alpha_j \sum_{i=1}^{U_{j,k,l}} \alpha_i \delta_i^{\lfloor t/\kappa_0 \rfloor} \mathbb{E} \left\| \mathbf{w}_i^{\lfloor t/\kappa_0 \rfloor} \right\|^2. \quad (81)$$

For the second term of (79), we have

$$\begin{aligned} & \frac{2\eta^2}{T} \sum_{t=0}^{T-1} \sum_{l=1}^L \alpha_l \sum_{k=1}^{B_l} \alpha_k \sum_{j=1}^{V_{k,l}} \alpha_j \sum_{i=1}^{U_{j,k,l}} \alpha_i \mathbb{E} \left\| \sum_{\tau=\bar{t}_0}^{t-1} \left[\tilde{g}(\tilde{\mathbf{w}}_i^{\tau,0}) \frac{\mathbf{1}_i^\tau}{p_i^\tau} - \sum_{i'=1}^{U_{j,k,l}} \alpha_{i'} \tilde{g}(\tilde{\mathbf{w}}_{i'}^{\tau,0}) \frac{\mathbf{1}_{i'}^\tau}{p_{i'}^\tau} \right] \right\|^2 \\ & = \frac{2\eta^2}{T} \sum_{t=0}^{T-1} \sum_{l=1}^L \alpha_l \sum_{k=1}^{B_l} \alpha_k \sum_{j=1}^{V_{k,l}} \alpha_j \sum_{i=1}^{U_{j,k,l}} \alpha_i \mathbb{E} \left\| \sum_{\tau=\bar{t}_0}^{t-1} \left[\tilde{g}(\tilde{\mathbf{w}}_i^{\tau,0}) \frac{\mathbf{1}_i^\tau}{p_i^\tau} \pm \nabla \tilde{f}_i(\tilde{\mathbf{w}}_i^{\tau,0}) \pm \sum_{i'=1}^{U_{j,k,l}} \alpha_{i'} \nabla \tilde{f}_i(\tilde{\mathbf{w}}_{i'}^{\tau,0}) - \sum_{i'=1}^{U_{j,k,l}} \alpha_{i'} \tilde{g}(\tilde{\mathbf{w}}_{i'}^{\tau,0}) \frac{\mathbf{1}_{i'}^\tau}{p_{i'}^\tau} \right] \right\|^2 \\ & \leq \frac{4\eta^2}{T} \sum_{t=0}^{T-1} \sum_{l=1}^L \alpha_l \sum_{k=1}^{B_l} \alpha_k \sum_{j=1}^{V_{k,l}} \alpha_j \sum_{i=1}^{U_{j,k,l}} \alpha_i \mathbb{E} \left\| \sum_{\tau=\bar{t}_0}^{t-1} \left[\left(\tilde{g}(\tilde{\mathbf{w}}_i^{\tau,0}) \frac{\mathbf{1}_i^\tau}{p_i^\tau} - \nabla \tilde{f}_i(\tilde{\mathbf{w}}_i^{\tau,0}) \right) - \sum_{i'=1}^{U_{j,k,l}} \alpha_{i'} \left(\tilde{g}(\tilde{\mathbf{w}}_{i'}^{\tau,0}) \frac{\mathbf{1}_{i'}^\tau}{p_{i'}^\tau} - \nabla \tilde{f}_i(\tilde{\mathbf{w}}_{i'}^{\tau,0}) \right) \right] \right\|^2 + \end{aligned}$$

$$\frac{4\eta^2}{T} \sum_{t=0}^{T-1} \sum_{l=1}^L \alpha_l \sum_{k=1}^{B_l} \alpha_k \sum_{j=1}^{V_{k,l}} \alpha_j \sum_{i=1}^{U_{j,k,l}} \alpha_i \mathbb{E} \left\| \sum_{\tau=\bar{l}_0}^{t-1} \left[\nabla \tilde{f}_i(\tilde{\mathbf{w}}_i^{\tau,0}) - \sum_{i'=1}^{U_{j,k,l}} \alpha_{i'} \nabla \tilde{f}_{i'}(\tilde{\mathbf{w}}_{i'}^{\tau,0}) \right] \right\|^2. \quad (82)$$

We calculate the first and the second terms of (82) in Lemma 5 and Lemma 6, respectively.

Lemma 5.

$$\begin{aligned} & \frac{4\eta^2}{T} \sum_{t=0}^{T-1} \sum_{l=1}^L \alpha_l \sum_{k=1}^{B_l} \alpha_k \sum_{j=1}^{V_{k,l}} \alpha_j \sum_{i=1}^{U_{j,k,l}} \alpha_i \mathbb{E} \left\| \sum_{\tau=\bar{l}_0}^{t-1} \left[\left(\tilde{g}(\tilde{\mathbf{w}}_i^{\tau,0}) \frac{\mathbf{1}_i^\tau}{p_i^\tau} - \nabla \tilde{f}_i(\tilde{\mathbf{w}}_i^{\tau,0}) \right) - \sum_{i'=1}^{U_{j,k,l}} \alpha_{i'} \left(\tilde{g}(\tilde{\mathbf{w}}_{i'}^{\tau,0}) \frac{\mathbf{1}_{i'}^\tau}{p_{i'}^\tau} - \nabla \tilde{f}_{i'}(\tilde{\mathbf{w}}_{i'}^{\tau,0}) \right) \right] \right\|^2 \\ & \leq 8\kappa_0 \eta^2 \sigma^2 + 8\kappa_0 \eta^2 G^2 \cdot \varphi_{w,L_1}, \end{aligned} \quad (83)$$

where $\varphi_{w,L_1} = \frac{1}{T} \sum_{l=1}^L \alpha_l \sum_{k=1}^{B_l} \alpha_k \sum_{j=1}^{V_{k,l}} \alpha_j \sum_{i=1}^{U_{j,k,l}} \alpha_i \sum_{t=0}^{T-1} \left(\frac{1-p_i^t}{p_i^t} \right)$.

Lemma 6.

$$\begin{aligned} & \frac{4\eta^2}{T} \sum_{t=0}^{T-1} \sum_{l=1}^L \alpha_l \sum_{k=1}^{B_l} \alpha_k \sum_{j=1}^{V_{k,l}} \alpha_j \sum_{i=1}^{U_{j,k,l}} \alpha_i \mathbb{E} \left\| \sum_{\tau=\bar{l}_0}^{t-1} \left[\nabla \tilde{f}_i(\tilde{\mathbf{w}}_i^{\tau,0}) - \sum_{i'=1}^{U_{j,k,l}} \alpha_{i'} \nabla \tilde{f}_{i'}(\tilde{\mathbf{w}}_{i'}^{\tau,0}) \right] \right\|^2 \\ & \leq 20\kappa_0^2 \eta^2 \varepsilon_{vc}^2 + 40\kappa_0^2 \eta^2 \beta^2 \cdot \bar{\mathbf{e}}_{\mathcal{D}} + \frac{40\kappa_0^2 \eta^2 \beta^2}{T} \sum_{t=0}^{T-1} \sum_{l=1}^L \alpha_l \sum_{k=1}^{B_l} \alpha_k \sum_{j=1}^{V_{k,l}} \alpha_j \sum_{i=1}^{U_{j,k,l}} \alpha_i \mathbb{E} \|\tilde{\mathbf{w}}_j^t - \tilde{\mathbf{w}}_i^t\|^2, \end{aligned} \quad (84)$$

where $\bar{\mathbf{e}}_{\mathcal{D}} = \frac{1}{T} \sum_{t=0}^{T-1} \sum_{l=1}^L \alpha_l \sum_{k=1}^{B_l} \alpha_k \sum_{j=1}^{V_{k,l}} \alpha_j \sum_{i=1}^{U_{j,k,l}} \alpha_i \delta_i^t \mathbb{E} \|\mathbf{w}_i^t\|^2$.

Using Lemma 5 and Lemma 6, we write

$$\frac{1}{T} \sum_{t=0}^T \sum_{l=1}^L \alpha_l \sum_{k=1}^{B_l} \alpha_k \sum_{j=1}^{V_{k,l}} \alpha_j \sum_{i=1}^{U_{j,k,l}} \alpha_i \mathbb{E} \|\tilde{\mathbf{w}}_j^t - \tilde{\mathbf{w}}_i^t\|^2 \leq \frac{8\kappa_0 \eta^2 \sigma^2 + 20\kappa_0^2 \eta^2 \varepsilon_{vc}^2 + 8\kappa_0 \eta^2 G^2 \cdot \varphi_{w,L_1} + 40\kappa_0^2 \eta^2 \beta^2 \cdot \bar{\mathbf{e}}_{\mathcal{D}} + 8 \cdot \mathbf{e}_{p,L_1}}{1 - 40\kappa_0^2 \eta^2 \beta^2}, \quad (85)$$

where $\mathbf{e}_{p,L_1} = \frac{1}{T} \sum_{t=0}^{T-1} \sum_{l=1}^L \alpha_l \sum_{k=1}^{B_l} \alpha_k \sum_{j=1}^{V_{k,l}} \alpha_j \sum_{i=1}^{U_{j,k,l}} \alpha_i \delta_i^{\lfloor t/\kappa_0 \rfloor} \mathbb{E} \|\mathbf{w}_i^{\lfloor t/\kappa_0 \rfloor}\|^2$.

Now multiplying both sides of (85) by $12\beta^2$, we get

$$\begin{aligned} & \frac{12\beta^2}{T} \sum_{t=0}^T \sum_{l=1}^L \alpha_l \sum_{k=1}^{B_l} \alpha_k \sum_{j=1}^{V_{k,l}} \alpha_j \sum_{i=1}^{U_{j,k,l}} \alpha_i \mathbb{E} \|\tilde{\mathbf{w}}_j^t - \tilde{\mathbf{w}}_i^t\|^2 \\ & \leq \frac{96\kappa_0 \eta^2 \beta^2 \sigma^2 + 240\kappa_0^2 \eta^2 \beta^2 \varepsilon_{vc}^2 + 96\kappa_0 \eta^2 \beta^2 G^2 \cdot \varphi_{w,L_1} + 480\kappa_0^2 \eta^2 \beta^4 \cdot \bar{\mathbf{e}}_{\mathcal{D}} + 96\beta^2 \cdot \mathbf{e}_{p,L_1}}{1 - 40\kappa_0^2 \eta^2 \beta^2}. \end{aligned} \quad (86)$$

When $\eta \leq \frac{1}{2\sqrt{10}\kappa_0\beta}$, we have $1 - 40\kappa_0^2 \eta^2 \beta^2 \geq 1$, and the previous assumption of $\eta \leq \frac{1}{\beta}$ is automatically satisfied. As such, we write

$$\begin{aligned} & \frac{12\beta^2}{T} \sum_{t=0}^T \sum_{l=1}^L \alpha_l \sum_{k=1}^{B_l} \alpha_k \sum_{j=1}^{V_{k,l}} \alpha_j \sum_{i=1}^{U_{j,k,l}} \alpha_i \mathbb{E} \|\tilde{\mathbf{w}}_j^t - \tilde{\mathbf{w}}_i^t\|^2 \\ & \leq 96\kappa_0 \eta^2 \beta^2 \sigma^2 + 240\kappa_0^2 \eta^2 \beta^2 \varepsilon_{vc}^2 + 96\kappa_0 \eta^2 \beta^2 G^2 \cdot \varphi_{w,L_1} + 480\kappa_0^2 \eta^2 \beta^4 \cdot \bar{\mathbf{e}}_{\mathcal{D}} + 96\beta^2 \cdot \mathbf{e}_{p,L_1} \\ & \approx \mathcal{O}(\kappa_0 \eta^2 \beta^2 \sigma^2) + \mathcal{O}(\kappa_0^2 \eta^2 \beta^2 \varepsilon_{vc}^2) + \mathcal{O}(\kappa_0 \eta^2 \beta^2 G^2 \cdot \varphi_{w,L_1}) + \mathcal{O}(\delta^{\text{th}} \beta^2 D^2). \end{aligned} \quad (87)$$

A. Missing Proof of Lemma 5

$$\begin{aligned} & 4\eta^2 \sum_{l=1}^L \alpha_l \sum_{k=1}^{B_l} \alpha_k \sum_{j=1}^{V_{k,l}} \alpha_j \sum_{i=1}^{U_{j,k,l}} \alpha_i \mathbb{E} \left\| \sum_{\tau=\bar{l}_0}^{t-1} \left\{ \left(\tilde{g}(\tilde{\mathbf{w}}_i^{\tau,0}) \frac{\mathbf{1}_i^\tau}{p_i^\tau} - \nabla \tilde{f}_i(\tilde{\mathbf{w}}_i^{\tau,0}) \right) - \sum_{i'=1}^{U_{j,k,l}} \alpha_{i'} \left(\tilde{g}(\tilde{\mathbf{w}}_{i'}^{\tau,0}) \frac{\mathbf{1}_{i'}^\tau}{p_{i'}^\tau} - \nabla \tilde{f}_{i'}(\tilde{\mathbf{w}}_{i'}^{\tau,0}) \right) \right\} \right\|^2, \\ & \stackrel{(a)}{=} 4\eta^2 \sum_{l=1}^L \alpha_l \sum_{k=1}^{B_l} \alpha_k \sum_{j=1}^{V_{k,l}} \alpha_j \left\{ \sum_{i=1}^{U_{j,k,l}} \alpha_i \mathbb{E} \left\| \sum_{\tau=\bar{l}_0}^{t-1} \left(\tilde{g}(\tilde{\mathbf{w}}_i^{\tau,0}) \frac{\mathbf{1}_i^\tau}{p_i^\tau} - \nabla \tilde{f}_i(\tilde{\mathbf{w}}_i^{\tau,0}) \right) \right\|^2 - \mathbb{E} \left\| \sum_{\tau=\bar{l}_0}^{t-1} \sum_{i'=1}^{U_{j,k,l}} \alpha_{i'} \left(\tilde{g}(\tilde{\mathbf{w}}_{i'}^{\tau,0}) \frac{\mathbf{1}_{i'}^\tau}{p_{i'}^\tau} - \nabla \tilde{f}_{i'}(\tilde{\mathbf{w}}_{i'}^{\tau,0}) \right) \right\|^2 \right\}, \\ & \stackrel{(b)}{=} 4\eta^2 \sum_{l=1}^L \alpha_l \sum_{k=1}^{B_l} \alpha_k \sum_{j=1}^{V_{k,l}} \alpha_j \left\{ \sum_{i=1}^{U_{j,k,l}} \alpha_i \sum_{\tau=\bar{l}_0}^{t-1} \mathbb{E} \left\| \tilde{g}(\tilde{\mathbf{w}}_i^{\tau,0}) \frac{\mathbf{1}_i^\tau}{p_i^\tau} \pm \tilde{g}(\tilde{\mathbf{w}}_i^{\tau,0}) - \nabla \tilde{f}_i(\tilde{\mathbf{w}}_i^{\tau,0}) \right\|^2 - \right. \\ & \quad \left. \sum_{\tau=\bar{l}_0}^{t-1} \mathbb{E} \left\| \sum_{i'=1}^{U_{j,k,l}} \alpha_{i'} \left(\tilde{g}(\tilde{\mathbf{w}}_{i'}^{\tau,0}) \frac{\mathbf{1}_{i'}^\tau}{p_{i'}^\tau} \pm \tilde{g}(\tilde{\mathbf{w}}_{i'}^{\tau,0}) - \nabla \tilde{f}_{i'}(\tilde{\mathbf{w}}_{i'}^{\tau,0}) \right) \right\|^2 \right\}, \end{aligned}$$

$$\begin{aligned}
& \stackrel{(c)}{=} 8\eta^2 \sum_{l=1}^L \alpha_l \sum_{k=1}^{B_l} \alpha_k \sum_{j=1}^{V_{k,l}} \alpha_j \sum_{i=1}^{U_{j,k,l}} \alpha_i \sum_{\tau=\bar{t}_0}^{t-1} \mathbb{E} \left\{ \left\| \left(\frac{\mathbf{1}_i^\tau}{p_i^\tau} - 1 \right) \tilde{g}(\tilde{\mathbf{w}}_i^{\tau,0}) \right\|^2 + \left\| \tilde{g}(\tilde{\mathbf{w}}_i^{\tau,0}) - \nabla \tilde{f}_i(\tilde{\mathbf{w}}_i^{\tau,0}) \right\|^2 \right\} - \\
& 8\eta^2 \sum_{l=1}^L \alpha_l \sum_{k=1}^{B_l} \alpha_k \sum_{j=1}^{V_{k,l}} \alpha_j \sum_{i=1}^{U_{j,k,l}} \sum_{\tau=\bar{t}_0}^{t-1} \sum_{i'=1}^{U_{j,k,l}} \alpha_{i'}^2 \mathbb{E} \left\{ \left\| \left(\frac{\mathbf{1}_{i'}^\tau}{p_{i'}^\tau} - 1 \right) \tilde{g}(\tilde{\mathbf{w}}_{i'}^{\tau,0}) \right\|^2 + \left\| \tilde{g}(\tilde{\mathbf{w}}_{i'}^{\tau,0}) - \nabla \tilde{f}_{i'}(\tilde{\mathbf{w}}_{i'}^{\tau,0}) \right\|^2 \right\}, \\
& \stackrel{(d)}{\leq} 8\eta^2 \sum_{l=1}^L \alpha_l \sum_{k=1}^{B_l} \alpha_k \sum_{j=1}^{V_{k,l}} \alpha_j \sum_{i=1}^{U_{j,k,l}} \alpha_i \sum_{\tau=\bar{t}_0}^{t-1} \left\{ \left(\frac{1-p_i^\tau}{p_i^\tau} \right) \mathbb{E} \left\| \tilde{g}(\tilde{\mathbf{w}}_i^{\tau,0}) \right\|^2 + \sigma^2 \right\} - \\
& 8\eta^2 \sum_{l=1}^L \alpha_l \sum_{k=1}^{B_l} \alpha_k \sum_{j=1}^{V_{k,l}} \alpha_j \sum_{\tau=\bar{t}_0}^{t-1} \sum_{i=1}^{U_{j,k,l}} \alpha_i^2 \left\{ \left(\frac{1-p_i^\tau}{p_i^\tau} \right) \mathbb{E} \left\| \tilde{g}(\tilde{\mathbf{w}}_i^{\tau,0}) \right\|^2 + \sigma^2 \right\}, \\
& \stackrel{(e)}{\leq} 8\kappa_0 \eta^2 \sigma^2 - 8\eta^2 \sum_{l=1}^L \alpha_l \sum_{k=1}^{B_l} \alpha_k \sum_{j=1}^{V_{k,l}} \alpha_j \sum_{\tau=\bar{t}_0}^{t-1} \sum_{i=1}^{U_{j,k,l}} \alpha_i^2 \sigma^2 + \\
& 8\eta^2 \sum_{l=1}^L \alpha_l \sum_{k=1}^{B_l} \alpha_k \sum_{j=1}^{V_{k,l}} \alpha_j \sum_{\tau=\bar{t}_0}^{t-1} \sum_{i=1}^{U_{j,k,l}} \alpha_i (1-\alpha_i) ([1-p_i^\tau]/p_i^\tau) \mathbb{E} \left\| \tilde{g}(\tilde{\mathbf{w}}_i^{\tau,0}) \right\|^2, \\
& \leq 8\kappa_0 \eta^2 \sigma^2 + 8\eta^2 \sum_{l=1}^L \alpha_l \sum_{k=1}^{B_l} \alpha_k \sum_{j=1}^{V_{k,l}} \alpha_j \sum_{\tau=\bar{t}_0}^{t-1} \sum_{i=1}^{U_{j,k,l}} \alpha_i \left(\frac{1-p_i^\tau}{p_i^\tau} \right) \mathbb{E} \left\| \tilde{g}(\tilde{\mathbf{w}}_i^{\tau,0}) \right\|^2, \tag{88}
\end{aligned}$$

where (a) stems from the fact that $\sum_{i=1}^n p_i \|\mathbf{x}_i - \bar{\mathbf{x}}\|^2 = \sum_{i=1}^n p_i \|\mathbf{x}_i\|^2 - \|\bar{\mathbf{x}}\|^2$, where $\bar{\mathbf{x}} = \sum_{i=1}^n p_i \mathbf{x}_i$ for any $0 \leq p_i \leq 1$ and $\sum_{i=1}^n p_i = 1$. Besides, (b) is true due to the time independence of the SGD assumption. Furthermore, in (c) and (d), we use the bounded divergence of the mini-batch gradient assumption and client independence property.

B. Missing Proof of Lemma 6

$$\begin{aligned}
& \frac{4\eta^2}{T} \sum_{t=0}^{T-1} \sum_{l=1}^L \alpha_l \sum_{k=1}^{B_l} \alpha_k \sum_{j=1}^{V_{k,l}} \alpha_j \sum_{i=1}^{U_{j,k,l}} \alpha_i \mathbb{E} \left\| \sum_{\tau=\bar{t}_0}^{t-1} \left[\nabla \tilde{f}_i(\tilde{\mathbf{w}}_i^{\tau,0}) - \sum_{i'=1}^{U_{j,k,l}} \alpha_{i'} \nabla \tilde{f}_{i'}(\tilde{\mathbf{w}}_{i'}^{\tau,0}) \right] \right\|^2 \\
& = \frac{4\kappa_0 \eta^2}{T} \sum_{t=0}^{T-1} \sum_{l=1}^L \alpha_l \sum_{k=1}^{B_l} \alpha_k \sum_{j=1}^{V_{k,l}} \alpha_j \sum_{i=1}^{U_{j,k,l}} \alpha_i \sum_{\tau=\bar{t}_0}^{t-1} \mathbb{E} \left\| \left(\nabla \tilde{f}_i(\tilde{\mathbf{w}}_i^{\tau,0}) - \nabla \tilde{f}_i(\tilde{\mathbf{w}}_i^\tau) \right) + \left(\nabla \tilde{f}_i(\tilde{\mathbf{w}}_i^\tau) - \nabla \tilde{f}_i(\tilde{\mathbf{w}}_j^\tau) \right) + \right. \\
& \quad \left(\nabla \tilde{f}_i(\tilde{\mathbf{w}}_j^\tau) - \sum_{i'=1}^{U_{j,k,l}} \alpha_{i'} \nabla \tilde{f}_{i'}(\tilde{\mathbf{w}}_j^\tau) \right) + \left(\sum_{i'=1}^{U_{j,k,l}} \alpha_{i'} \nabla \tilde{f}_{i'}(\tilde{\mathbf{w}}_j^\tau) - \sum_{i'=1}^{U_{j,k,l}} \alpha_{i'} \nabla \tilde{f}_{i'}(\tilde{\mathbf{w}}_i^\tau) \right) + \\
& \quad \left. \left(\sum_{i'=1}^{U_{j,k,l}} \alpha_{i'} \nabla \tilde{f}_{i'}(\tilde{\mathbf{w}}_i^\tau) - \sum_{i'=1}^{U_{j,k,l}} \alpha_{i'} \nabla \tilde{f}_{i'}(\tilde{\mathbf{w}}_{i'}^{\tau,0}) \right) \right\|^2 \\
& \leq \frac{20\kappa_0^2 \eta^2}{T} \sum_{t=0}^{T-1} \sum_{l=1}^L \alpha_l \sum_{k=1}^{B_l} \alpha_k \sum_{j=1}^{V_{k,l}} \alpha_j \sum_{i=1}^{U_{j,k,l}} \alpha_i \left[2\beta^2 \mathbb{E} \|\tilde{\mathbf{w}}_i^t - \tilde{\mathbf{w}}_i^{t,0}\|^2 + \varepsilon_{\text{vc}}^2 + 2\beta^2 \mathbb{E} \|\tilde{\mathbf{w}}_j^t - \tilde{\mathbf{w}}_i^t\|^2 \right] \\
& \leq 20\kappa_0^2 \eta^2 \varepsilon_{\text{vc}}^2 + 40\kappa_0^2 \eta^2 \beta^2 \cdot \bar{\varepsilon}_\delta + \frac{40\kappa_0^2 \eta^2 \beta^2}{T} \sum_{t=0}^{T-1} \sum_{l=1}^L \alpha_l \sum_{k=1}^{B_l} \alpha_k \sum_{j=1}^{V_{k,l}} \alpha_j \sum_{i=1}^{U_{j,k,l}} \alpha_i \mathbb{E} \|\tilde{\mathbf{w}}_j^t - \tilde{\mathbf{w}}_i^t\|^2, \tag{89}
\end{aligned}$$

where $\bar{\varepsilon}_\delta = \frac{1}{T} \sum_{t=0}^{T-1} \sum_{l=1}^L \alpha_l \sum_{k=1}^{B_l} \alpha_k \sum_{j=1}^{V_{k,l}} \alpha_j \sum_{i=1}^{U_{j,k,l}} \alpha_i \delta_i^t \mathbb{E} \|\mathbf{w}_i^t\|^2$. ■

APPENDIX C PROOF OF LEMMA 2

Lemma 2. When $\eta \leq 1/[2\sqrt{10}\kappa_0\kappa_1\beta]$, the difference between the sBS model parameters and VC model parameters, i.e., the L_2 term of (56), is upper bounded as

$$\begin{aligned}
& \frac{\beta^2}{T} \sum_{t=0}^{T-1} \sum_{l=1}^L \alpha_l \sum_{k=1}^{B_l} \alpha_k \sum_{j=1}^{V_{k,l}} \alpha_j \mathbb{E} \|\tilde{\mathbf{w}}_k^t - \tilde{\mathbf{w}}_j^t\|^2 \\
& \leq \mathcal{O}(\beta^4 \kappa_0^4 \kappa_1^4 \eta^4 \varepsilon_{\text{vc}}^2) + \mathcal{O}(\kappa_0^2 \kappa_1^2 \eta^2 \beta^2 \varepsilon_{\text{sbs}}^2) + \mathcal{O}(\kappa_0 \kappa_1 \eta^2 \sigma^2 \beta^2) + \mathcal{O}(\delta^h \beta^2 D^2) + \\
& \quad \mathcal{O}(\kappa_0^3 \kappa_1^3 \beta^4 \eta^4 G^2 \cdot \varphi_{\mathbf{w},L_1}(\boldsymbol{\delta}, \mathbf{f}, \mathbf{P})) + \mathcal{O}(\kappa_0 \kappa_1 \beta^2 \eta^2 \cdot \varphi_{\mathbf{w},L_2}(\boldsymbol{\delta}, \mathbf{f}, \mathbf{P})), \tag{90}
\end{aligned}$$

where $\varphi_{\mathbf{w},L_2}(\boldsymbol{\delta}, \mathbf{f}, \mathbf{P}) = [1/T] \sum_{t=0}^{T-1} \sum_{l=1}^L \alpha_l \sum_{k=1}^{B_l} \alpha_k \sum_{j=1}^{V_{k,l}} \alpha_j \sum_{i=1}^{U_{j,k,l}} \alpha_i^2 (1/p_i^t - 1)$.

Proof.

$$\begin{aligned}
& \frac{1}{T} \sum_{t=0}^{T-1} \sum_{l=1}^L \alpha_l \sum_{k=1}^{B_l} \alpha_k \sum_{j=1}^{V_{k,l}} \alpha_j \mathbb{E} \left\| \tilde{\mathbf{w}}_k' - \tilde{\mathbf{w}}_j' \right\|^2 \\
&= \frac{1}{T} \sum_{t=0}^{T-1} \sum_{l=1}^L \alpha_l \sum_{k=1}^{B_l} \alpha_k \sum_{j=1}^{V_{k,l}} \alpha_j \mathbb{E} \left\| \tilde{\mathbf{w}}_k^{\bar{t}_1,0} - \eta \sum_{\tau=\bar{t}_1}^{t-1} \sum_{j'=1}^{V_{k,l}} \alpha_{j'} \sum_{i'=1}^{U_{j',k,l}} \alpha_{i'} \tilde{g} \left(\tilde{\mathbf{w}}_{i'}^{\tau,0} \right) \frac{\mathbf{1}_{i'}^\tau}{p_{i'}^\tau} - \tilde{\mathbf{w}}_j^{\bar{t}_1,0} + \eta \sum_{\tau=\bar{t}_1}^{t-1} \sum_{i=1}^{U_{j,k,l}} \alpha_i \tilde{g} \left(\tilde{\mathbf{w}}_i^{\tau,0} \right) \frac{\mathbf{1}_i^\tau}{p_i^\tau} \right\|^2, \\
&\leq \frac{2}{T} \sum_{t=0}^{T-1} \sum_{l=1}^L \alpha_l \sum_{k=1}^{B_l} \alpha_k \sum_{j=1}^{V_{k,l}} \alpha_j \mathbb{E} \left\| \tilde{\mathbf{w}}_k^{\bar{t}_1,0} - \tilde{\mathbf{w}}_j^{\bar{t}_1,0} \right\|^2 + \\
&\quad \frac{2\eta^2}{T} \sum_{t=0}^{T-1} \sum_{l=1}^L \alpha_l \sum_{k=1}^{B_l} \alpha_k \sum_{j=1}^{V_{k,l}} \alpha_j \mathbb{E} \left\| \sum_{\tau=\bar{t}_1}^{t-1} \left[\sum_{i=1}^{U_{j,k,l}} \alpha_i \tilde{g} \left(\tilde{\mathbf{w}}_i^{\tau,0} \right) \frac{\mathbf{1}_i^\tau}{p_i^\tau} - \sum_{j'=1}^{V_{k,l}} \alpha_{j'} \sum_{i'=1}^{U_{j',k,l}} \alpha_{i'} \tilde{g} \left(\tilde{\mathbf{w}}_{i'}^{\tau,0} \right) \frac{\mathbf{1}_{i'}^\tau}{p_{i'}^\tau} \right] \right\|^2,
\end{aligned} \tag{91}$$

where $\bar{t}_1 = \{(m\kappa_3 + t_3)\kappa_2 + t_2\}\kappa_1\kappa_0$ and the inequalities in the last term arise from Jensen inequality.

For the first term in (91), we have

$$\begin{aligned}
& 2 \sum_{l=1}^L \alpha_l \sum_{k=1}^{B_l} \alpha_k \sum_{j=1}^{V_{k,l}} \alpha_j \mathbb{E} \left\| \tilde{\mathbf{w}}_k^{\bar{t}_1,0} - \tilde{\mathbf{w}}_j^{\bar{t}_1,0} \right\|^2 \\
&\stackrel{(a)}{=} 2 \sum_{l=1}^L \alpha_l \sum_{k=1}^{B_l} \alpha_k \sum_{j=1}^{V_{k,l}} \alpha_j \mathbb{E} \left\| \tilde{\mathbf{w}}_k^{\bar{t}_1,0} - \mathbf{w}_k^{\bar{t}_1} + \mathbf{w}_j^{\bar{t}_1} - \tilde{\mathbf{w}}_j^{\bar{t}_1,0} \right\|^2, \\
&\leq 4 \sum_{l=1}^L \alpha_l \sum_{k=1}^{B_l} \alpha_k \sum_{j=1}^{V_{k,l}} \alpha_j \mathbb{E} \left\| \mathbf{w}_k^{\bar{t}_1} - \tilde{\mathbf{w}}_k^{\bar{t}_1,0} \right\|^2 + 4 \sum_{l=1}^L \alpha_l \sum_{k=1}^{B_l} \alpha_k \sum_{j=1}^{V_{k,l}} \alpha_j \mathbb{E} \left\| \mathbf{w}_j^{\bar{t}_1} - \tilde{\mathbf{w}}_j^{\bar{t}_1,0} \right\|^2, \\
&\stackrel{(b)}{\leq} 4 \sum_{l=1}^L \alpha_l \sum_{k=1}^{B_l} \alpha_k \sum_{j=1}^{V_{k,l}} \alpha_j \sum_{i=1}^{U_{j,k,l}} \alpha_i \delta_i^{\bar{t}_1} \mathbb{E} \left\| \mathbf{w}_i^{\bar{t}_1} \right\|^2 + 4 \sum_{l=1}^L \alpha_l \sum_{k=1}^{B_l} \alpha_k \sum_{j=1}^{V_{k,l}} \alpha_j \sum_{i=1}^{U_{j,k,l}} \alpha_i \delta_i^{\bar{t}_1} \mathbb{E} \left\| \mathbf{w}_i^{\bar{t}_1} \right\|^2, \\
&= 8 \sum_{l=1}^L \alpha_l \sum_{k=1}^{B_l} \alpha_k \sum_{j=1}^{V_{k,l}} \alpha_j \sum_{i=1}^{U_{j,k,l}} \alpha_i \delta_i^{\bar{t}_1} \mathbb{E} \left\| \mathbf{w}_i^{\bar{t}_1} \right\|^2,
\end{aligned} \tag{92}$$

where in (a) we use the fact that $\mathbf{w}_k^{\bar{t}_1} = \mathbf{w}_j^{\bar{t}_1}$ and (b) stems from following similar steps as in (73) and (72).

As such we derive the upper bound of the first term of (91) as

$$\begin{aligned}
& 2 \sum_{l=1}^L \alpha_l \sum_{k=1}^{B_l} \alpha_k \sum_{j=1}^{V_{k,l}} \alpha_j \mathbb{E} \left\| \tilde{\mathbf{w}}_k^{\bar{t}_1,0} - \tilde{\mathbf{w}}_j^{\bar{t}_1,0} \right\|^2 \\
&\leq \frac{8}{T} \sum_{t=0}^{T-1} \sum_{l=1}^L \alpha_l \sum_{k=1}^{B_l} \alpha_k \sum_{j=1}^{V_{k,l}} \alpha_j \sum_{i=1}^{U_{j,k,l}} \alpha_i \delta_i^{\lfloor t/(\kappa_0\kappa_1) \rfloor} \mathbb{E} \left\| \mathbf{w}_i^{\lfloor t/(\kappa_0\kappa_1) \rfloor} \right\|^2 \approx \mathcal{O}(\delta^{\text{th}} D^2).
\end{aligned} \tag{93}$$

For the second term in (91), we have

$$\begin{aligned}
& \frac{2\eta^2}{T} \sum_{t=0}^{T-1} \sum_{l=1}^L \alpha_l \sum_{k=1}^{B_l} \alpha_k \sum_{j=1}^{V_{k,l}} \alpha_j \mathbb{E} \left\| \sum_{\tau=\bar{t}_1}^{t-1} \left(\sum_{i=1}^{U_{j,k,l}} \alpha_i \tilde{g} \left(\tilde{\mathbf{w}}_i^{\tau,0} \right) \frac{\mathbf{1}_i^\tau}{p_i^\tau} - \sum_{j'=1}^{V_{k,l}} \alpha_{j'} \sum_{i'=1}^{U_{j',k,l}} \alpha_{i'} \tilde{g} \left(\tilde{\mathbf{w}}_{i'}^{\tau,0} \right) \frac{\mathbf{1}_{i'}^\tau}{p_{i'}^\tau} \right) \right\|^2 \\
&= \frac{2\eta^2}{T} \sum_{t=0}^{T-1} \sum_{l=1}^L \alpha_l \sum_{k=1}^{B_l} \alpha_k \sum_{j=1}^{V_{k,l}} \alpha_j \mathbb{E} \left\| \sum_{\tau=\bar{t}_1}^{t-1} \left[\left\{ \sum_{i=1}^{U_{j,k,l}} \alpha_i \tilde{g} \left(\tilde{\mathbf{w}}_i^{\tau,0} \right) \frac{\mathbf{1}_i^\tau}{p_i^\tau} - \sum_{i=1}^{U_{j,k,l}} \alpha_i \nabla \tilde{f}_i \left(\tilde{\mathbf{w}}_i^{\tau,0} \right) \right\} + \right. \right. \\
&\quad \left. \left\{ \sum_{j'=1}^{V_{k,l}} \alpha_{j'} \sum_{i'=1}^{U_{j',k,l}} \alpha_{i'} \nabla \tilde{f}_{i'} \left(\tilde{\mathbf{w}}_{i'}^{\tau,0} \right) - \sum_{j'=1}^{V_{k,l}} \alpha_{j'} \sum_{i'=1}^{U_{j',k,l}} \alpha_{i'} \tilde{g} \left(\tilde{\mathbf{w}}_{i'}^{\tau,0} \right) \frac{\mathbf{1}_{i'}^\tau}{p_{i'}^\tau} \right\} + \right. \\
&\quad \left. \left. \left\{ \sum_{i=1}^{U_{j,k,l}} \alpha_i \nabla \tilde{f}_i \left(\tilde{\mathbf{w}}_i^{\tau,0} \right) - \sum_{j'=1}^{V_{k,l}} \alpha_{j'} \sum_{i'=1}^{U_{j',k,l}} \alpha_{i'} \nabla \tilde{f}_{i'} \left(\tilde{\mathbf{w}}_{i'}^{\tau,0} \right) \right\} \right] \right\|^2, \\
&\leq \frac{4\eta^2}{T} \sum_{t=0}^{T-1} \sum_{l=1}^L \alpha_l \sum_{k=1}^{B_l} \alpha_k \sum_{j=1}^{V_{k,l}} \alpha_j \mathbb{E} \left\| \sum_{\tau=\bar{t}_1}^{t-1} \left[\left\{ \sum_{i=1}^{U_{j,k,l}} \alpha_i \tilde{g} \left(\tilde{\mathbf{w}}_i^{\tau,0} \right) \frac{\mathbf{1}_i^\tau}{p_i^\tau} - \sum_{i=1}^{U_{j,k,l}} \alpha_i \nabla \tilde{f}_i \left(\tilde{\mathbf{w}}_i^{\tau,0} \right) \right\} + \right. \right. \\
&\quad \left. \left\{ \sum_{j'=1}^{V_{k,l}} \alpha_{j'} \sum_{i'=1}^{U_{j',k,l}} \alpha_{i'} \nabla \tilde{f}_{i'} \left(\tilde{\mathbf{w}}_{i'}^{\tau,0} \right) - \sum_{j'=1}^{V_{k,l}} \alpha_{j'} \sum_{i'=1}^{U_{j',k,l}} \alpha_{i'} \tilde{g} \left(\tilde{\mathbf{w}}_{i'}^{\tau,0} \right) \frac{\mathbf{1}_{i'}^\tau}{p_{i'}^\tau} \right\} \right] \right\|^2 +
\end{aligned}$$

$$\frac{4\eta^2}{T} \sum_{t=0}^{T-1} \sum_{l=1}^L \alpha_l \sum_{k=1}^{B_l} \alpha_k \sum_{j=1}^{V_{k,l}} \alpha_j \mathbb{E} \left\| \sum_{\tau=\bar{t}_1}^{t-1} \left[\sum_{i=1}^{U_{j,k,l}} \alpha_i \nabla \tilde{f}_i(\tilde{\mathbf{w}}_i^{\tau,0}) - \sum_{j'=1}^{V_{k,l}} \alpha_{j'} \sum_{i'=1}^{U_{j',k,l}} \alpha_{i'} \nabla \tilde{f}_{i'}(\tilde{\mathbf{w}}_{i'}^{\tau,0}) \right] \right\|^2, \quad (94)$$

Lemma 7.

$$\begin{aligned} & \frac{4\eta^2}{T} \sum_{t=0}^{T-1} \sum_{l=1}^L \alpha_l \sum_{k=1}^{B_l} \alpha_k \sum_{j=1}^{V_{k,l}} \alpha_j \mathbb{E} \left\| \sum_{\tau=\bar{t}_1}^{t-1} \left[\left\{ \sum_{i=1}^{U_{j,k,l}} \alpha_i \tilde{g}(\tilde{\mathbf{w}}_i^{\tau,0}) \frac{\mathbf{1}_i^\tau}{p_i^\tau} - \sum_{i=1}^{U_{j,k,l}} \alpha_i \nabla \tilde{f}_i(\tilde{\mathbf{w}}_i^{\tau,0}) \right\} + \right. \right. \\ & \quad \left. \left. \left\{ \sum_{j'=1}^{V_{k,l}} \alpha_{j'} \sum_{i'=1}^{U_{j',k,l}} \alpha_{i'} \nabla \tilde{f}_{i'}(\tilde{\mathbf{w}}_{i'}^{\tau,0}) - \sum_{j'=1}^{V_{k,l}} \alpha_{j'} \sum_{i'=1}^{U_{j',k,l}} \alpha_{i'} \tilde{g}(\tilde{\mathbf{w}}_{i'}^{\tau,0}) \frac{\mathbf{1}_{i'}^\tau}{p_{i'}^\tau} \right\} \right] \right\|^2 \\ & \leq 8\kappa_0 \kappa_1 \eta^2 \sigma^2 \sum_{l=1}^L \alpha_l \sum_{k=1}^{B_l} \alpha_k \sum_{j=1}^{V_{k,l}} \alpha_j \sum_{i=1}^{U_{j,k,l}} \alpha_i^2 + 8\kappa_0 \kappa_1 \eta^2 \cdot \varphi_{w,L_2} \\ & \approx \mathcal{O}(\kappa_0 \kappa_1 \eta^2 \sigma^2) + \mathcal{O}(\kappa_0 \kappa_1 \eta^2 \cdot \varphi_{w,L_2}), \end{aligned} \quad (95)$$

$$\approx \mathcal{O}(\kappa_0 \kappa_1 \eta^2 \sigma^2) + \mathcal{O}(\kappa_0 \kappa_1 \eta^2 \cdot \varphi_{w,L_2}), \quad (96)$$

where $\varphi_{w,L_2} = \frac{1}{T} \sum_{t=0}^{T-1} \sum_{l=1}^L \alpha_l \sum_{k=1}^{B_l} \alpha_k \sum_{j=1}^{V_{k,l}} \alpha_j \sum_{i=1}^{U_{j,k,l}} \alpha_i^2 \left(\frac{1}{p_i^\tau} - 1 \right)$.

Lemma 8.

$$\begin{aligned} & \frac{4\eta^2}{T} \sum_{t=0}^{T-1} \sum_{l=1}^L \alpha_l \sum_{k=1}^{B_l} \alpha_k \sum_{j=1}^{V_{k,l}} \alpha_j \mathbb{E} \left\| \sum_{\tau=\bar{t}_1}^{t-1} \left[\sum_{i=1}^{U_{j,k,l}} \alpha_i \nabla \tilde{f}_i(\tilde{\mathbf{w}}_i^{\tau,0}) - \sum_{j'=1}^{V_{k,l}} \alpha_{j'} \sum_{i'=1}^{U_{j',k,l}} \alpha_{i'} \nabla \tilde{f}_{i'}(\tilde{\mathbf{w}}_{i'}^{\tau,0}) \right] \right\|^2 \\ & \leq \mathcal{O}(\beta^2 \kappa_0^4 \kappa_1^2 \eta^4 \varepsilon_{vc}^2) + \mathcal{O}(\kappa_0^2 \kappa_1^2 \eta^2 \varepsilon_{sbs}^2) + \mathcal{O}(\beta^2 \sigma^2 \kappa_0^3 \kappa_1^2 \eta^4) + \mathcal{O}(\delta^{\text{th}} D^2 \beta^2 \kappa_0^2 \kappa_1^2 \eta^2) + \\ & \quad \mathcal{O}(\beta^2 \kappa_0^3 \kappa_1^2 \eta^4 G^2 \cdot \varphi_{w,L_1}) + \frac{40\beta^2 \kappa_0^2 \kappa_1^2 \eta^2}{T} \sum_{t=0}^{T-1} \sum_{l=1}^L \alpha_l \sum_{k=1}^{B_l} \alpha_k \sum_{j=1}^{V_{k,l}} \alpha_j \mathbb{E} \|\tilde{\mathbf{w}}_k^t - \tilde{\mathbf{w}}_j^t\|^2. \end{aligned} \quad (97)$$

Now, using Lemma 7, Lemma 8 and assuming $\eta \leq \frac{1}{2\sqrt{10}\kappa_0 \kappa_1 \beta}$, we have the following

$$\begin{aligned} & \frac{\beta^2}{T} \sum_{t=0}^{T-1} \sum_{l=1}^L \alpha_l \sum_{k=1}^{B_l} \alpha_k \sum_{j=1}^{V_{k,l}} \alpha_j \mathbb{E} \|\tilde{\mathbf{w}}_k^t - \tilde{\mathbf{w}}_j^t\|^2 \\ & \leq \mathcal{O}(\delta^{\text{th}} \beta^2 D^2) + \mathcal{O}(\kappa_0 \kappa_1 \eta^2 \sigma^2 \beta^2) + \mathcal{O}(\kappa_0 \kappa_1 \beta^2 \eta^2 \cdot \varphi_{w,L_2}) + \mathcal{O}(\beta^4 \kappa_0^4 \kappa_1^2 \eta^4 \varepsilon_{vc}^2) + \mathcal{O}(\kappa_0^2 \kappa_1^2 \eta^2 \beta^2 \varepsilon_{sbs}^2) + \\ & \quad \mathcal{O}(\sigma^2 \kappa_0^3 \kappa_1^2 \beta^4 \eta^4) + \mathcal{O}(\delta^{\text{th}} D^2 \kappa_0^2 \kappa_1^2 \eta^2 \beta^4) + \mathcal{O}(\kappa_0^3 \kappa_1^2 \beta^4 \eta^4 G^2 \cdot \varphi_{w,L_1}) \\ & \approx \mathcal{O}(\beta^4 \kappa_0^4 \kappa_1^2 \eta^4 \varepsilon_{vc}^2) + \mathcal{O}(\kappa_0^2 \kappa_1^2 \eta^2 \beta^2 \varepsilon_{sbs}^2) + \mathcal{O}(\kappa_0 \kappa_1 \eta^2 \sigma^2 \beta^2) + \mathcal{O}(\delta^{\text{th}} \beta^2 D^2) + \\ & \quad \mathcal{O}(\kappa_0^3 \kappa_1^2 \beta^4 \eta^4 G^2 \cdot \varphi_{w,L_1}) + \mathcal{O}(\kappa_0 \kappa_1 \beta^2 \eta^2 \cdot \varphi_{w,L_2}). \end{aligned} \quad (98)$$

A. Missing Proof of Lemma 7

$$\begin{aligned} & \frac{4\eta^2}{T} \sum_{t=0}^{T-1} \sum_{l=1}^L \alpha_l \sum_{k=1}^{B_l} \alpha_k \sum_{j=1}^{V_{k,l}} \alpha_j \mathbb{E} \left\| \sum_{\tau=\bar{t}_1}^{t-1} \left[\left\{ \sum_{i=1}^{U_{j,k,l}} \alpha_i \tilde{g}(\tilde{\mathbf{w}}_i^{\tau,0}) \frac{\mathbf{1}_i^\tau}{p_i^\tau} - \sum_{i=1}^{U_{j,k,l}} \alpha_i \nabla \tilde{f}_i(\tilde{\mathbf{w}}_i^{\tau,0}) \right\} + \right. \right. \\ & \quad \left. \left. \left\{ \sum_{j'=1}^{V_{k,l}} \alpha_{j'} \sum_{i'=1}^{U_{j',k,l}} \alpha_{i'} \nabla \tilde{f}_{i'}(\tilde{\mathbf{w}}_{i'}^{\tau,0}) - \sum_{j'=1}^{V_{k,l}} \alpha_{j'} \sum_{i'=1}^{U_{j',k,l}} \alpha_{i'} \tilde{g}(\tilde{\mathbf{w}}_{i'}^{\tau,0}) \frac{\mathbf{1}_{i'}^\tau}{p_{i'}^\tau} \right\} \right] \right\|^2 \\ & \stackrel{(a)}{=} \frac{4\eta^2}{T} \sum_{t=0}^{T-1} \sum_{l=1}^L \alpha_l \sum_{k=1}^{B_l} \alpha_k \sum_{j=1}^{V_{k,l}} \alpha_j \mathbb{E} \left\| \sum_{\tau=\bar{t}_1}^{t-1} \left[\sum_{i=1}^{U_{j,k,l}} \alpha_i \tilde{g}(\tilde{\mathbf{w}}_i^{\tau,0}) \frac{\mathbf{1}_i^\tau}{p_i^\tau} - \sum_{i=1}^{U_{j,k,l}} \alpha_i \nabla \tilde{f}_i(\tilde{\mathbf{w}}_i^{\tau,0}) \right] \right\|^2 - \\ & \quad \frac{4\eta^2}{T} \sum_{t=0}^{T-1} \sum_{l=1}^L \alpha_l \sum_{k=1}^{B_l} \alpha_k \sum_{j=1}^{V_{k,l}} \alpha_j \mathbb{E} \left\| \sum_{\tau=\bar{t}_1}^{t-1} \sum_{j'=1}^{V_{k,l}} \alpha_{j'} \sum_{i'=1}^{U_{j',k,l}} \alpha_{i'} \left[\tilde{g}(\tilde{\mathbf{w}}_{i'}^{\tau,0}) \frac{\mathbf{1}_{i'}^\tau}{p_{i'}^\tau} - \nabla \tilde{f}_{i'}(\tilde{\mathbf{w}}_{i'}^{\tau,0}) \right] \right\|^2 \\ & \stackrel{(b)}{=} \frac{4\eta^2}{T} \sum_{t=0}^{T-1} \sum_{l=1}^L \alpha_l \sum_{k=1}^{B_l} \alpha_k \sum_{j=1}^{V_{k,l}} \alpha_j \sum_{\tau=\bar{t}_1}^{t-1} \mathbb{E} \left\| \sum_{i=1}^{U_{j,k,l}} \alpha_i \left[\tilde{g}(\tilde{\mathbf{w}}_i^{\tau,0}) \frac{\mathbf{1}_i^\tau}{p_i^\tau} - \nabla \tilde{f}_i(\tilde{\mathbf{w}}_i^{\tau,0}) \right] \right\|^2 - \\ & \quad \frac{4\eta^2}{T} \sum_{t=0}^{T-1} \sum_{l=1}^L \alpha_l \sum_{k=1}^{B_l} \alpha_k \sum_{\tau=\bar{t}_1}^{t-1} \mathbb{E} \left\| \sum_{j'=1}^{V_{k,l}} \alpha_{j'} \sum_{i'=1}^{U_{j',k,l}} \alpha_{i'} \left[\tilde{g}(\tilde{\mathbf{w}}_{i'}^{\tau,0}) \frac{\mathbf{1}_{i'}^\tau}{p_{i'}^\tau} - \nabla \tilde{f}_{i'}(\tilde{\mathbf{w}}_{i'}^{\tau,0}) \right] \right\|^2 \\ & \stackrel{(c)}{\leq} \frac{4\kappa_0 \kappa_1 \eta^2}{T} \sum_{t=0}^{T-1} \sum_{l=1}^L \alpha_l \sum_{k=1}^{B_l} \alpha_k \sum_{j=1}^{V_{k,l}} \alpha_j \mathbb{E} \left\| \sum_{i=1}^{U_{j,k,l}} \alpha_i \left[\tilde{g}(\tilde{\mathbf{w}}_i^{\tau,0}) \frac{\mathbf{1}_i^\tau}{p_i^\tau} - \nabla \tilde{f}_i(\tilde{\mathbf{w}}_i^{\tau,0}) \right] \right\|^2 - \end{aligned}$$

$$\begin{aligned}
& \frac{4\kappa_0\kappa_1\eta^2}{T} \sum_{t=0}^{T-1} \sum_{l=1}^L \alpha_l \sum_{k=1}^{B_l} \alpha_k \mathbb{E} \left\| \sum_{j'=1}^{V_{k,l}} \alpha_{j'} \sum_{i'=1}^{U_{j',k,l}} \alpha_{i'} \left[\tilde{g}(\tilde{\mathbf{w}}_{i'}^{t,0}) \frac{\mathbf{1}_{i'}^t}{p_{i'}^t} - \nabla \tilde{f}_{i'}(\tilde{\mathbf{w}}_{i'}^{t,0}) \right] \right\|^2 \\
&= \frac{4\kappa_0\kappa_1\eta^2}{T} \sum_{t=0}^{T-1} \sum_{l=1}^L \alpha_l \sum_{k=1}^{B_l} \alpha_k \sum_{j=1}^{V_{k,l}} \alpha_j \sum_{i=1}^{U_{j,k,l}} \alpha_i^2 \mathbb{E} \left\| \tilde{g}(\tilde{\mathbf{w}}_i^{t,0}) \frac{\mathbf{1}_i^t}{p_i^t} \pm \tilde{g}(\tilde{\mathbf{w}}_i^{t,0}) - \nabla \tilde{f}_i(\tilde{\mathbf{w}}_i^{t,0}) \right\|^2 - \\
&\quad \frac{4\kappa_0\kappa_1\eta^2}{T} \sum_{t=0}^{T-1} \sum_{l=1}^L \alpha_l \sum_{k=1}^{B_l} \alpha_k \sum_{j=1}^{V_{k,l}} \alpha_j^2 \sum_{i=1}^{U_{j,k,l}} \alpha_i^2 \mathbb{E} \left\| \tilde{g}(\tilde{\mathbf{w}}_i^{t,0}) \frac{\mathbf{1}_i^t}{p_i^t} \pm \tilde{g}(\tilde{\mathbf{w}}_i^{t,0}) - \nabla \tilde{f}_i(\tilde{\mathbf{w}}_i^{t,0}) \right\|^2 \\
&\leq \frac{8\kappa_0\kappa_1\eta^2}{T} \sum_{t=0}^{T-1} \sum_{l=1}^L \alpha_l \sum_{k=1}^{B_l} \alpha_k \sum_{j=1}^{V_{k,l}} \alpha_j \sum_{i=1}^{U_{j,k,l}} \alpha_i^2 \left[\mathbb{E} \left\| \left(\frac{\mathbf{1}_i^t}{p_i^t} - 1 \right) \tilde{g}(\tilde{\mathbf{w}}_i^{t,0}) \right\|^2 + \mathbb{E} \left\| \tilde{g}(\tilde{\mathbf{w}}_i^{t,0}) - \nabla \tilde{f}_i(\tilde{\mathbf{w}}_i^{t,0}) \right\|^2 \right] - \\
&\quad \frac{8\kappa_0\kappa_1\eta^2}{T} \sum_{t=0}^{T-1} \sum_{l=1}^L \alpha_l \sum_{k=1}^{B_l} \alpha_k \sum_{j=1}^{V_{k,l}} \alpha_j^2 \sum_{i=1}^{U_{j,k,l}} \alpha_i^2 \left[\mathbb{E} \left\| \left(\frac{\mathbf{1}_i^t}{p_i^t} - 1 \right) \tilde{g}(\tilde{\mathbf{w}}_i^{t,0}) \right\|^2 + \mathbb{E} \left\| \tilde{g}(\tilde{\mathbf{w}}_i^{t,0}) - \nabla \tilde{f}_i(\tilde{\mathbf{w}}_i^{t,0}) \right\|^2 \right] \\
&\leq \frac{8\kappa_0\kappa_1\eta^2 G^2}{T} \sum_{t=0}^{T-1} \sum_{l=1}^L \alpha_l \sum_{k=1}^{B_l} \alpha_k \sum_{j=1}^{V_{k,l}} \alpha_j \sum_{i=1}^{U_{j,k,l}} \alpha_i^2 \left(\frac{1}{p_i^t} - 1 \right) + 8\kappa_0\kappa_1\eta^2 \sigma^2 G^2 \sum_{l=1}^L \alpha_l \sum_{k=1}^{B_l} \alpha_k \sum_{j=1}^{V_{k,l}} \alpha_j \sum_{i=1}^{U_{j,k,l}} \alpha_i^2 - \\
&\quad \frac{8\kappa_0\kappa_1\eta^2 G^2}{T} \sum_{t=0}^{T-1} \sum_{l=1}^L \alpha_l \sum_{k=1}^{B_l} \alpha_k \sum_{j=1}^{V_{k,l}} \alpha_j^2 \sum_{i=1}^{U_{j,k,l}} \alpha_i^2 \left(\frac{1}{p_i^t} - 1 \right) - 8\kappa_0\kappa_1\eta^2 \sigma^2 G^2 \sum_{l=1}^L \alpha_l \sum_{k=1}^{B_l} \alpha_k \sum_{j=1}^{V_{k,l}} \alpha_j^2 \sum_{i=1}^{U_{j,k,l}} \alpha_i^2 \\
&\leq 8\kappa_0\kappa_1\eta^2 \sigma^2 \sum_{l=1}^L \alpha_l \sum_{k=1}^{B_l} \alpha_k \sum_{j=1}^{V_{k,l}} \alpha_j \sum_{i=1}^{U_{j,k,l}} \alpha_i^2 + 8\kappa_0\kappa_1\eta^2 \cdot \varphi_{w,L_2}, \tag{99}
\end{aligned}$$

where $\varphi_{w,L_2} = \frac{1}{T} \sum_{t=0}^{T-1} \sum_{l=1}^L \alpha_l \sum_{k=1}^{B_l} \alpha_k \sum_{j=1}^{V_{k,l}} \alpha_j \sum_{i=1}^{U_{j,k,l}} \alpha_i^2 \left(\frac{1}{p_i^t} - 1 \right)$.

B. Missing Proof of Lemma 8

$$\begin{aligned}
& \frac{4\eta^2}{T} \sum_{t=0}^{T-1} \sum_{l=1}^L \alpha_l \sum_{k=1}^{B_l} \alpha_k \sum_{j=1}^{V_{k,l}} \alpha_j \mathbb{E} \left\| \sum_{\tau=\bar{t}_1}^{t-1} \left[\sum_{i=1}^{U_{j,k,l}} \alpha_i \nabla \tilde{f}_i(\tilde{\mathbf{w}}_i^{\tau,0}) - \sum_{j'=1}^{V_{k,l}} \alpha_{j'} \sum_{i'=1}^{U_{j',k,l}} \alpha_{i'} \nabla \tilde{f}_{i'}(\tilde{\mathbf{w}}_{i'}^{\tau,0}) \right] \right\|^2 \\
&= \frac{4\kappa_0\kappa_1\eta^2}{T} \sum_{t=0}^{T-1} \sum_{l=1}^L \alpha_l \sum_{k=1}^{B_l} \alpha_k \sum_{j=1}^{V_{k,l}} \alpha_j \sum_{\tau=\bar{t}_1}^{t-1} \mathbb{E} \left\| \left(\sum_{i=1}^{U_{j,k,l}} \alpha_i [\nabla \tilde{f}_i(\tilde{\mathbf{w}}_i^{\tau,0}) - \nabla \tilde{f}_i(\tilde{\mathbf{w}}_j^{\tau})] \right) + \right. \\
&\quad \left(\sum_{i=1}^{U_{j,k,l}} \alpha_i [\nabla \tilde{f}_i(\tilde{\mathbf{w}}_j^{\tau}) - \nabla \tilde{f}_i(\tilde{\mathbf{w}}_k^{\tau})] \right) + \left(\sum_{i=1}^{U_{j,k,l}} \alpha_i \nabla \tilde{f}_i(\tilde{\mathbf{w}}_k^{\tau}) - \sum_{j'=1}^{V_{k,l}} \alpha_{j'} \sum_{i'=1}^{U_{j',k,l}} \alpha_{i'} \nabla \tilde{f}_{i'}(\tilde{\mathbf{w}}_k^{\tau}) \right) + \\
&\quad \left. \left(\sum_{j'=1}^{V_{k,l}} \alpha_{j'} \sum_{i'=1}^{U_{j',k,l}} \alpha_{i'} [\nabla \tilde{f}_{i'}(\tilde{\mathbf{w}}_k^{\tau}) - \nabla \tilde{f}_{i'}(\tilde{\mathbf{w}}_j^{\tau})] \right) + \left(\sum_{j'=1}^{V_{k,l}} \alpha_{j'} \sum_{i'=1}^{U_{j',k,l}} \alpha_{i'} [\nabla \tilde{f}_{i'}(\tilde{\mathbf{w}}_j^{\tau}) - \nabla \tilde{f}_{i'}(\tilde{\mathbf{w}}_{i'}^{\tau,0})] \right) \right\|^2 \\
&\leq 20\kappa_0^2\kappa_1^2\eta^2\varepsilon_{\text{sbs}}^2 + \frac{40\beta^2\kappa_0^2\kappa_1^2\eta^2}{T} \sum_{t=0}^{T-1} \sum_{l=1}^L \alpha_l \sum_{k=1}^{B_l} \alpha_k \sum_{j=1}^{V_{k,l}} \alpha_j \mathbb{E} \|\tilde{\mathbf{w}}_k^t - \tilde{\mathbf{w}}_j^t\|^2 + \frac{80\beta^2\kappa_0^2\kappa_1^2\eta^2}{T} \sum_{t=0}^{T-1} \sum_{l=1}^L \alpha_l \sum_{k=1}^{B_l} \alpha_k \sum_{j=1}^{V_{k,l}} \alpha_j \sum_{i=1}^{U_{j,k,l}} \alpha_i \mathbb{E} \|\tilde{\mathbf{w}}_j^t - \tilde{\mathbf{w}}_i^t\|^2 + \\
&\quad \frac{80\beta^2\kappa_0^2\kappa_1^2\eta^2}{T} \sum_{t=0}^{T-1} \sum_{l=1}^L \alpha_l \sum_{k=1}^{B_l} \alpha_k \sum_{j=1}^{V_{k,l}} \alpha_j \sum_{i=1}^{U_{j,k,l}} \alpha_i \mathbb{E} \|\tilde{\mathbf{w}}_i^t - \tilde{\mathbf{w}}_i^{t,0}\|^2 \\
&\approx \mathcal{O}(\beta^2\kappa_0^4\kappa_1^2\eta^4\varepsilon_{\text{vc}}^2) + \mathcal{O}(\kappa_0^2\kappa_1^2\eta^2\varepsilon_{\text{sbs}}^2) + \mathcal{O}(\beta^2\sigma^2\kappa_0^3\kappa_1^2\eta^4) + \mathcal{O}(\delta^{\text{th}}D^2\beta^2\kappa_0^2\kappa_1^2\eta^2) + \mathcal{O}(\beta^2\kappa_0^3\kappa_1^2\eta^4G^2 \cdot \varphi_{w,L_1}) + \\
&\quad \frac{40\beta^2\kappa_0^2\kappa_1^2\eta^2}{T} \sum_{t=0}^{T-1} \sum_{l=1}^L \alpha_l \sum_{k=1}^{B_l} \alpha_k \sum_{j=1}^{V_{k,l}} \alpha_j \mathbb{E} \|\tilde{\mathbf{w}}_k^t - \tilde{\mathbf{w}}_j^t\|^2. \tag{100}
\end{aligned}$$

which concludes the proof of Lemma 8. ■

APPENDIX D PROOF OF LEMMA 3

Lemma 3. When $\eta \leq 1/[2\sqrt{14}\kappa_0\kappa_1\kappa_2\beta]$, the average difference between the sBS and mBS model parameters, i.e., the L_3 term of (56), is upper bounded as

$$[\beta^2/T] \sum_{t=0}^{T-1} \sum_{l=1}^L \alpha_l \sum_{k=1}^{B_l} \alpha_k \mathbb{E} \|\tilde{\mathbf{w}}_l^t - \tilde{\mathbf{w}}_k^t\|^2$$

$$\leq \mathcal{O}(\kappa_0^3 \kappa_1^2 \kappa_2^2 \eta^4 \beta^4 \varepsilon_{\text{c}}^2) + \mathcal{O}(\kappa_0^4 \kappa_1^4 \kappa_2^2 \eta^4 \beta^4 \varepsilon_{\text{sbs}}^2) + \mathcal{O}(\kappa_0^2 \kappa_1^2 \kappa_2^2 \eta^2 \beta^4 \varepsilon_{\text{mbs}}^2) + \mathcal{O}(\kappa_0 \kappa_1 \kappa_2 \eta^2 \beta^2 \sigma^2) + \mathcal{O}(\delta^{\text{th}} \beta^2 D^2) + \mathcal{O}(\kappa_0^3 \kappa_1^2 \kappa_2^2 \eta^4 \beta^4 G^2 \cdot \varphi_{\text{w},L_1}(\boldsymbol{\delta}, \mathbf{f}, \mathbf{P})) + \mathcal{O}(\kappa_0^2 \kappa_1^2 \kappa_2^2 \beta^4 \eta^4 \cdot \varphi_{\text{w},L_2}(\boldsymbol{\delta}, \mathbf{f}, \mathbf{P})) + \mathcal{O}(\kappa_0 \kappa_1 \kappa_2 \eta^2 \beta^2 G^2 \cdot \varphi_{\text{w},L_3}(\boldsymbol{\delta}, \mathbf{f}, \mathbf{P})). \quad (101)$$

where $\varphi_{\text{w},L_3}(\boldsymbol{\delta}, \mathbf{f}, \mathbf{P}) = [1/T] \sum_{l=1}^L \alpha_l \sum_{k=1}^{B_l} \alpha_k \sum_{j=1}^{V_{k,l}} \alpha_j^2 \sum_{i=1}^{U_{j,k,l}} \alpha_i^2 \sum_{t=0}^{T-1} (1/p_i^t - 1)$.

Proof.

$$\begin{aligned} & \frac{1}{T} \sum_{t=0}^{T-1} \sum_{l=1}^L \alpha_l \sum_{k=1}^{B_l} \alpha_k \mathbb{E} \|\tilde{\mathbf{w}}_l^t - \tilde{\mathbf{w}}_k^t\|^2 \\ &= \sum_{l=1}^L \alpha_l \sum_{k=1}^{B_l} \alpha_k \mathbb{E} \left\| \tilde{\mathbf{w}}_l^{\bar{t}_2,0} - \tilde{\mathbf{w}}_k^{\bar{t}_2,0} - \eta \sum_{\tau=\bar{t}_2}^{t-1} \sum_{k'=1}^{B_l} \alpha_{k'} \sum_{j'=1}^{V_{k',l}} \alpha_{j'} \sum_{i'=1}^{U_{j',k',l}} \alpha_{i'} \tilde{g}(\tilde{\mathbf{w}}_{i'}^{\tau,0}) \frac{\mathbf{1}_{i'}^\tau}{p_{i'}^\tau} + \eta \sum_{\tau=\bar{t}_2}^{t-1} \sum_{j=1}^{V_{k,l}} \alpha_j \sum_{i=1}^{U_{j,k,l}} \alpha_i \tilde{g}(\tilde{\mathbf{w}}_i^{\tau,0}) \frac{\mathbf{1}_i^\tau}{p_i^\tau} \right\|^2, \\ &\leq \frac{2}{T} \sum_{t=0}^{T-1} \sum_{l=1}^L \alpha_l \sum_{k=1}^{B_l} \alpha_k \mathbb{E} \|\tilde{\mathbf{w}}_l^{\bar{t}_2,0} - \tilde{\mathbf{w}}_k^{\bar{t}_2,0}\|^2 + \frac{2\eta^2}{T} \sum_{t=0}^{T-1} \sum_{l=1}^L \alpha_l \sum_{k=1}^{B_l} \alpha_k \mathbb{E} \left\| \sum_{\tau=\bar{t}_2}^{t-1} \left[\sum_{j=1}^{V_{k,l}} \alpha_j \sum_{i=1}^{U_{j,k,l}} \alpha_i \tilde{g}(\tilde{\mathbf{w}}_i^{\tau,0}) \frac{\mathbf{1}_i^\tau}{p_i^\tau} - \sum_{k'=1}^{B_l} \alpha_{k'} \sum_{j'=1}^{V_{k',l}} \alpha_{j'} \sum_{i'=1}^{U_{j',k',l}} \alpha_{i'} \tilde{g}(\tilde{\mathbf{w}}_{i'}^{\tau,0}) \frac{\mathbf{1}_{i'}^\tau}{p_{i'}^\tau} \right] \right\|^2, \end{aligned} \quad (102)$$

where $\bar{t}_2 = (m\kappa_3 + t_3)\kappa_2\kappa_1\kappa_0$ and the inequalities in the last term arise from Jensen inequality.

For the first term in (102), we have

$$\begin{aligned} & 2 \sum_{l=1}^L \alpha_l \sum_{k=1}^{B_l} \alpha_k \mathbb{E} \|\tilde{\mathbf{w}}_l^{\bar{t}_2,0} - \tilde{\mathbf{w}}_k^{\bar{t}_2,0}\|^2 \\ &\stackrel{(a)}{=} 2 \sum_{l=1}^L \alpha_l \sum_{k=1}^{B_l} \alpha_k \mathbb{E} \|\tilde{\mathbf{w}}_l^{\bar{t}_2,0} - \mathbf{w}_l^{\bar{t}_2} + \mathbf{w}_k^{\bar{t}_2} - \tilde{\mathbf{w}}_k^{\bar{t}_2,0}\|^2, \\ &\leq 4 \sum_{l=1}^L \alpha_l \sum_{k=1}^{B_l} \alpha_k \mathbb{E} \|\mathbf{w}_l^{\bar{t}_2} - \tilde{\mathbf{w}}_l^{\bar{t}_2,0}\|^2 + 4 \sum_{l=1}^L \alpha_l \sum_{k=1}^{B_l} \alpha_k \mathbb{E} \|\mathbf{w}_k^{\bar{t}_2} - \tilde{\mathbf{w}}_k^{\bar{t}_2,0}\|^2, \\ &\stackrel{(b)}{\leq} 4 \sum_{l=1}^L \alpha_l \sum_{k=1}^{B_l} \alpha_k \sum_{j=1}^{V_{k,l}} \alpha_j \sum_{i=1}^{U_{j,k,l}} \alpha_i \delta_i^{\bar{t}_2} \mathbb{E} \|\mathbf{w}_i^{\bar{t}_2}\|^2 + 4 \sum_{l=1}^L \alpha_l \sum_{k=1}^{B_l} \alpha_k \sum_{j=1}^{V_{k,l}} \alpha_j \sum_{i=1}^{U_{j,k,l}} \alpha_i \delta_i^{\bar{t}_2} \mathbb{E} \|\mathbf{w}_i^{\bar{t}_2}\|^2, \\ &= 8 \sum_{l=1}^L \alpha_l \sum_{k=1}^{B_l} \alpha_k \sum_{j=1}^{V_{k,l}} \alpha_j \sum_{i=1}^{U_{j,k,l}} \alpha_i \delta_i^{\bar{t}_2} \mathbb{E} \|\mathbf{w}_i^{\bar{t}_2}\|^2, \end{aligned} \quad (103)$$

where in (a) we use the fact that $\mathbf{w}_l^{\bar{t}_2} = \mathbf{w}_k^{\bar{t}_2}$. Moreover, (b) appears following similar steps as in (74) and (73).

As such, we have

$$\begin{aligned} & \frac{2}{T} \sum_{t=0}^{T-1} \sum_{l=1}^L \alpha_l \sum_{k=1}^{B_l} \alpha_k \mathbb{E} \|\tilde{\mathbf{w}}_l^{\bar{t}_2,0} - \tilde{\mathbf{w}}_k^{\bar{t}_2,0}\|^2 \\ &\leq \frac{8}{T} \sum_{t=0}^{T-1} \sum_{l=1}^L \alpha_l \sum_{k=1}^{B_l} \alpha_k \sum_{j=1}^{V_{k,l}} \alpha_j \sum_{i=1}^{U_{j,k,l}} \alpha_i \delta_i^{\lfloor \frac{t}{\kappa_0 \kappa_1 \kappa_2} \rfloor} \mathbb{E} \|\mathbf{w}_i^{\lfloor \frac{t}{\kappa_0 \kappa_1 \kappa_2} \rfloor}\|^2 \\ &\approx \mathcal{O}(\delta^{\text{th}} D^2). \end{aligned} \quad (104)$$

For the second term in (102), we have

$$\begin{aligned} & \frac{2\eta^2}{T} \sum_{t=0}^{T-1} \sum_{l=1}^L \alpha_l \sum_{k=1}^{B_l} \alpha_k \mathbb{E} \left\| \sum_{\tau=\bar{t}_2}^{t-1} \left(\sum_{j=1}^{V_{k,l}} \alpha_j \sum_{i=1}^{U_{j,k,l}} \alpha_i \tilde{g}(\tilde{\mathbf{w}}_i^{\tau,0}) \frac{\mathbf{1}_i^\tau}{p_i^\tau} - \sum_{k'=1}^{B_l} \alpha_{k'} \sum_{j'=1}^{V_{k',l}} \alpha_{j'} \sum_{i'=1}^{U_{j',k',l}} \alpha_{i'} \tilde{g}(\tilde{\mathbf{w}}_{i'}^{\tau,0}) \frac{\mathbf{1}_{i'}^\tau}{p_{i'}^\tau} \right) \right\|^2 \\ &= \frac{2\eta^2}{T} \sum_{t=0}^{T-1} \sum_{l=1}^L \alpha_l \sum_{k=1}^{B_l} \alpha_k \mathbb{E} \left\| \sum_{\tau=\bar{t}_2}^{t-1} \left[\sum_{j=1}^{V_{k,l}} \alpha_j \sum_{i=1}^{U_{j,k,l}} \alpha_i \left(\tilde{g}(\tilde{\mathbf{w}}_i^{\tau,0}) \frac{\mathbf{1}_i^\tau}{p_i^\tau} - \nabla \tilde{f}_i(\tilde{\mathbf{w}}_i^{\tau,0}) \right) - \sum_{k'=1}^{B_l} \alpha_{k'} \sum_{j'=1}^{V_{k',l}} \alpha_{j'} \sum_{i'=1}^{U_{j',k',l}} \alpha_{i'} \left(\tilde{g}(\tilde{\mathbf{w}}_{i'}^{\tau,0}) \frac{\mathbf{1}_{i'}^\tau}{p_{i'}^\tau} - \nabla \tilde{f}_{i'}(\tilde{\mathbf{w}}_{i'}^{\tau,0}) \right) \right] \right\|^2 \\ &\quad + \sum_{k'=1}^{B_l} \alpha_{k'} \sum_{j'=1}^{V_{k',l}} \alpha_{j'} \sum_{i'=1}^{U_{j',k',l}} \alpha_{i'} \nabla \tilde{f}_{i'}(\tilde{\mathbf{w}}_{i'}^{\tau,0}) - \sum_{j=1}^{V_{k,l}} \alpha_j \sum_{i=1}^{U_{j,k,l}} \alpha_i \nabla \tilde{f}_i(\tilde{\mathbf{w}}_i^{\tau,0}) \right\|^2, \\ &\leq \frac{4\eta^2}{T} \sum_{t=0}^{T-1} \sum_{l=1}^L \alpha_l \sum_{k=1}^{B_l} \alpha_k \mathbb{E} \left\| \sum_{\tau=\bar{t}_2}^{t-1} \left[\sum_{j=1}^{V_{k,l}} \alpha_j \sum_{i=1}^{U_{j,k,l}} \alpha_i \left(\tilde{g}(\tilde{\mathbf{w}}_i^{\tau,0}) \frac{\mathbf{1}_i^\tau}{p_i^\tau} - \nabla \tilde{f}_i(\tilde{\mathbf{w}}_i^{\tau,0}) \right) - \sum_{k'=1}^{B_l} \alpha_{k'} \sum_{j'=1}^{V_{k',l}} \alpha_{j'} \sum_{i'=1}^{U_{j',k',l}} \alpha_{i'} \left(\tilde{g}(\tilde{\mathbf{w}}_{i'}^{\tau,0}) \frac{\mathbf{1}_{i'}^\tau}{p_{i'}^\tau} - \nabla \tilde{f}_{i'}(\tilde{\mathbf{w}}_{i'}^{\tau,0}) \right) \right] \right\|^2 + \\ &\quad \frac{4\eta^2}{T} \sum_{t=0}^{T-1} \sum_{l=1}^L \alpha_l \sum_{k=1}^{B_l} \alpha_k \mathbb{E} \left\| \sum_{\tau=\bar{t}_2}^{t-1} \left[\sum_{k'=1}^{B_l} \alpha_{k'} \sum_{j'=1}^{V_{k',l}} \alpha_{j'} \sum_{i'=1}^{U_{j',k',l}} \alpha_{i'} \nabla \tilde{f}_{i'}(\tilde{\mathbf{w}}_{i'}^{\tau,0}) - \sum_{j=1}^{V_{k,l}} \alpha_j \sum_{i=1}^{U_{j,k,l}} \alpha_i \nabla \tilde{f}_i(\tilde{\mathbf{w}}_i^{\tau,0}) \right] \right\|^2, \end{aligned} \quad (105)$$

Lemma 9.

$$\begin{aligned}
& \frac{4\eta^2}{T} \sum_{t=0}^{T-1} \sum_{l=1}^L \alpha_l \sum_{k=1}^{B_l} \alpha_k \mathbb{E} \left\| \sum_{\tau=\bar{\tau}_2}^{t-1} \left[\sum_{j=1}^{V_{k,l}} \alpha_j \sum_{i=1}^{U_{j,k,l}} \alpha_i \left(\tilde{g}(\tilde{\mathbf{w}}_i^{\tau,0}) \frac{\mathbf{1}_i^\tau}{p_i^\tau} - \nabla \tilde{f}_i(\tilde{\mathbf{w}}_i^{\tau,0}) \right) - \sum_{k'=1}^{B_l} \alpha_{k'} \sum_{j'=1}^{V_{k',l}} \alpha_{j'} \sum_{i'=1}^{U_{j',k',l}} \alpha_{i'} \left(\tilde{g}(\tilde{\mathbf{w}}_{i'}^{\tau,0}) \frac{\mathbf{1}_{i'}^\tau}{p_{i'}^\tau} - \nabla \tilde{f}_{i'}(\tilde{\mathbf{w}}_{i'}^{\tau,0}) \right) \right] \right\|^2 \\
& \leq 8\kappa_0 \kappa_1 \kappa_2 \eta^2 \sigma^2 \sum_{l=1}^L \alpha_l \sum_{k=1}^{B_l} \alpha_k \sum_{j=1}^{V_{k,l}} \alpha_j^2 \sum_{i=1}^{U_{j,k,l}} \alpha_i^2 + 8\kappa_0 \kappa_1 \kappa_2 \eta^2 G^2 \cdot \varphi_{w,L_3} \\
& \approx \mathcal{O}(\kappa_0 \kappa_1 \kappa_2 \eta^2 \sigma^2) + \mathcal{O}(\kappa_0 \kappa_1 \kappa_2 \eta^2 G^2 \cdot \varphi_{w,L_3}),
\end{aligned} \tag{106}$$

where $\varphi_{w,L_3} = \frac{1}{T} \sum_{l=1}^L \alpha_l \sum_{k=1}^{B_l} \alpha_k \sum_{j=1}^{V_{k,l}} \alpha_j^2 \sum_{i=1}^{U_{j,k,l}} \alpha_i^2 \sum_{t=0}^{T-1} \left(\frac{1}{p_i^t} - 1 \right)$.

Lemma 10.

$$\begin{aligned}
& \frac{4\eta^2}{T} \sum_{t=0}^{T-1} \sum_{l=1}^L \alpha_l \sum_{k=1}^{B_l} \alpha_k \mathbb{E} \left\| \sum_{\tau=\bar{\tau}_2}^{t-1} \left[\sum_{k'=1}^{B_l} \alpha_{k'} \sum_{j'=1}^{V_{k',l}} \alpha_{j'} \sum_{i'=1}^{U_{j',k',l}} \alpha_{i'} \nabla \tilde{f}_{i'}(\tilde{\mathbf{w}}_{i'}^{\tau,0}) - \sum_{j=1}^{V_{k,l}} \alpha_j \sum_{i=1}^{U_{j,k,l}} \alpha_i \nabla \tilde{f}_i(\tilde{\mathbf{w}}_i^{\tau,0}) \right] \right\|^2 \\
& \leq \mathcal{O}(\kappa_0^3 \kappa_1^2 \kappa_2^2 \eta^4 \beta^2 \sigma^2) + \mathcal{O}(\kappa_0^3 \kappa_1^2 \kappa_2^2 \eta^4 \beta^2 \varepsilon_{vc}^2) + \mathcal{O}(\kappa_0^4 \kappa_1^4 \kappa_2^2 \eta^4 \beta^2 \varepsilon_{sbs}^2) + \mathcal{O}(\kappa_0^2 \kappa_1^2 \kappa_2^2 \eta^2 \beta^2 \varepsilon_{mbs}^2) + \mathcal{O}(\delta^{th} \kappa_0^2 \kappa_1^2 \kappa_2^2 \eta^2 \beta^2 D^2) + \\
& \quad \mathcal{O}(\kappa_0^3 \kappa_1^2 \kappa_2^2 \eta^4 \beta^2 G^2 \cdot \varphi_{w,L_1}) + \mathcal{O}(\kappa_0^2 \kappa_1^2 \kappa_2^2 \beta^2 \eta^4 \cdot \varphi_{w,L_2}) + \frac{56\kappa_0^2 \kappa_1^2 \kappa_2^2 \eta^2 \beta^2}{T} \sum_{t=0}^{T-1} \sum_{l=1}^L \alpha_l \sum_{k=1}^{B_l} \alpha_k \mathbb{E} \|\tilde{\mathbf{w}}_l^t - \tilde{\mathbf{w}}_k^t\|^2.
\end{aligned} \tag{107}$$

Using Lemma 9 and Lemma 10, when $\eta \leq \frac{1}{2\sqrt{14}\kappa_0 \kappa_1 \kappa_2 \beta}$, we have

$$\begin{aligned}
& \frac{\beta^2}{T} \sum_{t=0}^{T-1} \sum_{l=1}^L \alpha_l \sum_{k=1}^{B_l} \alpha_k \mathbb{E} \|\tilde{\mathbf{w}}_l^t - \tilde{\mathbf{w}}_k^t\|^2 \\
& \leq \mathcal{O}(\delta^{th} \beta^2 D^2) + \mathcal{O}(\kappa_0 \kappa_1 \kappa_2 \eta^2 \beta^2 \sigma^2) + \mathcal{O}(\kappa_0 \kappa_1 \kappa_2 \eta^2 \beta^2 G^2 \cdot \varphi_{w,L_3}) + \mathcal{O}(\kappa_0^3 \kappa_1^2 \kappa_2^2 \eta^4 \beta^4 \sigma^2) + \mathcal{O}(\kappa_0^3 \kappa_1^2 \kappa_2^2 \eta^4 \beta^4 \varepsilon_{vc}^2) + \\
& \quad \mathcal{O}(\kappa_0^4 \kappa_1^4 \kappa_2^2 \eta^4 \beta^4 \varepsilon_{sbs}^2) + \mathcal{O}(\kappa_0^2 \kappa_1^2 \kappa_2^2 \eta^2 \beta^4 \varepsilon_{mbs}^2) + \mathcal{O}(\delta^{th} \kappa_0^2 \kappa_1^2 \kappa_2^2 \eta^2 \beta^4 D^2) + \mathcal{O}(\kappa_0^3 \kappa_1^2 \kappa_2^2 \eta^4 \beta^4 G^2 \cdot \varphi_{w,L_1}) + \mathcal{O}(\kappa_0^2 \kappa_1^2 \kappa_2^2 \beta^4 \eta^4 \cdot \varphi_{w,L_2}) \\
& \approx \mathcal{O}(\kappa_0^3 \kappa_1^2 \kappa_2^2 \eta^4 \beta^4 \varepsilon_{vc}^2) + \mathcal{O}(\kappa_0^4 \kappa_1^4 \kappa_2^2 \eta^4 \beta^4 \varepsilon_{sbs}^2) + \mathcal{O}(\kappa_0^2 \kappa_1^2 \kappa_2^2 \eta^2 \beta^4 \varepsilon_{mbs}^2) + \mathcal{O}(\kappa_0 \kappa_1 \kappa_2 \eta^2 \beta^2 \sigma^2) + \mathcal{O}(\delta^{th} \beta^2 D^2) + \\
& \quad \mathcal{O}(\kappa_0^3 \kappa_1^2 \kappa_2^2 \eta^4 \beta^4 G^2 \cdot \varphi_{w,L_1}) + \mathcal{O}(\kappa_0^2 \kappa_1^2 \kappa_2^2 \beta^4 \eta^4 \cdot \varphi_{w,L_2}) + \mathcal{O}(\kappa_0 \kappa_1 \kappa_2 \eta^2 \beta^2 G^2 \cdot \varphi_{w,L_3}).
\end{aligned} \tag{108}$$

A. Missing Proof of Lemma 9

$$\begin{aligned}
& \frac{4\eta^2}{T} \sum_{t=0}^{T-1} \sum_{l=1}^L \alpha_l \sum_{k=1}^{B_l} \alpha_k \mathbb{E} \left\| \sum_{\tau=\bar{\tau}_2}^{t-1} \left[\sum_{j=1}^{V_{k,l}} \alpha_j \sum_{i=1}^{U_{j,k,l}} \alpha_i \left(\tilde{g}(\tilde{\mathbf{w}}_i^{\tau,0}) \frac{\mathbf{1}_i^\tau}{p_i^\tau} - \nabla \tilde{f}_i(\tilde{\mathbf{w}}_i^{\tau,0}) \right) - \sum_{k'=1}^{B_l} \alpha_{k'} \sum_{j'=1}^{V_{k',l}} \alpha_{j'} \sum_{i'=1}^{U_{j',k',l}} \alpha_{i'} \left(\tilde{g}(\tilde{\mathbf{w}}_{i'}^{\tau,0}) \frac{\mathbf{1}_{i'}^\tau}{p_{i'}^\tau} - \nabla \tilde{f}_{i'}(\tilde{\mathbf{w}}_{i'}^{\tau,0}) \right) \right] \right\|^2 \\
& \stackrel{(a)}{=} \frac{4\eta^2}{T} \sum_{t=0}^{T-1} \sum_{l=1}^L \alpha_l \sum_{k=1}^{B_l} \alpha_k \mathbb{E} \left\| \sum_{\tau=\bar{\tau}_2}^{t-1} \left[\sum_{j=1}^{V_{k,l}} \alpha_j \sum_{i=1}^{U_{j,k,l}} \alpha_i \left(\tilde{g}(\tilde{\mathbf{w}}_i^{\tau,0}) \frac{\mathbf{1}_i^\tau}{p_i^\tau} - \nabla \tilde{f}_i(\tilde{\mathbf{w}}_i^{\tau,0}) \right) \right] \right\|^2 - \\
& \quad \frac{4\eta^2}{T} \sum_{t=0}^{T-1} \sum_{l=1}^L \alpha_l \mathbb{E} \left\| \sum_{\tau=\bar{\tau}_2}^{t-1} \left[\sum_{k'=1}^{B_l} \alpha_{k'} \sum_{j'=1}^{V_{k',l}} \alpha_{j'} \sum_{i'=1}^{U_{j',k',l}} \alpha_{i'} \left(\tilde{g}(\tilde{\mathbf{w}}_{i'}^{\tau,0}) \frac{\mathbf{1}_{i'}^\tau}{p_{i'}^\tau} - \nabla \tilde{f}_{i'}(\tilde{\mathbf{w}}_{i'}^{\tau,0}) \right) \right] \right\|^2 \\
& \stackrel{(b)}{=} \frac{4\eta^2}{T} \sum_{t=0}^{T-1} \sum_{l=1}^L \alpha_l \sum_{k=1}^{B_l} \sum_{\tau=\bar{\tau}_2}^{t-1} \mathbb{E} \left\| \sum_{j=1}^{V_{k,l}} \alpha_j \sum_{i=1}^{U_{j,k,l}} \alpha_i \left(\tilde{g}(\tilde{\mathbf{w}}_i^{\tau,0}) \frac{\mathbf{1}_i^\tau}{p_i^\tau} - \nabla \tilde{f}_i(\tilde{\mathbf{w}}_i^{\tau,0}) \right) \right\|^2 - \\
& \quad \frac{4\eta^2}{T} \sum_{t=0}^{T-1} \sum_{l=1}^L \alpha_l \sum_{\tau=\bar{\tau}_2}^{t-1} \mathbb{E} \left\| \sum_{k'=1}^{B_l} \alpha_{k'} \sum_{j'=1}^{V_{k',l}} \alpha_{j'} \sum_{i'=1}^{U_{j',k',l}} \alpha_{i'} \left(\tilde{g}(\tilde{\mathbf{w}}_{i'}^{\tau,0}) \frac{\mathbf{1}_{i'}^\tau}{p_{i'}^\tau} - \nabla \tilde{f}_{i'}(\tilde{\mathbf{w}}_{i'}^{\tau,0}) \right) \right\|^2 \\
& \stackrel{(c)}{\leq} \frac{4\kappa_0 \kappa_1 \kappa_2 \eta^2}{T} \sum_{t=0}^{T-1} \sum_{l=1}^L \alpha_l \sum_{k=1}^{B_l} \alpha_k \mathbb{E} \left\| \sum_{j=1}^{V_{k,l}} \alpha_j \sum_{i=1}^{U_{j,k,l}} \alpha_i \left(\tilde{g}(\tilde{\mathbf{w}}_i^{t,0}) \frac{\mathbf{1}_i^t}{p_i^t} - \nabla \tilde{f}_i(\tilde{\mathbf{w}}_i^{t,0}) \right) \right\|^2 - \\
& \quad \frac{4\kappa_0 \kappa_1 \kappa_2 \eta^2}{T} \sum_{t=0}^{T-1} \sum_{l=1}^L \alpha_l \mathbb{E} \left\| \sum_{k'=1}^{B_l} \alpha_{k'} \sum_{j'=1}^{V_{k',l}} \alpha_{j'} \sum_{i'=1}^{U_{j',k',l}} \alpha_{i'} \left(\tilde{g}(\tilde{\mathbf{w}}_{i'}^{t,0}) \frac{\mathbf{1}_{i'}^t}{p_{i'}^t} - \nabla \tilde{f}_{i'}(\tilde{\mathbf{w}}_{i'}^{t,0}) \right) \right\|^2 \\
& \stackrel{(d)}{=} \frac{4\kappa_0 \kappa_1 \kappa_2 \eta^2}{T} \sum_{t=0}^{T-1} \sum_{l=1}^L \alpha_l \sum_{k=1}^{B_l} \sum_{j=1}^{V_{k,l}} \alpha_j^2 \sum_{i=1}^{U_{j,k,l}} \alpha_i^2 \mathbb{E} \left\| \tilde{g}(\tilde{\mathbf{w}}_i^{t,0}) \frac{\mathbf{1}_i^t}{p_i^t} \pm \tilde{g}(\tilde{\mathbf{w}}_i^{t,0}) - \nabla \tilde{f}_i(\tilde{\mathbf{w}}_i^{t,0}) \right\|^2 - \\
& \quad \frac{4\kappa_0 \kappa_1 \kappa_2 \eta^2}{T} \sum_{t=0}^{T-1} \sum_{l=1}^L \alpha_l \sum_{k=1}^{B_l} \sum_{j=1}^{V_{k,l}} \alpha_j^2 \sum_{i=1}^{U_{j,k,l}} \alpha_i^2 \mathbb{E} \left\| \tilde{g}(\tilde{\mathbf{w}}_i^{t,0}) \frac{\mathbf{1}_i^t}{p_i^t} \pm \tilde{g}(\tilde{\mathbf{w}}_i^{t,0}) - \nabla \tilde{f}_i(\tilde{\mathbf{w}}_i^{t,0}) \right\|^2
\end{aligned}$$

$$\begin{aligned}
&\leq 8\kappa_0\kappa_1\kappa_2\eta^2\sigma^2 \sum_{l=1}^L \alpha_l \sum_{k=1}^{B_l} \alpha_k \sum_{j=1}^{V_{k,l}} \alpha_j^2 \sum_{i=1}^{U_{j,k,l}} \alpha_i^2 + 8\kappa_0\kappa_1\kappa_2\eta^2G^2 \cdot \varphi_{w,L_3} \\
&\approx \mathcal{O}(\kappa_0\kappa_1\kappa_2\eta^2\sigma^2) + \mathcal{O}(\kappa_0\kappa_1\kappa_2\eta^2G^2 \cdot \varphi_{w,L_3}),
\end{aligned} \tag{109}$$

where $\varphi_{w,L_3} = \frac{1}{T} \sum_{l=1}^L \alpha_l \sum_{k=1}^{B_l} \alpha_k \sum_{j=1}^{V_{k,l}} \alpha_j^2 \sum_{i=1}^{U_{j,k,l}} \alpha_i^2 \sum_{t=0}^{T-1} \left(\frac{1}{p_i^t} - 1 \right)$.

B. Missing Proof of Lemma 10

$$\begin{aligned}
&\frac{4\eta^2}{T} \sum_{t=0}^{T-1} \sum_{l=1}^L \alpha_l \sum_{k=1}^{B_l} \alpha_k \mathbb{E} \left\| \sum_{\tau=\tau_2}^{t-1} \left[\sum_{k'=1}^{B_l} \alpha_{k'} \sum_{j'=1}^{V_{k',l}} \alpha_{j'} \sum_{i'=1}^{U_{j',k',l}} \alpha_{i'} \nabla \tilde{f}_{i'}(\tilde{\mathbf{w}}_{i'}^{\tau,0}) - \sum_{j=1}^{V_{k,l}} \alpha_j \sum_{i=1}^{U_{j,k,l}} \alpha_i \nabla \tilde{f}_i(\tilde{\mathbf{w}}_i^{\tau,0}) \right] \right\|^2 \\
&= \frac{4\kappa_0\kappa_1\kappa_2\eta^2}{T} \sum_{t=0}^{T-1} \sum_{l=1}^L \alpha_l \sum_{k=1}^{B_l} \alpha_k \sum_{\tau=\tau_2}^{t-1} \mathbb{E} \left\| \left(\sum_{j=1}^{V_{k,l}} \alpha_j \sum_{i=1}^{U_{j,k,l}} \alpha_i [\nabla \tilde{f}_i(\tilde{\mathbf{w}}_i^{\tau,0}) - \nabla \tilde{f}_i(\tilde{\mathbf{w}}_j^{\tau})] \right) + \right. \\
&\quad \left(\sum_{j=1}^{V_{k,l}} \alpha_j \sum_{i=1}^{U_{j,k,l}} \alpha_i [\nabla \tilde{f}_i(\tilde{\mathbf{w}}_j^{\tau}) - \nabla \tilde{f}_i(\tilde{\mathbf{w}}_k^{\tau})] \right) + \left(\sum_{j=1}^{V_{k,l}} \alpha_j \sum_{i=1}^{U_{j,k,l}} \alpha_i [\nabla \tilde{f}_i(\tilde{\mathbf{w}}_k^{\tau}) - \nabla \tilde{f}_i(\tilde{\mathbf{w}}_l^{\tau})] \right) + \\
&\quad \left(\sum_{j=1}^{V_{k,l}} \alpha_j \sum_{i=1}^{U_{j,k,l}} \alpha_i \nabla \tilde{f}_i(\tilde{\mathbf{w}}_l^{\tau}) - \sum_{k'=1}^{B_l} \alpha_{k'} \sum_{j'=1}^{V_{k',l}} \alpha_{j'} \sum_{i'=1}^{U_{j',k',l}} \alpha_{i'} \nabla \tilde{f}_{i'}(\tilde{\mathbf{w}}_l^{\tau}) \right) + \\
&\quad \left(\sum_{k'=1}^{B_l} \alpha_{k'} \sum_{j'=1}^{V_{k',l}} \alpha_{j'} \sum_{i'=1}^{U_{j',k',l}} \alpha_{i'} [\nabla \tilde{f}_{i'}(\tilde{\mathbf{w}}_l^{\tau}) - \nabla \tilde{f}_{i'}(\tilde{\mathbf{w}}_k^{\tau})] \right) + \\
&\quad \left(\sum_{k'=1}^{B_l} \alpha_{k'} \sum_{j'=1}^{V_{k',l}} \alpha_{j'} \sum_{i'=1}^{U_{j',k',l}} \alpha_{i'} [\nabla \tilde{f}_{i'}(\tilde{\mathbf{w}}_k^{\tau}) - \nabla \tilde{f}_{i'}(\tilde{\mathbf{w}}_j^{\tau})] \right) + \\
&\quad \left. \left(\sum_{k'=1}^{B_l} \alpha_{k'} \sum_{j'=1}^{V_{k',l}} \alpha_{j'} \sum_{i'=1}^{U_{j',k',l}} \alpha_{i'} [\nabla \tilde{f}_{i'}(\tilde{\mathbf{w}}_j^{\tau}) - \nabla \tilde{f}_{i'}(\tilde{\mathbf{w}}_{i'}^{\tau,0})] \right) \right\|^2 \\
&\leq 28\kappa_0^2\kappa_1^2\kappa_2^2\eta^2\beta^2\epsilon_{\text{mbs}}^2 + \frac{128\kappa_0^2\kappa_1^2\kappa_2^2\eta^2\beta^2}{T} \sum_{t=0}^{T-1} \sum_{l=1}^L \alpha_l \sum_{k=1}^{B_l} \alpha_k \sum_{j=1}^{V_{k,l}} \alpha_j \sum_{i=1}^{U_{j,k,l}} \alpha_i \mathbb{E} \|\tilde{\mathbf{w}}_i^t - \tilde{\mathbf{w}}_i^{t,0}\|^2 + \\
&\quad \frac{128\kappa_0^2\kappa_1^2\kappa_2^2\eta^2\beta^2}{T} \sum_{t=0}^{T-1} \sum_{l=1}^L \alpha_l \sum_{k=1}^{B_l} \alpha_k \sum_{j=1}^{V_{k,l}} \alpha_j \sum_{i=1}^{U_{j,k,l}} \alpha_i \mathbb{E} \|\tilde{\mathbf{w}}_j^t - \tilde{\mathbf{w}}_i^t\|^2 + \\
&\quad \frac{56\kappa_0^2\kappa_1^2\kappa_2^2\eta^2\beta^2}{T} \sum_{t=0}^{T-1} \sum_{l=1}^L \alpha_l \sum_{k=1}^{B_l} \alpha_k \sum_{j=1}^{V_{k,l}} \alpha_j \mathbb{E} \|\tilde{\mathbf{w}}_k^t - \tilde{\mathbf{w}}_j^t\|^2 + \\
&\quad \frac{56\kappa_0^2\kappa_1^2\kappa_2^2\eta^2\beta^2}{T} \sum_{t=0}^{T-1} \sum_{l=1}^L \alpha_l \sum_{k=1}^{B_l} \alpha_k \mathbb{E} \|\tilde{\mathbf{w}}_l^t - \tilde{\mathbf{w}}_k^t\|^2 \\
&\leq \mathcal{O}(\kappa_0^2\kappa_1^2\kappa_2^2\eta^2\beta^2\epsilon_{\text{mbs}}^2) + \mathcal{O}(\delta^{\text{th}}\kappa_0^2\kappa_1^2\kappa_2^2\eta^2\beta^2D^2) + \mathcal{O}(\kappa_0^3\kappa_1^2\kappa_2^2\eta^4\beta^2\sigma^2) + \mathcal{O}(\kappa_0^3\kappa_1^2\kappa_2^2\eta^4\beta^2\epsilon_{\text{vc}}^2) + \\
&\quad \mathcal{O}(\kappa_0^3\kappa_1^2\kappa_2^2\eta^4\beta^2G^2 \cdot \varphi_{w,L_1}) + \mathcal{O}(\delta^{\text{th}}\kappa_0^2\kappa_1^2\kappa_2^2\eta^2\beta^2D^2) + \mathcal{O}(\beta^4\kappa_0^6\kappa_1^4\kappa_2^2\eta^6\epsilon_{\text{vc}}^2) + \mathcal{O}(\kappa_0^4\kappa_1^4\kappa_2^2\eta^4\beta^2\epsilon_{\text{sbs}}^2) + \\
&\quad \mathcal{O}(\kappa_0^3\kappa_1^3\kappa_2^2\eta^4\sigma^2\beta^2) + \mathcal{O}(\delta^{\text{th}}\kappa_0^2\kappa_1^2\kappa_2^2\eta^2\beta^2D^2) + \mathcal{O}(\kappa_0^5\kappa_1^4\kappa_2^2\beta^4\eta^6G^2 \cdot \varphi_{w,L_1}) + \\
&\quad \mathcal{O}(\kappa_0^2\kappa_1^2\kappa_2^2\beta^2\eta^4 \cdot \varphi_{w,L_2}) + \frac{56\kappa_0^2\kappa_1^2\kappa_2^2\eta^2\beta^2}{T} \sum_{t=0}^{T-1} \sum_{l=1}^L \alpha_l \sum_{k=1}^{B_l} \alpha_k \mathbb{E} \|\tilde{\mathbf{w}}_l^t - \tilde{\mathbf{w}}_k^t\|^2 \\
&\approx \mathcal{O}(\kappa_0^3\kappa_1^2\kappa_2^2\eta^4\beta^2\sigma^2) + \mathcal{O}(\kappa_0^3\kappa_1^2\kappa_2^2\eta^4\beta^2\epsilon_{\text{vc}}^2) + \mathcal{O}(\kappa_0^4\kappa_1^4\kappa_2^2\eta^4\beta^2\epsilon_{\text{sbs}}^2) + \mathcal{O}(\kappa_0^2\kappa_1^2\kappa_2^2\eta^2\beta^2\epsilon_{\text{mbs}}^2) + \\
&\quad \mathcal{O}(\delta^{\text{th}}\kappa_0^2\kappa_1^2\kappa_2^2\eta^2\beta^2D^2) + \mathcal{O}(\kappa_0^3\kappa_1^2\kappa_2^2\eta^4\beta^2G^2 \cdot \varphi_{w,L_1}) + \\
&\quad \mathcal{O}(\kappa_0^2\kappa_1^2\kappa_2^2\beta^2\eta^4 \cdot \varphi_{w,L_2}) + \frac{56\kappa_0^2\kappa_1^2\kappa_2^2\eta^2\beta^2}{T} \sum_{t=0}^{T-1} \sum_{l=1}^L \alpha_l \sum_{k=1}^{B_l} \alpha_k \mathbb{E} \|\tilde{\mathbf{w}}_l^t - \tilde{\mathbf{w}}_k^t\|^2.
\end{aligned} \tag{110}$$

■

APPENDIX E
PROOF OF LEMMA 4

Lemma 4. When $\eta \leq 1/[6\sqrt{2}\kappa_0\kappa_1\kappa_2\kappa_3\beta]$, the average difference between the global and the mBS models, i.e., the L_4 term, is bounded as follows:

$$\begin{aligned} [\beta^2/T] \sum_{t=0}^{T-1} \sum_{l=1}^L \alpha_l \mathbb{E} \|\tilde{\mathbf{w}}^t - \tilde{\mathbf{w}}_l^t\|^2 &\leq \mathcal{O}(\kappa_0^4 \kappa_1^4 \kappa_2^2 \kappa_3^2 \eta^4 \beta^4 \epsilon_{\text{vc}}^2) + \mathcal{O}(\kappa_0^4 \kappa_1^4 \kappa_2^2 \kappa_3^2 \eta^4 \beta^4 \epsilon_{\text{sbs}}^2) + \\ &\mathcal{O}(\kappa_0^4 \kappa_1^4 \kappa_2^2 \kappa_3^2 \eta^4 \beta^6 \epsilon_{\text{mbs}}^2) + \mathcal{O}(\kappa_0^2 \kappa_1^2 \kappa_2^2 \kappa_3^2 \beta^4 \eta^2 \epsilon^2) + \mathcal{O}(\kappa_0 \kappa_1 \kappa_2 \kappa_3 \beta^2 \eta^2 \sigma^2) + \mathcal{O}(\delta^{\text{th}} \beta^2 D^2) + \\ &\mathcal{O}(\kappa_0^3 \kappa_1^2 \kappa_2^2 \kappa_3^2 \eta^4 \beta^4 G^2 \cdot \varphi_{\text{w},L_1}(\boldsymbol{\delta}, \mathbf{f}, \mathbf{P})) + \mathcal{O}(\kappa_0^3 \kappa_1^3 \kappa_2^2 \kappa_3^2 \beta^4 \eta^4 \cdot \varphi_{\text{w},L_2}(\boldsymbol{\delta}, \mathbf{f}, \mathbf{P})) + \\ &\mathcal{O}(\kappa_0^3 \kappa_1^3 \kappa_2^3 \kappa_3^2 \eta^4 \beta^4 G^2 \cdot \varphi_{\text{w},L_3}(\boldsymbol{\delta}, \mathbf{f}, \mathbf{P})) + \mathcal{O}(\kappa_0 \kappa_1 \kappa_2 \kappa_3 \beta^2 \eta^2 G^2 \cdot \varphi_{\text{w},L_4}(\boldsymbol{\delta}, \mathbf{f}, \mathbf{P})), \end{aligned} \quad (111)$$

where $\varphi_{\text{w},L_4}(\boldsymbol{\delta}, \mathbf{f}, \mathbf{P}) = [1/T] \sum_{l=1}^L \alpha_l \sum_{k=1}^{B_l} \alpha_k^2 \sum_{j=1}^{V_{k,l}} \alpha_j^2 \sum_{i=1}^{U_{j,k,l}} \alpha_i^2 \sum_{t=0}^{T-1} (1/p_i^t - 1)$.

Proof.

$$\begin{aligned} &\frac{1}{T} \sum_{t=0}^{T-1} \sum_{l=1}^L \alpha_l \mathbb{E} \|\tilde{\mathbf{w}}^t - \tilde{\mathbf{w}}_l^t\|^2 \\ &= \frac{1}{T} \sum_{t=0}^{T-1} \sum_{l=1}^L \alpha_l \mathbb{E} \left\| \tilde{\mathbf{w}}^{m\Pi_{z=0}^3 \kappa_z, 0} - \eta \sum_{\tau=m\Pi_{z=0}^3 \kappa_z}^{t-1} \sum_{l'=1}^L \alpha_{l'} \sum_{k'=1}^{B_{l'}} \alpha_{k'} \sum_{j'=1}^{V_{k',l'}} \alpha_{j'} \sum_{i'=1}^{U_{j',k',l'}} \alpha_{i'} \tilde{g}(\tilde{\mathbf{w}}_{i'}^{\tau,0}) \frac{\mathbf{1}_{i'}^\tau}{p_{i'}^\tau} - \right. \\ &\quad \left. \left(\tilde{\mathbf{w}}_l^{m\Pi_{z=0}^3 \kappa_z, 0} - \eta \sum_{\tau=m\Pi_{z=0}^3 \kappa_z}^{t-1} \sum_{k=1}^{B_l} \alpha_k \sum_{j=1}^{V_{k,l}} \alpha_j \sum_{i=1}^{U_{j,k,l}} \alpha_i \tilde{g}(\tilde{\mathbf{w}}_i^{\tau,0}) \frac{\mathbf{1}_i^\tau}{p_i^\tau} \right) \right\|^2, \\ &\leq \frac{2}{T} \sum_{t=0}^{T-1} \sum_{l=1}^L \alpha_l \mathbb{E} \left\| \tilde{\mathbf{w}}^{m\Pi_{z=0}^3 \kappa_z, 0} - \tilde{\mathbf{w}}_l^{m\Pi_{z=0}^3 \kappa_z, 0} \right\|^2 + \\ &\quad \frac{2\eta^2}{T} \sum_{t=0}^{T-1} \sum_{l=1}^L \alpha_l \mathbb{E} \left\| \sum_{\tau=m\Pi_{z=0}^3 \kappa_z}^{t-1} \left[\sum_{k=1}^{B_l} \alpha_k \sum_{j=1}^{V_{k,l}} \alpha_j \sum_{i=1}^{U_{j,k,l}} \alpha_i \tilde{g}(\tilde{\mathbf{w}}_i^{\tau,0}) \frac{\mathbf{1}_i^\tau}{p_i^\tau} - \sum_{l'=1}^L \alpha_{l'} \sum_{k'=1}^{B_{l'}} \alpha_{k'} \sum_{j'=1}^{V_{k',l'}} \alpha_{j'} \sum_{i'=1}^{U_{j',k',l'}} \alpha_{i'} \tilde{g}(\tilde{\mathbf{w}}_{i'}^{\tau,0}) \frac{\mathbf{1}_{i'}^\tau}{p_{i'}^\tau} \right] \right\|^2, \end{aligned} \quad (112)$$

where the last inequality follows from Jensen inequality.

For the first term of (112), we have

$$\begin{aligned} &2 \sum_{l=1}^L \alpha_l \mathbb{E} \left\| \tilde{\mathbf{w}}^{m\Pi_{z=0}^3 \kappa_z, 0} - \tilde{\mathbf{w}}_l^{m\Pi_{z=0}^3 \kappa_z, 0} \right\|^2, \\ &\stackrel{(a)}{=} 2 \sum_{l=1}^L \alpha_l \mathbb{E} \left\| \tilde{\mathbf{w}}^{m\Pi_{z=0}^3 \kappa_z, 0} - \mathbf{w}^{m\Pi_{z=0}^3 \kappa_z} + \mathbf{w}_l^{m\Pi_{z=0}^3 \kappa_z} - \tilde{\mathbf{w}}_l^{m\Pi_{z=0}^3 \kappa_z, 0} \right\|^2, \\ &\stackrel{(b)}{\leq} 4 \sum_{l=1}^L \alpha_l \mathbb{E} \left\| \tilde{\mathbf{w}}^{m\Pi_{z=0}^3 \kappa_z, 0} - \mathbf{w}^{m\Pi_{z=0}^3 \kappa_z} \right\|^2 + 4 \sum_{l=1}^L \alpha_l \mathbb{E} \left\| \mathbf{w}_l^{m\Pi_{z=0}^3 \kappa_z} - \tilde{\mathbf{w}}_l^{m\Pi_{z=0}^3 \kappa_z, 0} \right\|^2, \\ &\leq 8 \sum_{l=1}^L \alpha_l \sum_{k=1}^{B_l} \alpha_k \sum_{j=1}^{V_{k,l}} \alpha_j \sum_{i=1}^{U_{j,k,l}} \alpha_i \delta_i^m \Pi_{z=0}^3 \kappa_z \mathbb{E} \left\| \mathbf{w}_i^{m\Pi_{z=0}^3 \kappa_z} \right\|^2, \end{aligned} \quad (113)$$

where in (a), we use the fact that $\mathbf{w}^{m\Pi_{z=0}^3 \kappa_z} = \mathbf{w}_l^{m\Pi_{z=0}^3 \kappa_z}$ and (b) stems from $\|\sum_{i=1}^n \mathbf{a}_i\|^2 \leq n \sum_{i=1}^n \|\mathbf{a}_i\|^2$. Moreover, the last inequality appears following steps as in (75) and (74).

As such, we simplify the first term as

$$\begin{aligned} &\frac{2}{T} \sum_{t=0}^{T-1} \sum_{l=1}^L \alpha_l \mathbb{E} \left\| \tilde{\mathbf{w}}^{m\Pi_{z=0}^3 \kappa_z, 0} - \tilde{\mathbf{w}}_l^{m\Pi_{z=0}^3 \kappa_z, 0} \right\|^2 \leq \frac{8}{T} \sum_{t=0}^{T-1} \sum_{l=1}^L \alpha_l \sum_{k=1}^{B_l} \alpha_k \sum_{j=1}^{V_{k,l}} \alpha_j \sum_{i=1}^{U_{j,k,l}} \alpha_i \delta_i^{\lfloor t/[\Pi_{z=0}^3 \kappa_z] \rfloor} \mathbb{E} \left\| \mathbf{w}_i^{\lfloor t/[\Pi_{z=0}^3 \kappa_z] \rfloor} \right\|^2 \\ &\approx \mathcal{O}(\delta^{\text{th}} D^2). \end{aligned} \quad (114)$$

The second term of (112) is further simplified as follows:

$$\begin{aligned} &\frac{2\eta^2}{T} \sum_{t=0}^{T-1} \sum_{l=1}^L \alpha_l \mathbb{E} \left\| \sum_{\tau=m\Pi_{z=0}^3 \kappa_z}^{t-1} \left[\sum_{k=1}^{B_l} \alpha_k \sum_{j=1}^{V_{k,l}} \alpha_j \sum_{i=1}^{U_{j,k,l}} \alpha_i \tilde{g}(\tilde{\mathbf{w}}_i^{\tau,0}) \frac{\mathbf{1}_i^\tau}{p_i^\tau} - \sum_{l'=1}^L \alpha_{l'} \sum_{k'=1}^{B_{l'}} \alpha_{k'} \sum_{j'=1}^{V_{k',l'}} \alpha_{j'} \sum_{i'=1}^{U_{j',k',l'}} \alpha_{i'} \tilde{g}(\tilde{\mathbf{w}}_{i'}^{\tau,0}) \frac{\mathbf{1}_{i'}^\tau}{p_{i'}^\tau} \right] \right\|^2 \\ &= \frac{2\eta^2}{T} \sum_{t=0}^{T-1} \sum_{l=1}^L \alpha_l \mathbb{E} \left\| \sum_{\tau=m\Pi_{z=0}^3 \kappa_z}^{t-1} \left[\sum_{k=1}^{B_l} \alpha_k \sum_{j=1}^{V_{k,l}} \alpha_j \sum_{i=1}^{U_{j,k,l}} \alpha_i \left(\tilde{g}(\tilde{\mathbf{w}}_i^{\tau,0}) \frac{\mathbf{1}_i^\tau}{p_i^\tau} - \nabla \tilde{f}_i(\tilde{\mathbf{w}}_i^{\tau,0}) \right) - \right. \right. \end{aligned}$$

$$\begin{aligned}
& \sum_{l'=1}^L \alpha_{l'} \sum_{k'=1}^{B_{l'}} \alpha_{k'} \sum_{j'=1}^{V_{k',l'}} \alpha_{j'} \sum_{i'=1}^{U_{j',k',l'}} \alpha_{i'} \left(\tilde{g}(\tilde{\mathbf{w}}_{i'}^{\tau,0}) \frac{\mathbf{1}_{i'}^{\tau}}{p_{i'}^{\tau}} - \tilde{f}_{i'}(\tilde{\mathbf{w}}_{i'}^{\tau,0}) \right) + \\
& \left\| \sum_{k=1}^{B_l} \alpha_k \sum_{j=1}^{V_{k,l}} \alpha_j \sum_{i=1}^{U_{j,k,l}} \alpha_i \nabla \tilde{f}_i(\tilde{\mathbf{w}}_i^{\tau,0}) - \sum_{l'=1}^L \alpha_{l'} \sum_{k'=1}^{B_{l'}} \alpha_{k'} \sum_{j'=1}^{V_{k',l'}} \alpha_{j'} \sum_{i'=1}^{U_{j',k',l'}} \alpha_{i'} \tilde{f}_{i'}(\tilde{\mathbf{w}}_{i'}^{\tau,0}) \right\|^2 \\
& \leq \frac{4\eta^2}{T} \sum_{t=0}^{T-1} \sum_{l=1}^L \alpha_l \mathbb{E} \left\| \sum_{\tau=m}^{t-1} \prod_{z=0}^{\tau} \kappa_z \left[\sum_{k=1}^{B_l} \alpha_k \sum_{j=1}^{V_{k,l}} \alpha_j \sum_{i=1}^{U_{j,k,l}} \alpha_i \left(\tilde{g}(\tilde{\mathbf{w}}_i^{\tau,0}) \frac{\mathbf{1}_i^{\tau}}{p_i^{\tau}} - \nabla \tilde{f}_i(\tilde{\mathbf{w}}_i^{\tau,0}) \right) - \right. \right. \\
& \quad \left. \sum_{l'=1}^L \alpha_{l'} \sum_{k'=1}^{B_{l'}} \alpha_{k'} \sum_{j'=1}^{V_{k',l'}} \alpha_{j'} \sum_{i'=1}^{U_{j',k',l'}} \alpha_{i'} \left(\tilde{g}(\tilde{\mathbf{w}}_{i'}^{\tau,0}) \frac{\mathbf{1}_{i'}^{\tau}}{p_{i'}^{\tau}} - \tilde{f}_{i'}(\tilde{\mathbf{w}}_{i'}^{\tau,0}) \right) \right] \right\|^2 + \\
& \quad \frac{4\eta^2}{T} \sum_{t=0}^{T-1} \sum_{l=1}^L \alpha_l \mathbb{E} \left\| \sum_{\tau=m}^{t-1} \prod_{z=0}^{\tau} \kappa_z \left[\sum_{k=1}^{B_l} \alpha_k \sum_{j=1}^{V_{k,l}} \alpha_j \sum_{i=1}^{U_{j,k,l}} \alpha_i \nabla \tilde{f}_i(\tilde{\mathbf{w}}_i^{\tau,0}) - \sum_{l'=1}^L \alpha_{l'} \sum_{k'=1}^{B_{l'}} \alpha_{k'} \sum_{j'=1}^{V_{k',l'}} \alpha_{j'} \sum_{i'=1}^{U_{j',k',l'}} \alpha_{i'} \tilde{f}_{i'}(\tilde{\mathbf{w}}_{i'}^{\tau,0}) \right] \right\|^2. \quad (115)
\end{aligned}$$

Lemma 11. *The first term of (115) is bounded as follow:*

$$\begin{aligned}
& \frac{4\eta^2}{T} \sum_{t=0}^{T-1} \sum_{l=1}^L \alpha_l \mathbb{E} \left\| \sum_{\tau=m}^{t-1} \prod_{z=0}^{\tau} \kappa_z \left[\sum_{k=1}^{B_l} \alpha_k \sum_{j=1}^{V_{k,l}} \alpha_j \sum_{i=1}^{U_{j,k,l}} \alpha_i \left(\tilde{g}(\tilde{\mathbf{w}}_i^{\tau,0}) \frac{\mathbf{1}_i^{\tau}}{p_i^{\tau}} - \nabla \tilde{f}_i(\tilde{\mathbf{w}}_i^{\tau,0}) \right) - \right. \right. \\
& \quad \left. \left. \sum_{l'=1}^L \alpha_{l'} \sum_{k'=1}^{B_{l'}} \alpha_{k'} \sum_{j'=1}^{V_{k',l'}} \alpha_{j'} \sum_{i'=1}^{U_{j',k',l'}} \alpha_{i'} \left(\tilde{g}(\tilde{\mathbf{w}}_{i'}^{\tau,0}) \frac{\mathbf{1}_{i'}^{\tau}}{p_{i'}^{\tau}} - \tilde{f}_{i'}(\tilde{\mathbf{w}}_{i'}^{\tau,0}) \right) \right] \right\|^2 \\
& \leq 8 \left(\prod_{z=0}^3 \kappa_z \right) \eta^2 \sigma^2 \sum_{l=1}^L \alpha_l \sum_{k=1}^{B_l} \alpha_k^2 \sum_{j=1}^{V_{k,l}} \alpha_j^2 \sum_{i=1}^{U_{j,k,l}} \alpha_i^2 + \frac{8 \left(\prod_{z=0}^3 \kappa_z \right) \eta^2 G^2}{T} \sum_{l=1}^L \alpha_l \sum_{k=1}^{B_l} \alpha_k^2 \sum_{j=1}^{V_{k,l}} \alpha_j^2 \sum_{i=1}^{U_{j,k,l}} \alpha_i^2 \sum_{t=0}^{T-1} \left(\frac{1-p_i^t}{p_i^t} \right) \\
& \approx \mathcal{O}(\kappa_0 \kappa_1 \kappa_2 \kappa_3 \eta^2 \sigma^2) + \mathcal{O}(\kappa_0 \kappa_1 \kappa_2 \kappa_3 \eta^2 G^2 \cdot \varphi_{w,L_4}), \quad (116)
\end{aligned}$$

where $\varphi_{w,L_4} = \frac{1}{T} \sum_{l=1}^L \alpha_l \sum_{k=1}^{B_l} \alpha_k^2 \sum_{j=1}^{V_{k,l}} \alpha_j^2 \sum_{i=1}^{U_{j,k,l}} \alpha_i^2 \sum_{t=0}^{T-1} \left(\frac{1-p_i^t}{p_i^t} \right)$.

Lemma 12. *The second term of (115) is bounded as follow:*

$$\begin{aligned}
& \frac{4\eta^2}{T} \sum_{t=0}^{T-1} \sum_{l=1}^L \alpha_l \mathbb{E} \left\| \sum_{\tau=m}^{t-1} \prod_{z=0}^{\tau} \kappa_z \left[\sum_{k=1}^{B_l} \alpha_k \sum_{j=1}^{V_{k,l}} \alpha_j \sum_{i=1}^{U_{j,k,l}} \alpha_i \nabla \tilde{f}_i(\tilde{\mathbf{w}}_i^{\tau,0}) - \sum_{l'=1}^L \alpha_{l'} \sum_{k'=1}^{B_{l'}} \alpha_{k'} \sum_{j'=1}^{V_{k',l'}} \alpha_{j'} \sum_{i'=1}^{U_{j',k',l'}} \alpha_{i'} \tilde{f}_{i'}(\tilde{\mathbf{w}}_{i'}^{\tau,0}) \right] \right\|^2 \\
& \leq \mathcal{O}(\kappa_0^4 \kappa_1^2 \kappa_2^2 \kappa_3^2 \eta^4 \beta^2 \varepsilon_{vc}^2) + \mathcal{O}(\kappa_0^4 \kappa_1^4 \kappa_2^2 \kappa_3^2 \eta^4 \beta^2 \varepsilon_{sbs}^2) + \mathcal{O}(\kappa_0^4 \kappa_1^4 \kappa_2^4 \kappa_3^2 \eta^4 \beta^4 \varepsilon_{mbs}^2) + \\
& \quad \mathcal{O}(\kappa_0^2 \kappa_1^2 \kappa_2^2 \kappa_3^2 \beta^2 \eta^2 \varepsilon^2) + \mathcal{O}(\kappa_0^2 \kappa_1^2 \kappa_2^2 \kappa_3^2 \eta^4 \beta^2 \sigma^2) + \mathcal{O}(\delta^{\text{th}} \kappa_0^2 \kappa_1^2 \kappa_2^2 \kappa_3^2 \eta^2 \beta^2 D^2) + \\
& \quad \mathcal{O}(\kappa_0^3 \kappa_1^2 \kappa_2^2 \kappa_3^2 \eta^4 \beta^2 G^2 \cdot \varphi_{w,L_1}) + \mathcal{O}(\kappa_0^3 \kappa_1^3 \kappa_2^2 \kappa_3^2 \beta^2 \eta^4 \cdot \varphi_{w,L_2}) + \\
& \quad \mathcal{O}(\kappa_0^3 \kappa_1^3 \kappa_2^3 \kappa_3^2 \eta^4 \beta^2 G^2 \cdot \varphi_{w,L_3}) + \frac{72(\beta \eta \kappa_0 \kappa_1 \kappa_2 \kappa_3)^2}{T} \sum_{t=0}^{T-1} \sum_{l=1}^L \alpha_l \mathbb{E} \left\| \tilde{\mathbf{w}}^t - \tilde{\mathbf{w}}_l^t \right\|^2. \quad (117)
\end{aligned}$$

Using Lemma 11 and Lemma 12, and assuming $\eta \leq \frac{1}{6\sqrt{2}\kappa_0 \kappa_1 \kappa_2 \kappa_3 \beta}$, we get

$$\begin{aligned}
& \frac{\beta^2}{T} \sum_{t=0}^{T-1} \sum_{l=1}^L \alpha_l \mathbb{E} \left\| \tilde{\mathbf{w}}^t - \tilde{\mathbf{w}}_l^t \right\|^2 \\
& \leq \mathcal{O}(\delta^{\text{th}} \beta^2 D^2) + \mathcal{O}(\kappa_0 \kappa_1 \kappa_2 \kappa_3 \beta^2 \eta^2 \sigma^2) + \mathcal{O}(\kappa_0 \kappa_1 \kappa_2 \kappa_3 \beta^2 \eta^2 G^2 \cdot \varphi_{w,L_4}) + \\
& \quad \mathcal{O}(\kappa_0^4 \kappa_1^2 \kappa_2^2 \kappa_3^2 \eta^4 \beta^4 \varepsilon_{vc}^2) + \mathcal{O}(\kappa_0^4 \kappa_1^4 \kappa_2^2 \kappa_3^2 \eta^4 \beta^4 \varepsilon_{sbs}^2) + \mathcal{O}(\kappa_0^4 \kappa_1^4 \kappa_2^4 \kappa_3^2 \eta^4 \beta^6 \varepsilon_{mbs}^2) + \\
& \quad \mathcal{O}(\kappa_0^2 \kappa_1^2 \kappa_2^2 \kappa_3^2 \beta^4 \eta^2 \varepsilon^2) + \mathcal{O}(\kappa_0^2 \kappa_1^2 \kappa_2^2 \kappa_3^2 \eta^4 \beta^4 \sigma^2) + \mathcal{O}(\delta^{\text{th}} \kappa_0^2 \kappa_1^2 \kappa_2^2 \kappa_3^2 \eta^2 \beta^4 D^2) + \\
& \quad \mathcal{O}(\kappa_0^3 \kappa_1^2 \kappa_2^2 \kappa_3^2 \eta^4 \beta^4 G^2 \cdot \varphi_{w,L_1}) + \mathcal{O}(\kappa_0^3 \kappa_1^3 \kappa_2^2 \kappa_3^2 \beta^4 \eta^4 \cdot \varphi_{w,L_2}) + \\
& \quad \mathcal{O}(\kappa_0^3 \kappa_1^3 \kappa_2^3 \kappa_3^2 \eta^4 \beta^4 G^2 \cdot \varphi_{w,L_3}) \\
& \approx \mathcal{O}(\kappa_0^4 \kappa_1^2 \kappa_2^2 \kappa_3^2 \eta^4 \beta^4 \varepsilon_{vc}^2) + \mathcal{O}(\kappa_0^4 \kappa_1^4 \kappa_2^2 \kappa_3^2 \eta^4 \beta^4 \varepsilon_{sbs}^2) + \mathcal{O}(\kappa_0^4 \kappa_1^4 \kappa_2^4 \kappa_3^2 \eta^4 \beta^6 \varepsilon_{mbs}^2) + \\
& \quad \mathcal{O}(\kappa_0^2 \kappa_1^2 \kappa_2^2 \kappa_3^2 \beta^4 \eta^2 \varepsilon^2) + \mathcal{O}(\kappa_0 \kappa_1 \kappa_2 \kappa_3 \beta^2 \eta^2 \sigma^2) + \mathcal{O}(\delta^{\text{th}} \beta^2 D^2) + \\
& \quad \mathcal{O}(\kappa_0^3 \kappa_1^2 \kappa_2^2 \kappa_3^2 \eta^4 \beta^4 G^2 \cdot \varphi_{w,L_1}) + \mathcal{O}(\kappa_0^3 \kappa_1^3 \kappa_2^2 \kappa_3^2 \beta^4 \eta^4 \cdot \varphi_{w,L_2}) + \\
& \quad \mathcal{O}(\kappa_0^3 \kappa_1^3 \kappa_2^3 \kappa_3^2 \eta^4 \beta^4 G^2 \cdot \varphi_{w,L_3}) + \mathcal{O}(\kappa_0 \kappa_1 \kappa_2 \kappa_3 \beta^2 \eta^2 G^2 \cdot \varphi_{w,L_4}). \quad (118)
\end{aligned}$$

A. Missing Proof of Lemma 11

$$\begin{aligned}
& \frac{4\eta^2}{T} \sum_{t=0}^{T-1} \sum_{l=1}^L \alpha_l \mathbb{E} \left\| \sum_{\tau=m}^{t-1} \prod_{z=0}^3 \kappa_z \left[\sum_{k=1}^{B_l} \alpha_k \sum_{j=1}^{V_{k,l}} \alpha_j \sum_{i=1}^{U_{j,k,l}} \alpha_i \left(\tilde{g}(\tilde{\mathbf{w}}_i^{\tau,0}) \frac{\mathbf{1}_i^\tau}{p_i^\tau} - \nabla \tilde{f}_i(\tilde{\mathbf{w}}_i^{\tau,0}) \right) - \right. \right. \\
& \quad \left. \left. \sum_{l'=1}^L \alpha_{l'} \sum_{k'=1}^{B_{l'}} \alpha_{k'} \sum_{j'=1}^{V_{k',l'}} \alpha_{j'} \sum_{i'=1}^{U_{j',k',l'}} \alpha_{i'} \left(\tilde{g}(\tilde{\mathbf{w}}_{i'}^{\tau,0}) \frac{\mathbf{1}_{i'}^\tau}{p_{i'}^\tau} - \tilde{f}_{i'}(\tilde{\mathbf{w}}_{i'}^{\tau,0}) \right) \right] \right\|^2 \\
& \stackrel{(a)}{=} \frac{4\eta^2}{T} \sum_{t=0}^{T-1} \sum_{l=1}^L \alpha_l \mathbb{E} \left\| \sum_{\tau=m}^{t-1} \prod_{z=0}^3 \kappa_z \left[\sum_{k=1}^{B_l} \alpha_k \sum_{j=1}^{V_{k,l}} \alpha_j \sum_{i=1}^{U_{j,k,l}} \alpha_i \left(\tilde{g}(\tilde{\mathbf{w}}_i^{\tau,0}) \frac{\mathbf{1}_i^\tau}{p_i^\tau} - \nabla \tilde{f}_i(\tilde{\mathbf{w}}_i^{\tau,0}) \right) \right] \right\|^2 - \\
& \quad \frac{4\eta^2}{T} \sum_{t=0}^{T-1} \mathbb{E} \left\| \sum_{\tau=m}^{t-1} \prod_{z=0}^3 \kappa_z \left[\sum_{l=1}^L \alpha_l \sum_{k=1}^{B_l} \alpha_k \sum_{j=1}^{V_{k,l}} \alpha_j \sum_{i=1}^{U_{j,k,l}} \alpha_i \left(\tilde{g}(\tilde{\mathbf{w}}_i^{\tau,0}) \frac{\mathbf{1}_i^\tau}{p_i^\tau} - \tilde{f}_i(\tilde{\mathbf{w}}_i^{\tau,0}) \right) \right] \right\|^2 \\
& \stackrel{(b)}{=} \frac{4\eta^2}{T} \sum_{t=0}^{T-1} \sum_{l=1}^L \alpha_l \sum_{\tau=m}^{t-1} \prod_{z=0}^3 \kappa_z \mathbb{E} \left\| \sum_{k=1}^{B_l} \alpha_k \sum_{j=1}^{V_{k,l}} \alpha_j \sum_{i=1}^{U_{j,k,l}} \alpha_i \left(\tilde{g}(\tilde{\mathbf{w}}_i^{\tau,0}) \frac{\mathbf{1}_i^\tau}{p_i^\tau} - \nabla \tilde{f}_i(\tilde{\mathbf{w}}_i^{\tau,0}) \right) \right\|^2 - \\
& \quad \frac{4\eta^2}{T} \sum_{t=0}^{T-1} \sum_{\tau=m}^{t-1} \prod_{z=0}^3 \kappa_z \mathbb{E} \left\| \sum_{l=1}^L \alpha_l \sum_{k=1}^{B_l} \alpha_k \sum_{j=1}^{V_{k,l}} \alpha_j \sum_{i=1}^{U_{j,k,l}} \alpha_i \left(\tilde{g}(\tilde{\mathbf{w}}_i^{\tau,0}) \frac{\mathbf{1}_i^\tau}{p_i^\tau} - \tilde{f}_i(\tilde{\mathbf{w}}_i^{\tau,0}) \right) \right\|^2 \\
& \stackrel{(c)}{\leq} \frac{4\kappa_0 \kappa_1 \kappa_2 \kappa_3 \eta^2}{T} \sum_{t=0}^{T-1} \sum_{l=1}^L \alpha_l \mathbb{E} \left\| \sum_{k=1}^{B_l} \alpha_k \sum_{j=1}^{V_{k,l}} \alpha_j \sum_{i=1}^{U_{j,k,l}} \alpha_i \left(\tilde{g}(\tilde{\mathbf{w}}_i^{t,0}) \frac{\mathbf{1}_i^t}{p_i^t} \pm \tilde{g}(\tilde{\mathbf{w}}_i^{t,0}) - \nabla \tilde{f}_i(\tilde{\mathbf{w}}_i^{t,0}) \right) \right\|^2 - \\
& \quad \frac{4\kappa_0 \kappa_1 \kappa_2 \kappa_3 \eta^2}{T} \sum_{t=0}^{T-1} \mathbb{E} \left\| \sum_{l=1}^L \alpha_l \sum_{k=1}^{B_l} \alpha_k \sum_{j=1}^{V_{k,l}} \alpha_j \sum_{i=1}^{U_{j,k,l}} \alpha_i \left(\tilde{g}(\tilde{\mathbf{w}}_i^{t,0}) \frac{\mathbf{1}_i^t}{p_i^t} \pm \tilde{g}(\tilde{\mathbf{w}}_i^{t,0}) - \tilde{f}_i(\tilde{\mathbf{w}}_i^{t,0}) \right) \right\|^2 \\
& \leq 8\kappa_0 \kappa_1 \kappa_2 \kappa_3 \eta^2 \sigma^2 \sum_{l=1}^L \alpha_l \sum_{k=1}^{B_l} \alpha_k^2 \sum_{j=1}^{V_{k,l}} \alpha_j^2 \sum_{i=1}^{U_{j,k,l}} \alpha_i^2 + \frac{8\kappa_0 \kappa_1 \kappa_2 \kappa_3 \eta^2 G^2}{T} \sum_{l=1}^L \alpha_l \sum_{k=1}^{B_l} \alpha_k^2 \sum_{j=1}^{V_{k,l}} \alpha_j^2 \sum_{i=1}^{U_{j,k,l}} \alpha_i^2 \sum_{t=0}^{T-1} \left(\frac{1-p_i^t}{p_i^t} \right) \\
& \approx \mathcal{O}(\kappa_0 \kappa_1 \kappa_2 \kappa_3 \eta^2 \sigma^2) + \mathcal{O}(\kappa_0 \kappa_1 \kappa_2 \kappa_3 \eta^2 G^2 \cdot \varphi_{w,L_4}), \tag{119}
\end{aligned}$$

where $\varphi_{w,L_4} = \frac{1}{T} \sum_{l=1}^L \alpha_l \sum_{k=1}^{B_l} \alpha_k^2 \sum_{j=1}^{V_{k,l}} \alpha_j^2 \sum_{i=1}^{U_{j,k,l}} \alpha_i^2 \sum_{t=0}^{T-1} \left(\frac{1-p_i^t}{p_i^t} \right)$.

B. Missing Proof of Lemma 12

$$\begin{aligned}
& \frac{4\eta^2}{T} \sum_{t=0}^{T-1} \sum_{l=1}^L \alpha_l \mathbb{E} \left\| \sum_{\tau=m}^{t-1} \prod_{z=0}^3 \kappa_z \left[\sum_{k=1}^{B_l} \alpha_k \sum_{j=1}^{V_{k,l}} \alpha_j \sum_{i=1}^{U_{j,k,l}} \alpha_i \nabla \tilde{f}_i(\tilde{\mathbf{w}}_i^{\tau,0}) - \sum_{l'=1}^L \alpha_{l'} \sum_{k'=1}^{B_{l'}} \alpha_{k'} \sum_{j'=1}^{V_{k',l'}} \alpha_{j'} \sum_{i'=1}^{U_{j',k',l'}} \alpha_{i'} \nabla \tilde{f}_{i'}(\tilde{\mathbf{w}}_{i'}^{\tau,0}) \right] \right\|^2 \\
& = \frac{4\kappa_0 \kappa_1 \kappa_2 \kappa_3 \eta^2}{T} \sum_{t=0}^{T-1} \sum_{l=1}^L \alpha_l \mathbb{E} \left\| \left(\sum_{k=1}^{B_l} \alpha_k \sum_{j=1}^{V_{k,l}} \alpha_j \sum_{i=1}^{U_{j,k,l}} \alpha_i [\nabla \tilde{f}_i(\tilde{\mathbf{w}}_i^{t,0}) - \nabla \tilde{f}_i(\tilde{\mathbf{w}}_j^t)] \right) + \right. \\
& \quad \left(\sum_{k=1}^{B_l} \alpha_k \sum_{j=1}^{V_{k,l}} \alpha_j \sum_{i=1}^{U_{j,k,l}} \alpha_i [\nabla \tilde{f}_i(\tilde{\mathbf{w}}_j^t) - \nabla \tilde{f}_i(\tilde{\mathbf{w}}_k^t)] \right) + \left(\sum_{k=1}^{B_l} \alpha_k \sum_{j=1}^{V_{k,l}} \alpha_j \sum_{i=1}^{U_{j,k,l}} \alpha_i [\nabla \tilde{f}_i(\tilde{\mathbf{w}}_k^t) - \nabla \tilde{f}_i(\tilde{\mathbf{w}}_l^t)] \right) + \\
& \quad \left(\sum_{k=1}^{B_l} \alpha_k \sum_{j=1}^{V_{k,l}} \alpha_j \sum_{i=1}^{U_{j,k,l}} \alpha_i [\nabla \tilde{f}_i(\tilde{\mathbf{w}}_l^t) - \nabla \tilde{f}_i(\tilde{\mathbf{w}}^t)] \right) + \left(\sum_{k=1}^{B_l} \alpha_k \sum_{j=1}^{V_{k,l}} \alpha_j \sum_{i=1}^{U_{j,k,l}} \alpha_i \nabla \tilde{f}_i(\tilde{\mathbf{w}}^t) - \right. \\
& \quad \left. \sum_{l'=1}^L \alpha_{l'} \sum_{k'=1}^{B_{l'}} \alpha_{k'} \sum_{j'=1}^{V_{k',l'}} \alpha_{j'} \sum_{i'=1}^{U_{j',k',l'}} \alpha_{i'} \tilde{f}_{i'}(\tilde{\mathbf{w}}^t) \right) + \left(\sum_{l'=1}^L \alpha_{l'} \sum_{k'=1}^{B_{l'}} \alpha_{k'} \sum_{j'=1}^{V_{k',l'}} \alpha_{j'} \sum_{i'=1}^{U_{j',k',l'}} \alpha_{i'} [\nabla \tilde{f}_{i'}(\tilde{\mathbf{w}}^t) - \nabla \tilde{f}_{i'}(\tilde{\mathbf{w}}_l^t)] \right) + \\
& \quad \left(\sum_{l'=1}^L \alpha_{l'} \sum_{k'=1}^{B_{l'}} \alpha_{k'} \sum_{j'=1}^{V_{k',l'}} \alpha_{j'} \sum_{i'=1}^{U_{j',k',l'}} \alpha_{i'} [\nabla \tilde{f}_{i'}(\tilde{\mathbf{w}}_l^t) - \nabla \tilde{f}_{i'}(\tilde{\mathbf{w}}_k^t)] \right) + \\
& \quad \left. \left(\sum_{l'=1}^L \alpha_{l'} \sum_{k'=1}^{B_{l'}} \alpha_{k'} \sum_{j'=1}^{V_{k',l'}} \alpha_{j'} \sum_{i'=1}^{U_{j',k',l'}} \alpha_{i'} [\nabla \tilde{f}_{i'}(\tilde{\mathbf{w}}_k^t) - \nabla \tilde{f}_{i'}(\tilde{\mathbf{w}}_j^t)] \right) \right\|^2
\end{aligned}$$

$$\begin{aligned}
& \left(\sum_{l'=1}^L \alpha_{l'} \sum_{k'=1}^{B_{l'}} \alpha_{k'} \sum_{j'=1}^{V_{k',l'}} \alpha_{j'} \sum_{i'=1}^{U_{j',k',l'}} \alpha_{i'} [\nabla \tilde{f}_{i'}(\bar{\mathbf{w}}_i^t) - \nabla \tilde{f}_{i'}(\bar{\mathbf{w}}_{i'}^{t,0})] \right)^2 \\
& \leq 36(\beta \varepsilon \eta \kappa_0 \kappa_1 \kappa_2 \kappa_3)^2 + \frac{144(\beta \eta \kappa_0 \kappa_1 \kappa_2 \kappa_3)^2}{T} \sum_{t=0}^{T-1} \sum_{l=1}^L \alpha_l \sum_{k=1}^{B_l} \alpha_k \sum_{j=1}^{V_{k,l}} \alpha_j \sum_{i=1}^{U_{j,k,l}} \alpha_i \mathbb{E} \left\| \tilde{\mathbf{w}}_i^t - \tilde{\mathbf{w}}_{i'}^{t,0} \right\|^2 + \\
& \quad \frac{144(\beta \eta \kappa_0 \kappa_1 \kappa_2 \kappa_3)^2}{T} \sum_{t=0}^{T-1} \sum_{l=1}^L \alpha_l \sum_{k=1}^{B_l} \alpha_k \sum_{j=1}^{V_{k,l}} \alpha_j \sum_{i=1}^{U_{j,k,l}} \alpha_i \mathbb{E} \left\| \bar{\mathbf{w}}_j^t - \bar{\mathbf{w}}_i^t \right\|^2 + \\
& \quad \frac{72(\beta \eta \kappa_0 \kappa_1 \kappa_2 \kappa_3)^2}{T} \sum_{t=0}^{T-1} \sum_{l=1}^L \alpha_l \sum_{k=1}^{B_l} \alpha_k \sum_{j=1}^{V_{k,l}} \alpha_j \mathbb{E} \left\| \bar{\mathbf{w}}_k^t - \bar{\mathbf{w}}_j^t \right\|^2 + \\
& \quad \frac{72(\beta \eta \kappa_0 \kappa_1 \kappa_2 \kappa_3)^2}{T} \sum_{t=0}^{T-1} \sum_{l=1}^L \alpha_l \sum_{k=1}^{B_l} \alpha_k \mathbb{E} \left\| \bar{\mathbf{w}}_l^t - \bar{\mathbf{w}}_k^t \right\|^2 + \\
& \quad \frac{72(\beta \eta \kappa_0 \kappa_1 \kappa_2 \kappa_3)^2}{T} \sum_{t=0}^{T-1} \sum_{l=1}^L \alpha_l \mathbb{E} \left\| \bar{\mathbf{w}}^t - \bar{\mathbf{w}}_l^t \right\|^2 \\
& \leq \mathcal{O}(\kappa_0^2 \kappa_1^2 \kappa_2^2 \kappa_3^2 \beta^2 \eta^2 \varepsilon^2) + \mathcal{O}(\delta^{\text{th}} \kappa_0^2 \kappa_1^2 \kappa_2^2 \kappa_3^2 \beta^2 \eta^2 D^2) + \mathcal{O}(\kappa_0^3 \kappa_1^2 \kappa_2^2 \kappa_3^2 \eta^4 \beta^2 \sigma^2) + \\
& \quad \mathcal{O}(\kappa_0^4 \kappa_1^2 \kappa_2^2 \kappa_3^2 \eta^4 \beta^2 \varepsilon_{\text{vc}}^2) + \mathcal{O}(\kappa_0^3 \kappa_1^2 \kappa_2^2 \kappa_3^2 \eta^4 \beta^2 G^2 \cdot \varphi_{\text{w},L_1}) + \mathcal{O}(\delta^{\text{th}} \kappa_0^2 \kappa_1^2 \kappa_2^2 \kappa_3^2 \eta^2 \beta^2 D^2) + \\
& \quad \mathcal{O}(\kappa_0^6 \kappa_1^4 \kappa_2^2 \kappa_3^2 \eta^6 \beta^4 \varepsilon_{\text{vc}}^2) + \mathcal{O}(\kappa_0^4 \kappa_1^4 \kappa_2^2 \kappa_3^2 \eta^4 \beta^2 \varepsilon_{\text{sbs}}^2) + \mathcal{O}(\kappa_0^3 \kappa_1^3 \kappa_2^2 \kappa_3^2 \eta^4 \sigma^2 \beta^2) + \\
& \quad \mathcal{O}(\delta^{\text{th}} \kappa_0^2 \kappa_1^2 \kappa_2^2 \kappa_3^2 \beta^2 \eta^2 D^2) + \mathcal{O}(\kappa_0^5 \kappa_1^4 \kappa_2^2 \kappa_3^2 \beta^4 \eta^6 G^2 \cdot \varphi_{\text{w},L_1}) + \mathcal{O}(\kappa_0^3 \kappa_1^3 \kappa_2^2 \kappa_3^2 \beta^2 \eta^4 \cdot \varphi_{\text{w},L_2}) + \\
& \quad \mathcal{O}(\kappa_0^5 \kappa_1^4 \kappa_2^4 \kappa_3^2 \eta^6 \beta^4 \varepsilon_{\text{vc}}^2) + \mathcal{O}(\kappa_0^6 \kappa_1^6 \kappa_2^4 \kappa_3^2 \eta^6 \beta^4 \varepsilon_{\text{sbs}}^2) + \mathcal{O}(\kappa_0^4 \kappa_1^4 \kappa_2^4 \kappa_3^2 \eta^4 \beta^4 \varepsilon_{\text{mbs}}^2) + \\
& \quad \mathcal{O}(\kappa_0^3 \kappa_1^3 \kappa_2^3 \kappa_3^2 \eta^4 \beta^2 \sigma^2) + \mathcal{O}(\delta^{\text{th}} \kappa_0^2 \kappa_1^2 \kappa_2^2 \kappa_3^2 \eta^2 \beta^2 D^2) + \mathcal{O}(\kappa_0^5 \kappa_1^4 \kappa_2^4 \kappa_3^2 \eta^6 \beta^4 G^2 \cdot \varphi_{\text{w},L_1}) + \\
& \quad \mathcal{O}(\kappa_0^4 \kappa_1^4 \kappa_2^4 \kappa_3^2 \beta^4 \eta^6 \cdot \varphi_{\text{w},L_2}) + \mathcal{O}(\kappa_0^3 \kappa_1^3 \kappa_2^3 \kappa_3^2 \eta^4 \beta^2 G^2 \cdot \varphi_{\text{w},L_3}) + \\
& \quad \frac{72(\beta \eta \kappa_0 \kappa_1 \kappa_2 \kappa_3)^2}{T} \sum_{t=0}^{T-1} \sum_{l=1}^L \alpha_l \mathbb{E} \left\| \bar{\mathbf{w}}^t - \bar{\mathbf{w}}_l^t \right\|^2 \\
& \approx \mathcal{O}(\kappa_0^4 \kappa_1^2 \kappa_2^2 \kappa_3^2 \eta^4 \beta^2 \varepsilon_{\text{vc}}^2) + \mathcal{O}(\kappa_0^4 \kappa_1^4 \kappa_2^2 \kappa_3^2 \eta^4 \beta^2 \varepsilon_{\text{sbs}}^2) + \mathcal{O}(\kappa_0^4 \kappa_1^4 \kappa_2^4 \kappa_3^2 \eta^4 \beta^4 \varepsilon_{\text{mbs}}^2) + \\
& \quad \mathcal{O}(\kappa_0^2 \kappa_1^2 \kappa_2^2 \kappa_3^2 \beta^2 \eta^2 \varepsilon^2) + \mathcal{O}(\kappa_0^3 \kappa_1^2 \kappa_2^2 \kappa_3^2 \eta^4 \beta^2 \sigma^2) + \mathcal{O}(\delta^{\text{th}} \kappa_0^2 \kappa_1^2 \kappa_2^2 \kappa_3^2 \eta^2 \beta^2 D^2) + \\
& \quad \mathcal{O}(\kappa_0^3 \kappa_1^2 \kappa_2^2 \kappa_3^2 \eta^4 \beta^2 G^2 \cdot \varphi_{\text{w},L_1}) + \mathcal{O}(\kappa_0^3 \kappa_1^3 \kappa_2^2 \kappa_3^2 \beta^2 \eta^4 \cdot \varphi_{\text{w},L_2}) + \\
& \quad \mathcal{O}(\kappa_0^3 \kappa_1^3 \kappa_2^3 \kappa_3^2 \eta^4 \beta^2 G^2 \cdot \varphi_{\text{w},L_3}) + \frac{72(\beta \eta \kappa_0 \kappa_1 \kappa_2 \kappa_3)^2}{T} \sum_{t=0}^{T-1} \sum_{l=1}^L \alpha_l \mathbb{E} \left\| \bar{\mathbf{w}}^t - \bar{\mathbf{w}}_l^t \right\|^2.
\end{aligned} \tag{121}$$

■